A chiral auxiliary approach to the synthesis of mechanically planar-chiral rotaxanes

Robert J. Bordoli

Thesis submitted in partial fulfilment of the requirement for a degree of Doctor of Philosophy at Queen Mary, University of London

For Nicola, Mum and Dad

Statement of originality

I, Robert J. Bordoli, confirm that the research included within this thesis is my own work or that where it has been carried out in collaboration with, or supported by others, that this is duly acknowledged below and my contribution indicated. Previously published material is also acknowledged below.

I attest that I have exercised reasonable care to ensure that the work is original, and does not to the best of my knowledge break any UK law, infringe any third party's copyright or other Intellectual Property Right, or contain any confidential material.

I accept that the College has the right to use plagiarism detection software to check the electronic version of the thesis.

I confirm that this thesis has not been previously submitted for the award of a degree by this or any other university.

Signature: 

Date: 20/04/2015

Details of collaboration and publications:

Bordoli, R. J.; Goldup, S. M. *J. Am. Chem. Soc.* **2014**, *136* (13), 4817.

Abstract

Rotaxanes are a class of compounds composed of two or more mechanically interlocked molecules. Mechanically planar chiral rotaxanes are a novel class of compound in that their chirality is due to the isomerism of a mechanical bond, as opposed to the covalent bonding of the individual components. We know of no method to synthesise enantiomerically pure samples of the mechanical isomers of a mechanically planar chiral rotaxane without resorting to advanced purification techniques. The lack of ready availability of these materials has hampered the full investigation of their properties and applications. Of particular interest are their properties as chiral reaction-spaces, such as ligands, organo-catalysts, and chiral resolution agents.

This thesis addresses these issues by developing a chiral-auxiliary approach toward the synthesis of mechanically planar chiral rotaxanes whereby an intermediate pair of diastereomeric rotaxanes are synthesised and separated using reliable and scalable standard laboratory techniques. Cleavage of the chiral auxiliary allows for the synthesis of enantiopure mechanically planar chiral rotaxanes. Tuning the structure of the mechanically interlocked components as well as the reaction conditions allows for control over the diastereoselectivity during the mechanical bond forming step.

Contents

Chapter 2: Synthesis of mechanically planar-chiral [2]rotaxanes

Chapter 3: Diastereoselective synthesis of mechanically planar chiral [2]rotaxanes

Chapter 4: Experimental section

Acknowledgements

I would firstly like to thank my supervisor, Dr Stephen Goldup, for the opportunity to undertake such an interesting project, and for his direction and support during my research as well as the preparation of this thesis. I thank Queen Mary University of London for their financial and administrative support.

I thank my colleagues in the Goldup group for their friendship and support over the last few years; a special thank you to Ben, Jess, Kajally, Ed, Luca, Joby, Marzia, Cath, and Jamie. Without you the lab would have been a much duller and quieter place! Particular thanks to Ben, Jess and Cath for being exceptional housemates.

The data acquisition undertaken during the preparation of this thesis was made much smoother with the excellent help of the technical and support staff in the School of Biological and Chemical Sciences. Thanks to Greg and Harold for keeping the NMR service up and running, to Ian for his help with acquiring mass-spectral data, and thanks to Majid for acquiring some challenging crystal structures.

I give thanks to my family for their love and support over the years. A special thank you to Mum and Dad, for giving me the freedom to make my own way, and for your enormous generosity over the years. Honourable mentions go to my uncle Nigel and aunt Linda for housing me when I ended up without anywhere to live, and my gran Margaret and sister Ruth for their support and encouragement.

Ultimately, thank you to Nicola, for your patience, love and support while writing up.

Abbreviations

AT	active template
CD	circular dichroism
CSP-HPLC	chiral stationary phase HPLC
CuAAC	copper mediated alkyne-azide-cycladdition
DME	1,2-dimethoxyethane
DMF	*N*,*N*'-dimethylformamide
GC-MS	gas chromatography – mass spectrometry
h	hour(s)
HPLC	high performance liquid chromatography
HRMS	high resolution mass spectrometry
IPA	isopropyl alcohol
LRMS	low resolution mass spectrometry
MIA	mechanically interlocked architecture
NMR	nuclear magnetic resonance (spectroscopy)
rt	room temperature
THF	tetrahydrofuran

Chapter 1 – Introduction to chirality, molecular structure and chemical topology

1.1 – Chemical topology

Chemists are naturally familiar with the description of molecular structures. By denoting the number and type of atoms in a molecule, their connectivity and the type of bond with which they are bound, and the spatial arrangement around atomic centres, we are able to accurately describe the structure of most organic compounds. However, in 1961 Frisch and Wasserman introduced a new term "chemical topology", in a paper of the same name, in which they described a number of molecules which required more complex descriptions.[1] They highlighted that a cyclic polyethylene chain can exist as both a simple ring and as a trefoil knot, and that while the two compounds have identical chemical bonding they are clearly two different isomers of the same species (Figure 1).

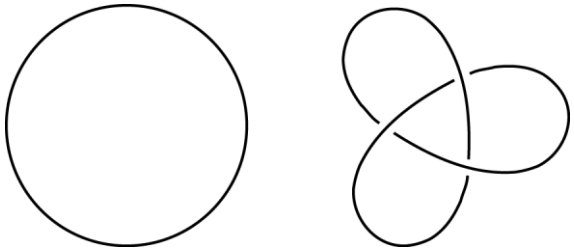

Figure 1: Topological isomers: a cyclic molecule in its ring (left) and trefoil knot (right) forms

These two isomers differ in their topology, where the topological description of the molecule concerns the connectivity of the structure but ignores bond lengths and angles. Topological deformation of the molecule enables us to arbitrarily stretch and bend bonds to rearrange the structure, as long as we do not 'cut' previously connected or 'join' unconnected sections of the molecule. This is analogous to the breaking or creation of a chemical bond. As the ring and knot forms cannot be interconverted through a topological deformation they are said to be *topological isomers*.

By extension, it is possible to arrange a pair of ring shaped molecules in two different ways, either as separate molecules or being interlinked (Figure 2). This second isomer (known as a *catenane*) is arranged such that the two individual components cannot be separated without first breaking a chemical bond, and the catenane therefore acts as a single molecule. The catenane is a topological isomer of the two rings, and the rings in the catenane are said to share a *topological bond*. The catenane is described as possessing a mechanical bond, where the strength of the mechanical bond is as strong as the weakest chemical bond in the catenane. The number of components in a catenane is denoted as a numerical prefix, the catenane shown in Figure 2 is a [2]catenane.

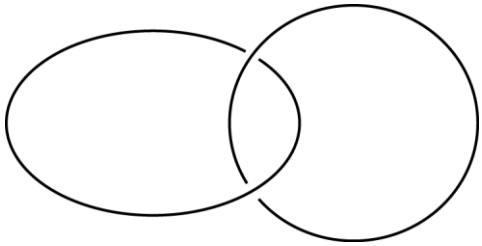

Figure 2: General structure of a [2]catanane

In their paper, Frisch and Wasserman note that a topologically trivial analogue of a catenane may also exist, in which a ring shaped molecule (macrocycle) is threaded with a linear molecule (thread) which has bulky end groups (stoppers) to prevent the ring slipping over. Although Frisch and Wasserman left this species un-named it would later become known as a rotaxane (Figure 3). The nomenclature of rotaxanes follows that of catenanes; a two component rotaxane is a [2]rotaxane.

The general term for a molecule with a mechanical bond is a *mechanically interlocked architecture* (MIA). Rotaxanes are atypical of most MIAs in that they are topologically trivial; the two (or more) components of a rotaxane can be deformed topologically to separate them. A rotaxane has no topological bond as the hypothetical expansion of the macrocycle would allow it to be separated from the thread. However, in chemical terms a rotaxane has a mechanical bond due to the inability of the macrocycle to fit over the bulky stoppers. As an aside, in cases where the macrocycle can slip off the thread such molecules are termed a 'pseudo-rotaxane'. This is unlike a catenane, in which you would have to pass one ring through another to separate the components. Like a catenane, a rotaxane possesses a mechanical bond and therefore a chemical bond must be broken to separate its two components.

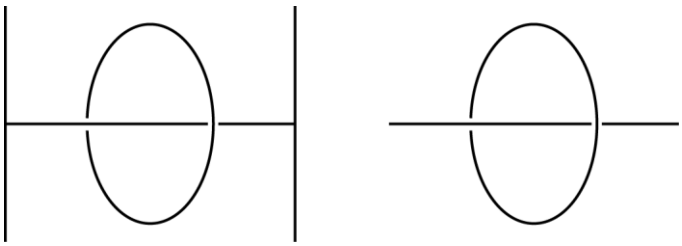

Figure 3: General structure of a [2]rotaxane (left) and a pseudo-rotaxane (right)

The term *mechanically interlocked architecture* (MIA) is a catch-all term used to describe compounds which possess a mechanical bond. There are a number of different subclasses of MIAs including rotaxanes, catenanes, molecular knots, Solomon links, and Borromean rings.

1.2 – Rotaxane syntheses

In the last 50 years a number of different methodologies have been developed to synthesise mechanically interlocked archtectures. Here we discuss the synthesis of rotaxanes in a historical context. A rotaxane forming reaction is termed a *rotaxanation*.

1.2.1 – Statistical synthesis

The first reported synthesis of a rotaxane was published in 1967 by Harrison and Harrison.[2] They treated a column of resin-bound macrocycle (**1**) with a solution of decane-1,10-diol (**2**) and triphenylmethyl chloride (**3**). The treatment was repeated 70 times and the resin-bound rotaxane (**4**) was hydrolysed from the resin to give the target rotaxane (**5**) in a 6% yield (Figure 4).

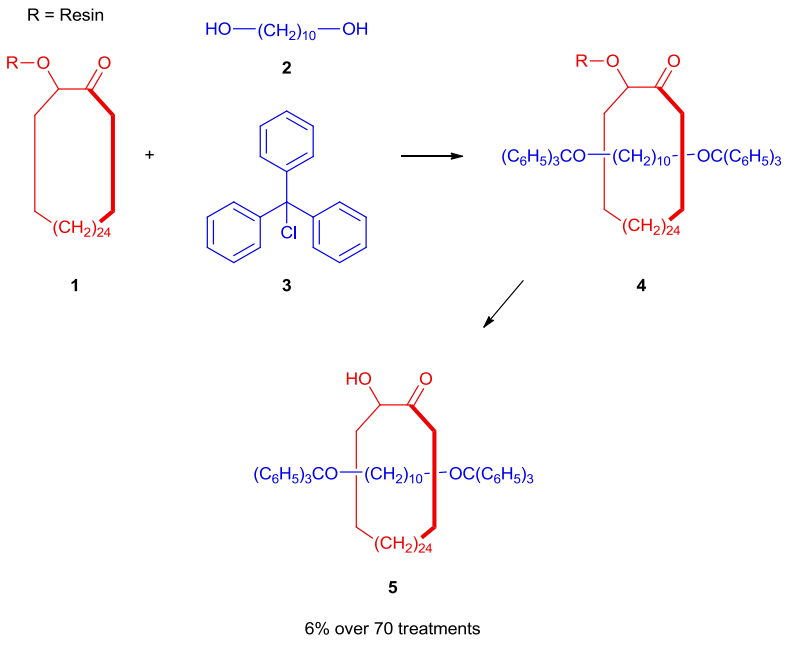

Figure 4: Harrison and Harrison's rotaxane synthesis

1.2.2 – Covalent directed synthesis

The low yield of Harrison's statistical approach left plenty of room for improvement. In 1969 Schill and Zollenkopf published a directed synthesis of a rotaxane based on chemistry they had developed for the synthesis of catenanes.[3] In their directed synthesis they took a pre-formed

threaded structure (**6**), 'capped' it with bulky end groups to form **7**, and then cleaved the covalent bonds between macrocycle and thread moieties to form [2]rotaxane **9**. The yield for the conversion of the capped pseudo-rotaxane (**7**, Figure 5) to the rotaxane **9** was 46%, a marked increase on Harrison's statistical synthesis.

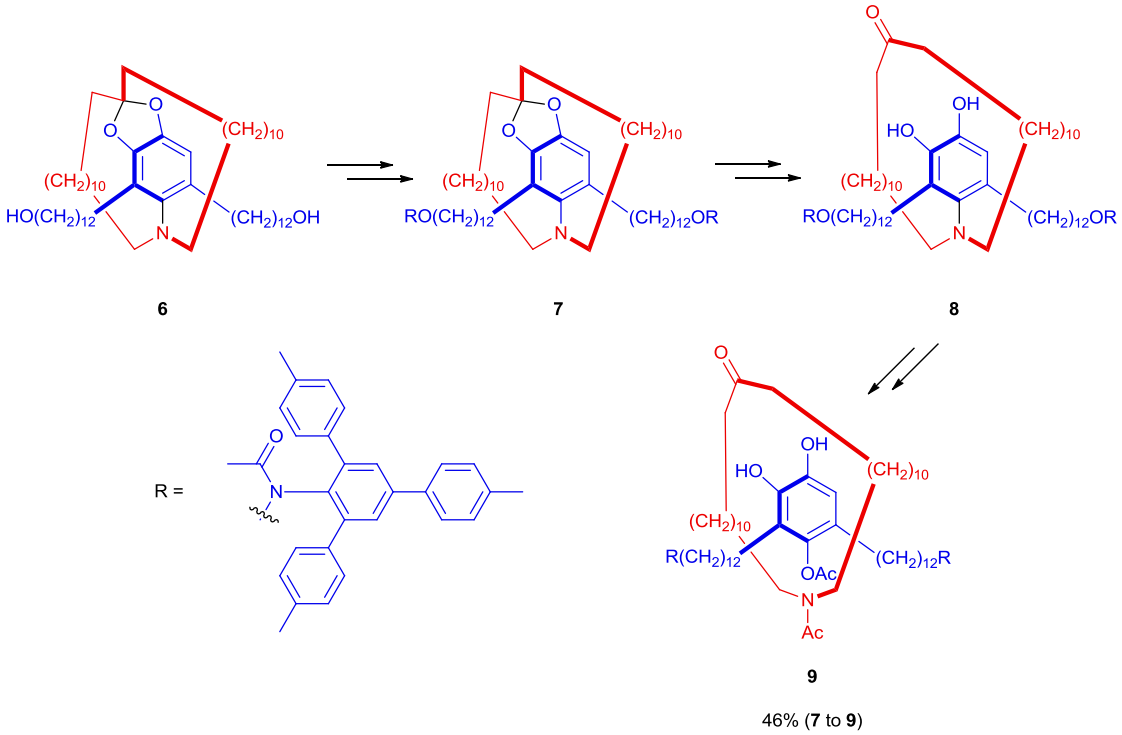

Figure 5: An abbreviated sequence for the synthesis of Schill's rotaxane

1.2.3 – Metal templated synthesis

The following years saw investigations into templated reactions. Sauvage and co-workers employed a tetrahedral copper(I) ion to coordinate two 1,10-phenanthrolene derivatives in a pseudo-rotaxane arrangement, pre-organising the components for the synthesis of a [2]catenane.[4] Their successful catenane synthesis showed that this was a viable approach, and Gibson and co-workers then demonstrated an analogous reaction using the same pseudorotaxane intermediate (**10**) in the synthesis of a [2]rotaxane (**12**), successfully generating the target rotaxane in 42% yield (Figure 6).[5]

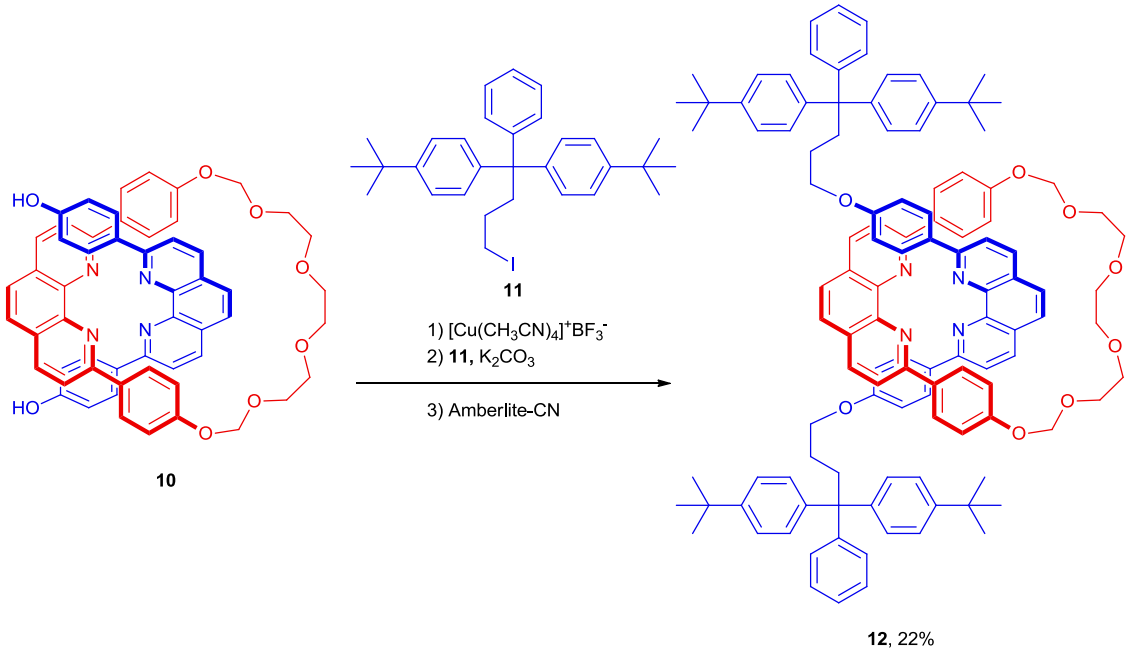

Figure 6: Gibson's copper(I) templated rotaxanation

A variety of metal template reactions were developed employing a number of metals, including copper, palladium, manganese, iron, cobalt, nickel, copper, zinc, cadmium and mercury.[6,7]

1.2.4 – Organic template-directed synthesis and rotaxane formation under thermodynamic control

Stoddart and co-workers later published a number of papers showing a metal-free template methodology which they used to synthesise [2]catenanes[8] and pseudo-rotaxanes.[9] Stoddart and co-workers followed this work employing a metal-free templated reaction in the synthesis of a [2]rotaxane (**16**). This method utilised the cation-pi interactions between a thread (**15**) containing a 1,4-bisphenol ether moiety and a tetracationic pre-macrocycle (**13**) containing two bipyridinium moieties.[10] They formed the mechanical bond by 'clipping' the macrocycle around the thread (through a double alkylation reaction with **14**) forming the rotaxane in a 10% yield (Figure 7). Here they were able to show that non-covalent interactions between purely organic molecules could construct complex molecular arrangements.

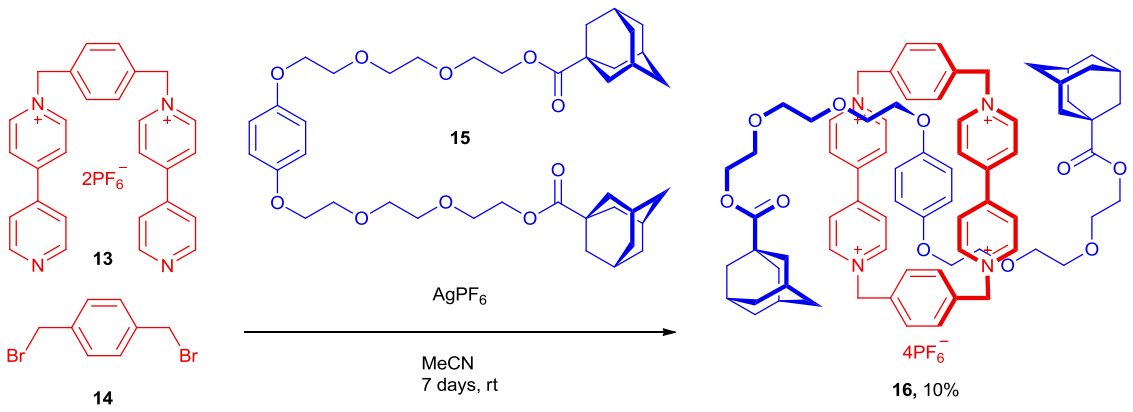

Figure 7: Stoddart's metal-free template directed [2]rotaxane synthesis

Busch and co-workers later synthesised a [2]rotaxane via a metal-free templated synthesis by incorporating crown-ether and ammonium moieties into the macrocycle and thread respectively. This method utilises favourable ion-dipole interactions between the positive dialkylammonium unit and the polar crown other moiety of dibenzo[24]crown-8 to pre-assemble a pseudo-rotaxane. Subsequent capping of the pseudo-rotaxane (**17**) with stopper **18** gave a relatively high yielding synthesis of rotaxanes without the use of metallic coordination to give the target rotaxane (**19**) in up to 22% yield (Figure 8).

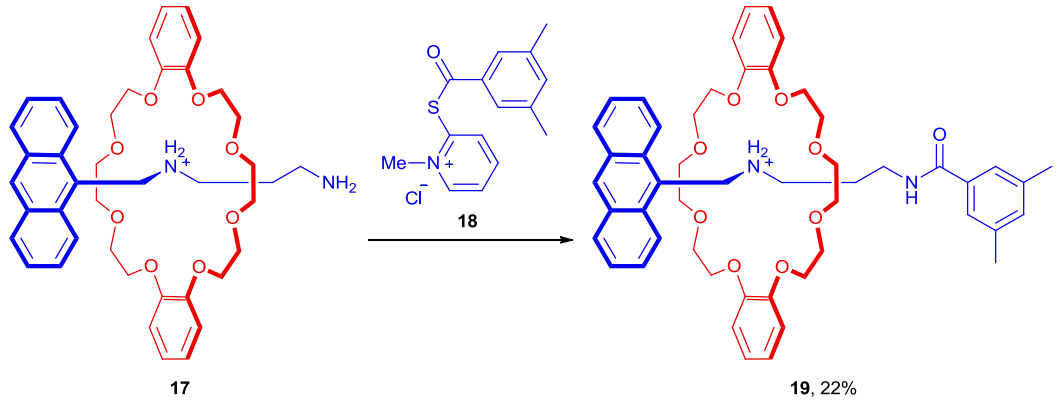

Figure 8: Busch's crown ether-ammonium templated rotaxane synthesis

After publishing a number of papers on ammonium-crown ether templated catenane syntheses Stoddart and co-workers published the synthesis of a switchable [2]rotaxane shuttle comprised of a crown ether macrocycle (**DB24C8**) and an ammonium based thread (**20**).[11] Rotaxane shuttles are rotaxanes which possess two or more stations in the thread over which the macrocycle preferentially sits. The position preferred by the macrocycle can be altered through chemical or photochemical stimuli (Figure 9). These systems are of interest as they may serve as chemical switches given that they are able to change function or state in a controllable manner.

The position of the macrocycle on the thread in rotaxane **22**+H can be altered through deprotonation of the ammonium moiety. On addition of diisopropylethylamine the crown ether shuttles to the bipyridinium station. It remains here until addition of acid reprotonates the amine and the crown ether macrocycle shuttles back to its original position (**22**).

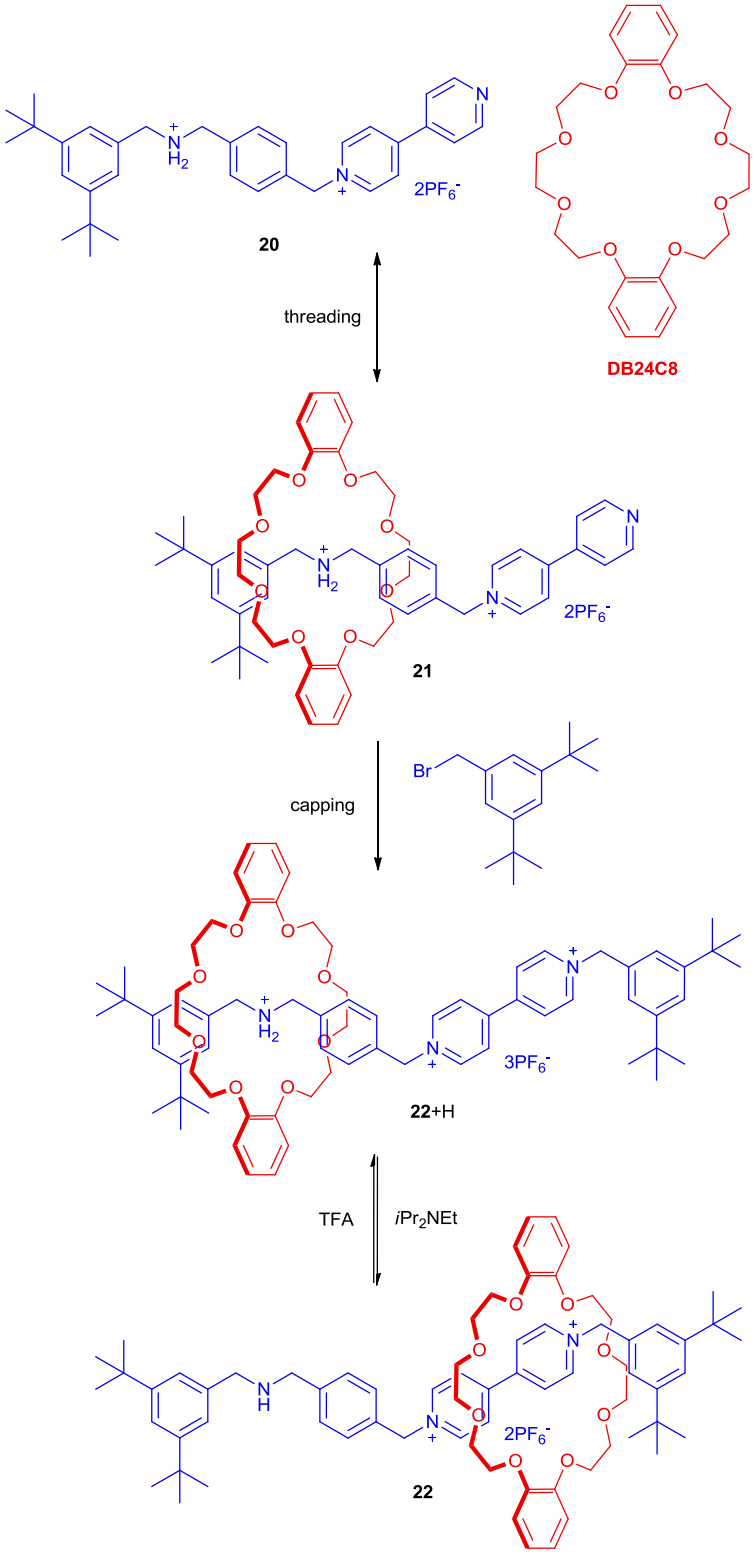

Figure 9: Stoddart's dialkylammonium-dibenzo[24]crown-8 based rotaxane

Stoddart and co-workers went on to develop the synthesis of rotaxanes under thermodynamic control, in which they designed a thermodynamically reversible step into the mechanical bond forming reaction.[12] Using the same dibenzylammonium ion/crown ether recognition motif as shown earlier, the self assembly of a [2]rotaxane was allowed through a reversible imine hydrolysis reaction of the thread. Reduction of the imine bonds afforded the kinetically inert [2]rotaxane ([**24**-H•DB24C8]•PF_6) in a reasonable yield (18%).

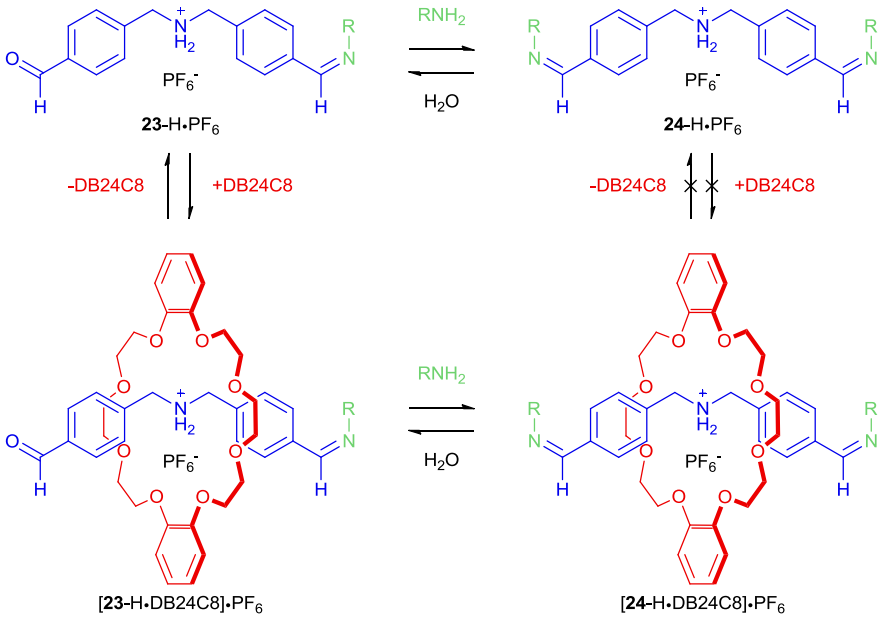

Figure 10: Synthesis of a [2]rotaxane under thermodynamic control.

1.2.5 – Active-metal template reaction

Metal templated reactions remained an efficient tool in the synthesis of rotaxanes and other MIAs for many years, but this methodology relies both on metal ion coordination as well as one or more subsequent reactions to form the mechanical bond. A more elegant solution would be to employ the coordinating metal as a catalyst in the mechanical bond-forming step. The Leigh group pioneered this methodology describing it as an "*active"-metal template* (AT) reaction.

In 2006 Leigh and co-workers published a paper which demonstrated the use of a copper(I)-catalysed acetylene-azide cycloaddition (CuAAC) as the mechanical bond forming step to synthesise a [2]rotaxane (**27**).[13] The rotaxanes were synthesised in one step from a macrocycle (**25**) and two 'half-threads' (**24** and **26**), each of which bore a bulky stopper moiety. By utilising the same tetrahedral geometry provided by a copper(I) centre as Sauvage had done previously Leigh and co-workers were able to produce rotaxanes in excellent yields. At the same time they

showed that both stoichiometric and catalytic variants of the AT-CuAAC reaction were possible.

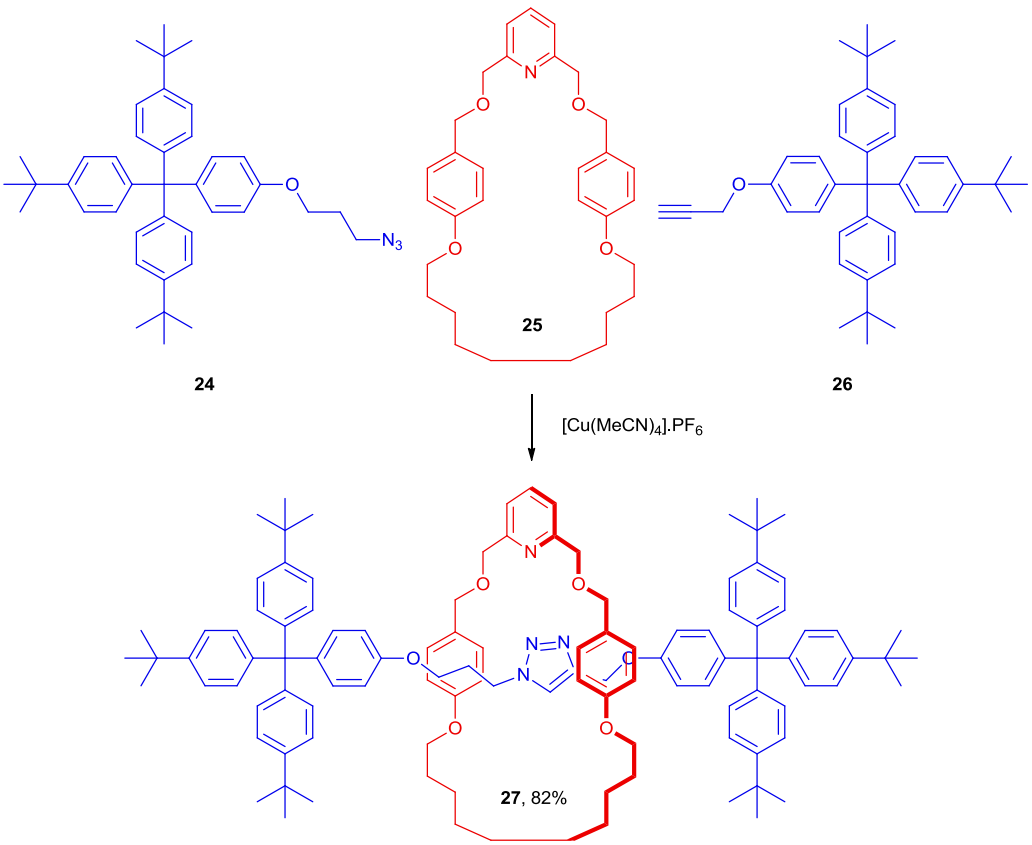

Figure 11: Leigh's catalytic 'click' rotaxanation

Leigh and co-workers later published an example of an active metal template rotaxanation using a palladium centre to perform an alkyne homocoupling reaction, giving evidence for the generality of the concept (Figure 12).[14]

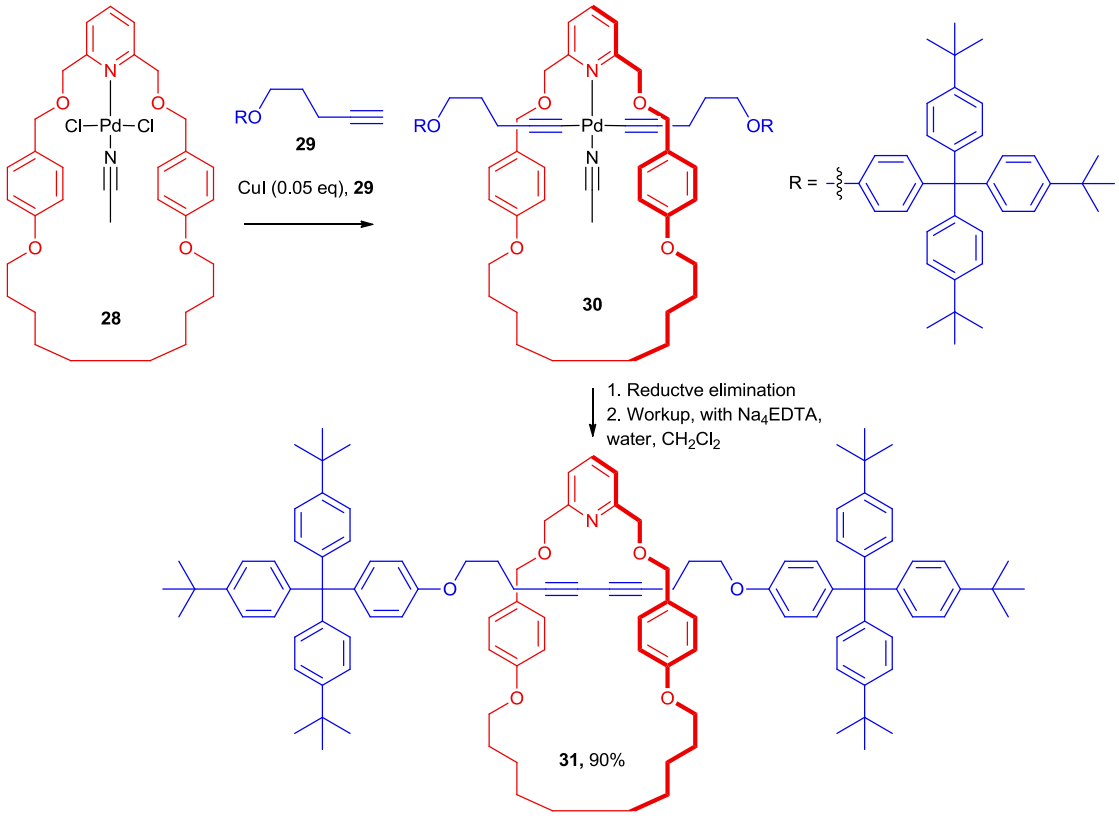

Figure 12: Leigh's palladium-mediated alkyne-homocoupling AT-rotaxanation

The relatively simple synthesis of the required reagents, and the broad functional tolerance of the CuAAC 'click' reaction has proven invaluable to the synthesis of these complex targets, and has proven to be a popular reaction for this reason. The Leigh group and others have shown that the application of the AT-CuAAC reaction can be used to synthesise a variety of complex mechanically interlocked structures, including catenanes,[15,16] rotaxanes,[17,18] and knots.[19]

1.2.6 – 'Size matters' - Small macrocycles in the AT-CuAAC reaction

One limitation of the existing methodologies was the requirement for relatively large structural motifs. Macrocycles typically possessed large cavities due to the thought that the bond-forming reaction required space to occur in. The large macrocycles therefore necessitated large bulky stoppers, which could suffer from issues with low solubility and protracted synthetic sequences. Goldup and co-workers sought to address this though development of 'small' rotaxanes, utilising the high efficiency of the AT-CuAAC reaction to thread small bipyridine containing macrocycles.[20] They investigated the effects of macrocycle size on AT-CuAAC rotaxanations, and probed the steric limits of the stoppers employed in these reactions. They found that the yield of the reaction increased on reduced macrocycle size, which was counterintuitive to the

prevailing thought that the reaction required space to take place in. In fact, the smallest macrocycle was successfully captured with a number of small half-threads, and in excellent yields. The combination of small, rigid stoppers and the reduced flexibility of the macrocycle gave quantitative conversion to the rotaxane product (Figure 13).

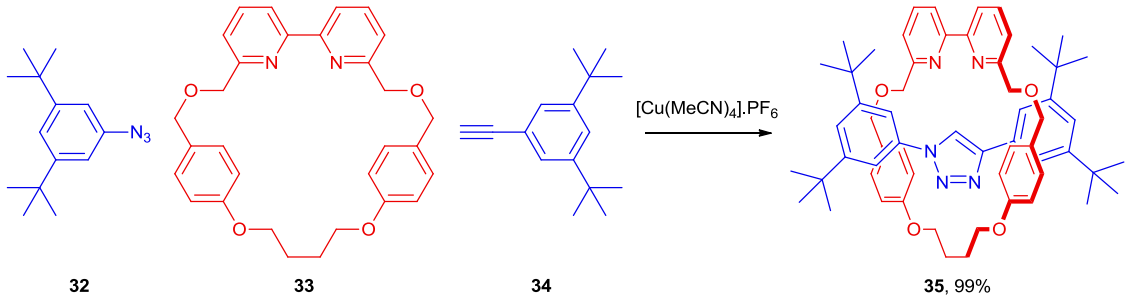

Figure 13: High yielding AT-CuAAC synthesis of a 'small' [2]rotaxane

The small macrocycle cavity prevents the two threads from approaching from the same face of the macrocycle, dramatically increasing the yield of the rotaxane forming reaction and reducing the yield of non-mechanically interlocked thread as a sideproduct. This methodology demonstrated a number of advantages of 'small' AT-CuAAC rotaxanations, including easy access to small half-threads as well as high yielding reactions. A variety of half threads were employed and demonstrated the synthesis of rotaxanes containing, simple di-alkyl arene stoppers (**34,** Figure 14), stoppers bearing single atom reactive functionalities (**36**), trialkylsilyl groups (**37**), fluorophores (**38**), and chiral pool materials (**39**). Some of these stoppers form rotaxanes with fully conjugated threads and open the possibility of extending this methodology toward the synthesis of oligomeric insulated molecular wires.

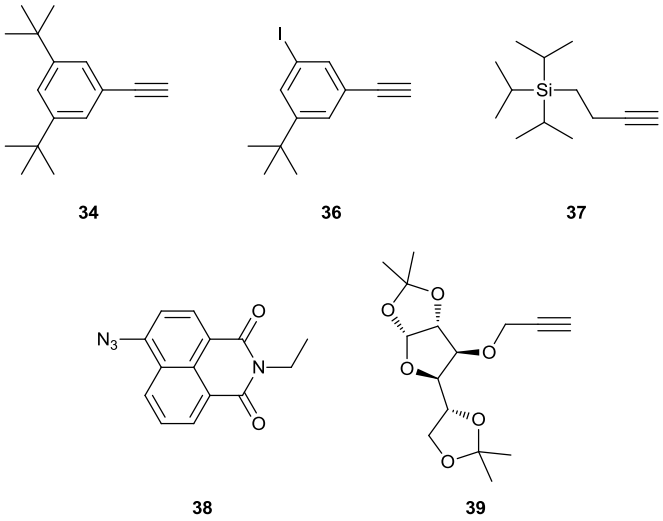

Figure 14: Stoppers employed in the synthesis of 'small' rotaxanes

1.3 – Chirality in mechanically interlocked architectures

1.3.1 – Sources of chirality

The simplest definition of chirality is that of molecules which exist as two non-superposable mirror images. These isomers are called *enantiomers*. The source of chirality can take many forms, the classic example being a tetrahedral carbon atom with four different substituents (**40**, Figure 15). However, compounds which do not possess asymmetrically substituted atoms may still be chiral. For example, if a molecule contains a set of substituents held in a spatial arrangement that is not superposable on its mirror image then it may also exist as two enantiomers, as in the case of spiroketones and allenes (**41** and **42** respectively, Figure 15). These compounds are *axially chiral*.

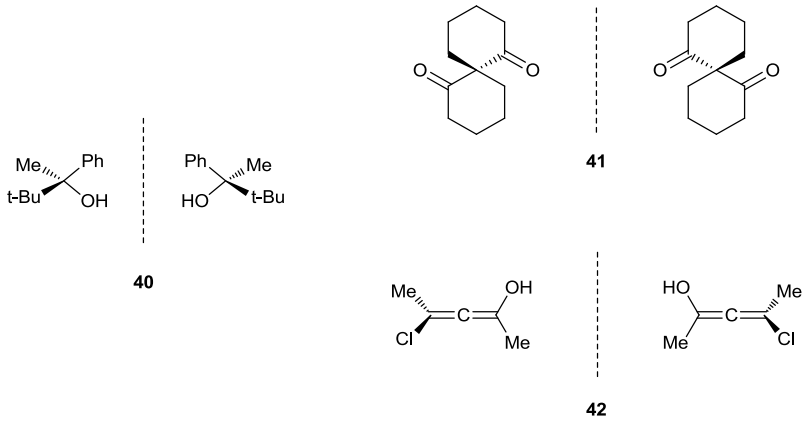

Figure 15: Sources of chirality

Similarly, compounds in which restricted rotation around a single bond prevents the interconversion of two conformational isomers results in two enantiomeric forms of a compound, known as atropisomers. These species can also be described as exhibiting *axial chirality*. Typical examples of axially chiral species include binapthylene and biphenyl derivatives (**43** and **44**, Figure 16).

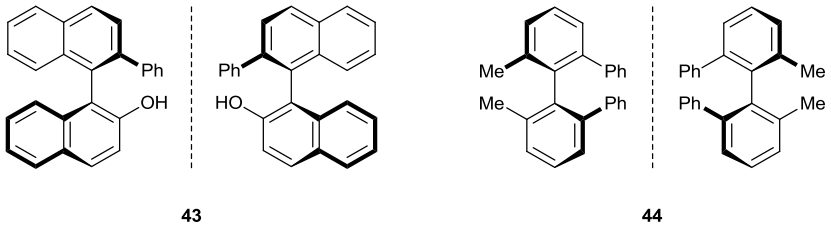

Figure 16: Axially chiral biaryl species

. Molecules in which two coplanar rings, each bearing dissymmetric functionality, and which cannot rotate easily about the chemical bond connecting them are decribed as being *planar chiral*. An example of this type of molecule is the ferrocene derivative **45** which can be used in the kinetic resolution of secondary alcohols.[21]

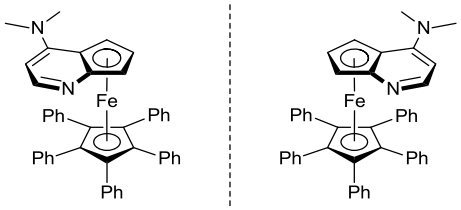

45

Figure 17: A planar chiral ferrocene derivative

Other types of chirality can arise indirectly from the covalent structure of a molecule, such as in the case of *helicenes* - molecules with a helical structure that most often arises due to steric hinderance forcing the molecule to adopt a twisted, non-planar configuration. Depending on the orientation of the twist the molecule exists either as right- or left-handed screw, which (similarly to the R- and S- notation used in stereochemical assignments) are denoted as M- or P-helicenes respectively.

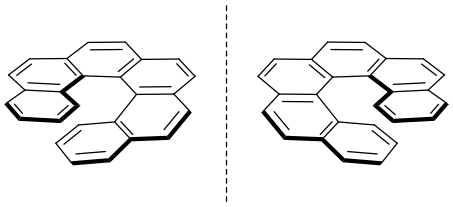

(P)-**46** (M)-**46**

Figure 18: The two helically shaped enantiomers of [6]helicene

1.3.2 – Applications of chiral rotaxanes

Mechanically interlocked architectures may possess elements of chirality such as those described above. Indeed, many examples of atropisomeric catenanes and rotaxanes can be found in the literature, as well as catenanes and rotaxanes containing centrochiral stereogenic centres. These elements of chirality have been employed in different ways to make functional systems.

Examples of rotaxanes containing a chiral centre have been employed as chiral switches. Leigh and co-workers have published a number of papers on switchable rotaxanes, which respond to stimuli enabling them to alter their function.

In 2002 Leigh and co-workers published a study into the induced circular dichroism in hydrogen bonded rotaxanes (**47**), in which they demonstrated the ability to alter the magnitude of the CD response through control of the intercomponent interactions through modification of solvent conditions or temperature (Figure 19).[22]

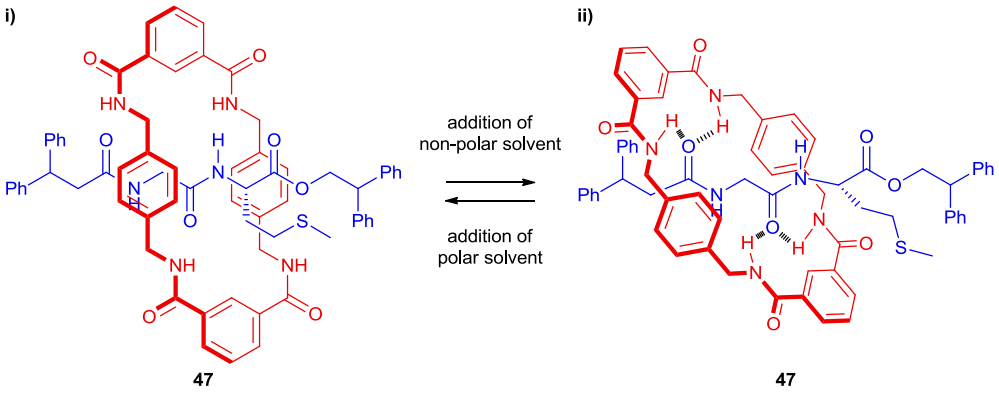

Figure 19: Leigh's peptide derived rotaxane in i) non-hydrogen bonded, and ii) hydrogen bonded states

This paved the way for further work and in 2003 Leigh and co-workers demonstrated a rotaxane shuttle (**48**) that exhibited chiroptical switching. The application of a chemical stimulus to the rotaxane resulted in the translation of the macrocycle between stations on the thread.[23] Once over a chiral station the macrocycle-amine interaction resulted in a UV active chromophore, which would otherwise be absent, allowing the rotaxane to act as a chiroptical switch (Figure 20).

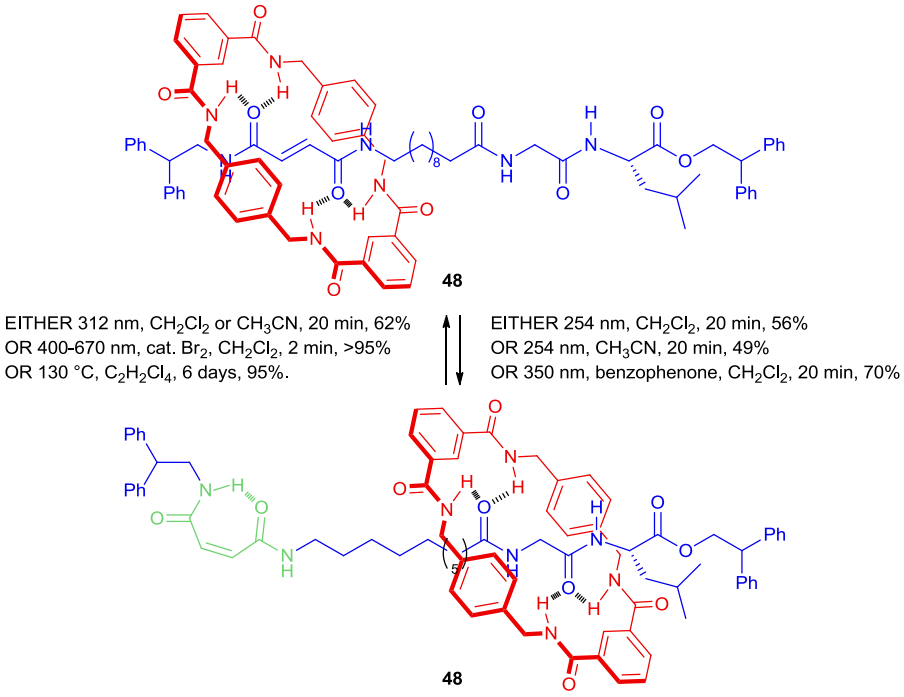

Figure 20: Leigh's chiroptical switch

This work was ultimately followed in 2014 by the development of a switchable [2]rotaxane organocatalyst (**49**).[24] This rotaxane could be switched between active and inactive states via the protonation or deprotonation of a secondary amine (Figure 21). Deprotonation of the amine caused the macrocycle to translate along the thread to a triazolium station, thereby revealing the amine and allowing it to catalyse an asymmetric Michael addition reaction.

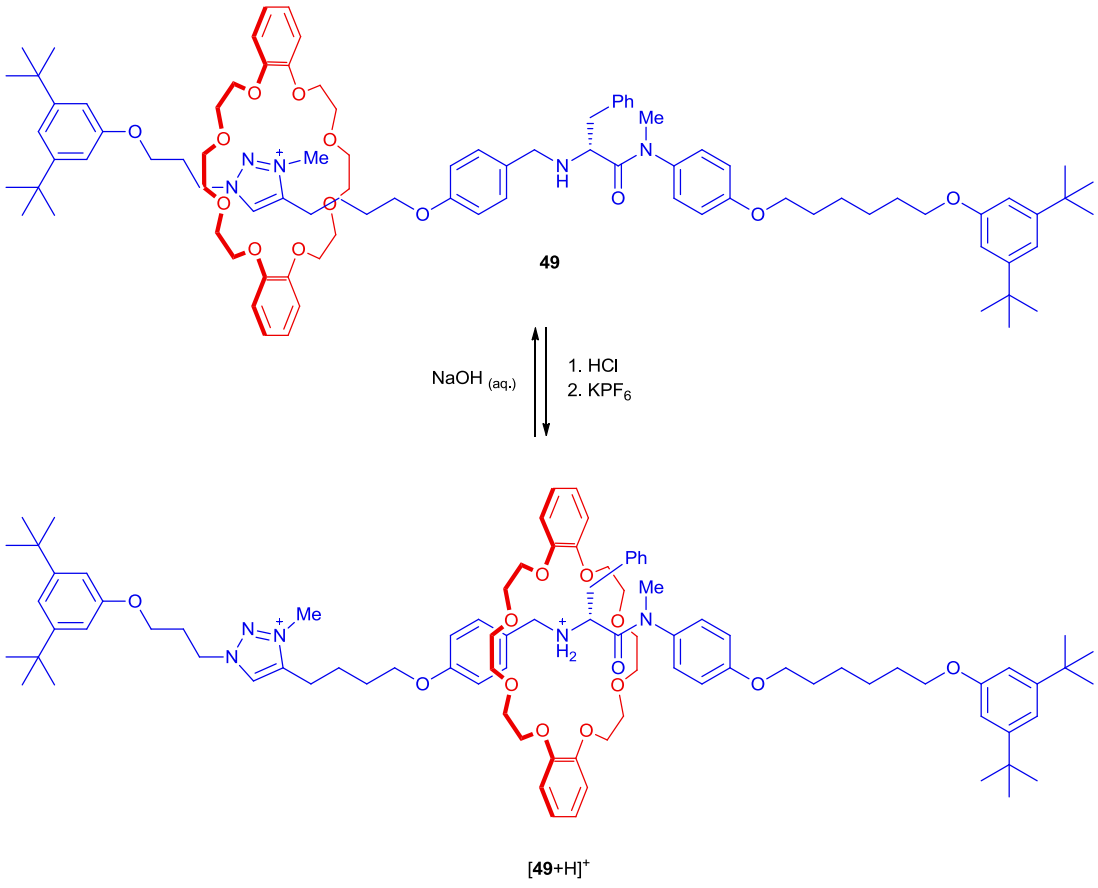

Figure 21: Leigh's switchable [2]rotaxane organocatalyst

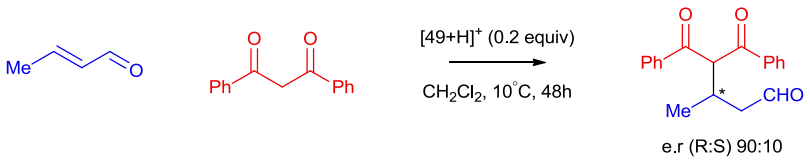

Figure 22: An example of an Asymmetric Michael addition mediated by a chiral rotaxane

In 2007, Nishibayashi and co-workers published the first example of a chiral ligand (**50**) based on a pseudo-rotaxane skeleton in the enantioselective transition-metal mediated hydrogenation of enamines (Figure 23 and Figure 24).[25] Their hydrogenation catalyst was effective, providing selectivity of up to 77% ee. They demonstrated that only the mechanically interlocked complex

was effective and that the macrocycle and thread components were individually much less efficient in performing the reaction.

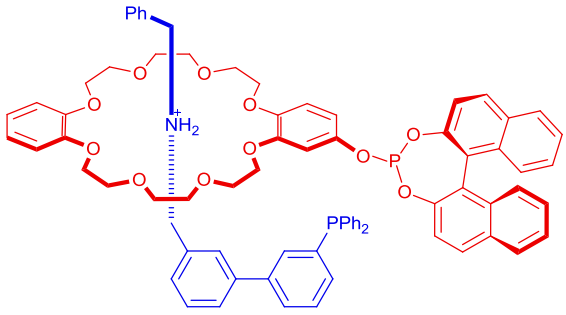

50

Figure 23: Nishibayashi's chiral pseudorotaxane ligand

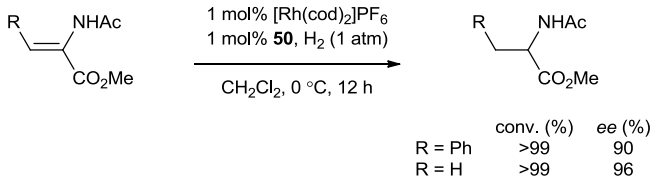

Figure 24: Scheme for and select examples of enantioselective hydrogenation using rotaxane 50

Ogoshi and co-workers demonstrated the synthesis of planar chiral [2]- and [3]rotaxanes through the threading of pillar[5]arenes followed by a CuAAC capping reaction.[26] Pillar[5]arenes are a cyclic pentamer, first reported by Ogoshi in 2008, and are themselves planar chiral.[27] They are able to form a number of conformations, but as the five units in the pentamer are able to freely rotate at 25 °C it is not possible to isolate these different conformations. However, they showed that by threading the cavity of the pillar[5]arene it is possible to prevent isomerisation of the conformers which results in the formation of two enantiomeric forms of the product rotaxane (Figure 25).

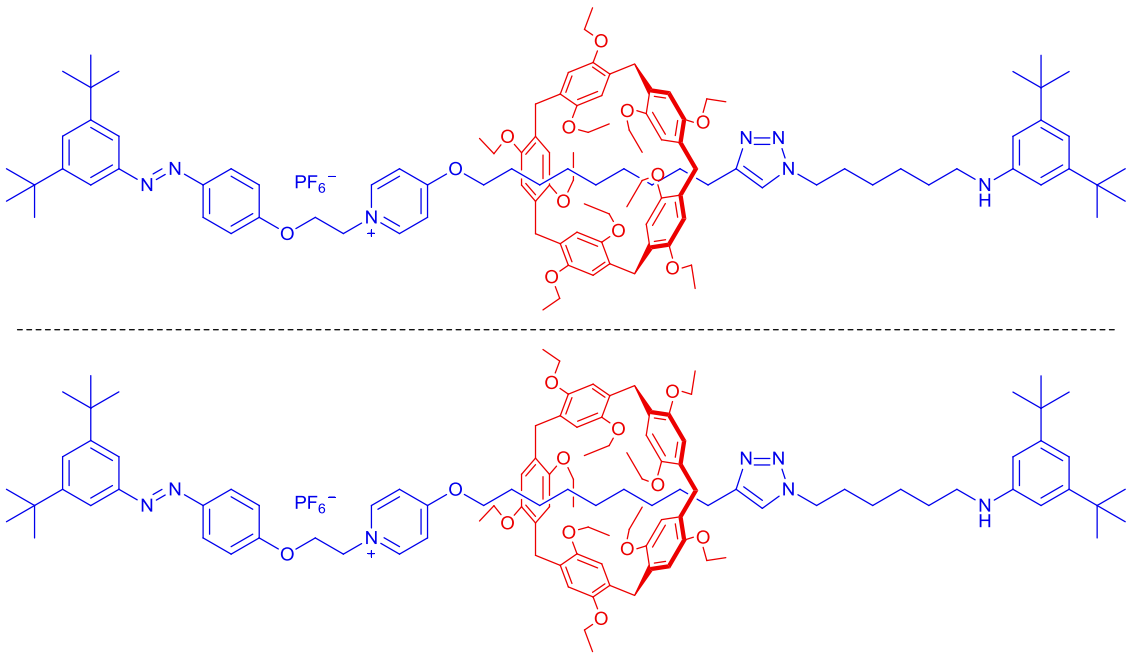

51

Figure 25: Ogoshi's enantiomeric pillar[5]arene based [2]rotaxane

1.3.3 – Mechanical chirality

Mechanically interlocked architectures can exist as stereoisomers, even without possessing a classic stereogenic element. Their chirality may arise purely from the relative orientation of their component(s). For example, as molecular trefoil knot (a single component MIA) can exist in two enantiomeric forms (**i**, Figure 26). Similarly, MIAs comprised of two or more components which are themselves achiral can exist as two enantiomers when interlocked, as was first noted for catenanes by Wasserman in 1961, and for rotaxanes by Schill in 1971.[28,29] Therefore, [2]catenanes exist as enantiomers if their two components are both rotationally unsymmetric (**ii**, Figure 26), and by extension polycatenanes may possess several centres of mechanical chirality if each ring is rotationally unsymmetric.

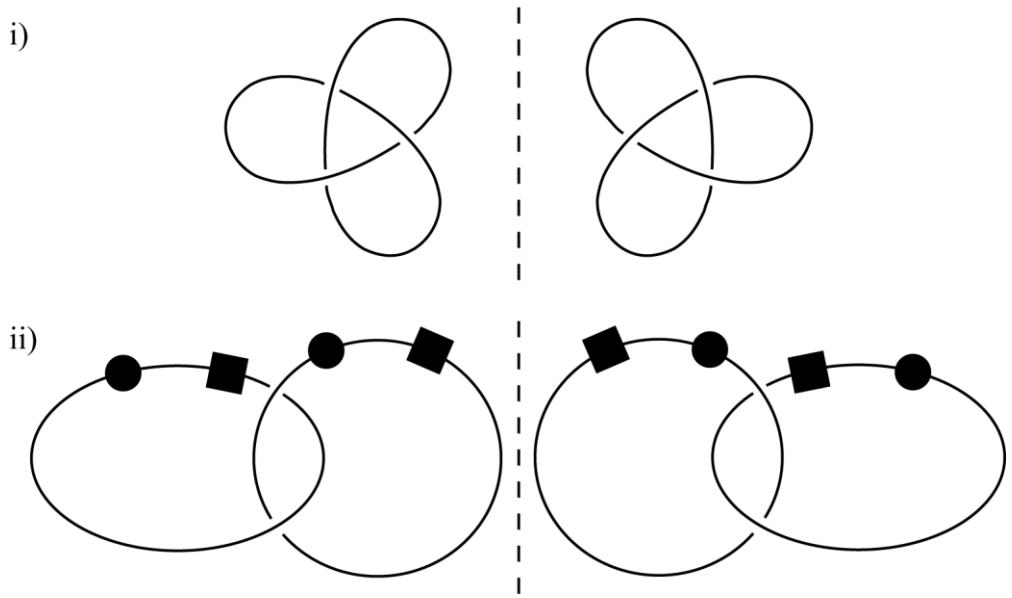

Figure 26: Examples of mechanically interlocked architectures, showing; i) enantiomers of a trefoil knot, and ii) enantiomers of a [2]catenane

The same logic applies to rotaxanes; a rotaxane comprised of a translationally asymmetric thread and a rotationally asymmetric macrocycle can be combined in two configurations which are enantiomers of each other. These rotaxanes are described as being mechanically planar-chiral.

1.4 – Mechanically planar-chiral rotaxanes

1.4.1 – Requirements for mechanical planar chirality

A rotaxane is chiral when a translationally asymmetric thread is interlocked with a rotationally asymmetric macrocycle (Figure 27). We describe these systems as being mechanically planar-chiral as the asymmetry of the molecule arises purely due to the configuration of the mechanical bond.

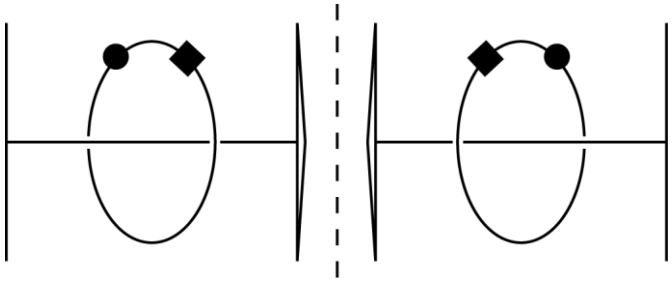

Figure 27: Two enantiomers of a mechanically planar chiral [2]rotaxane

The addition of further rotationally asymmetric macrocycles allows for more complex molecular configurations, each additional macrocycle forming a new stereogenic element due to its mechanical bond with the thread. Rotaxanes with two or more rotationally asymmetric macrocyclic components on an asymmetric thread can exist as diastereomers (Figure 28, shown with stereochemical assignment).

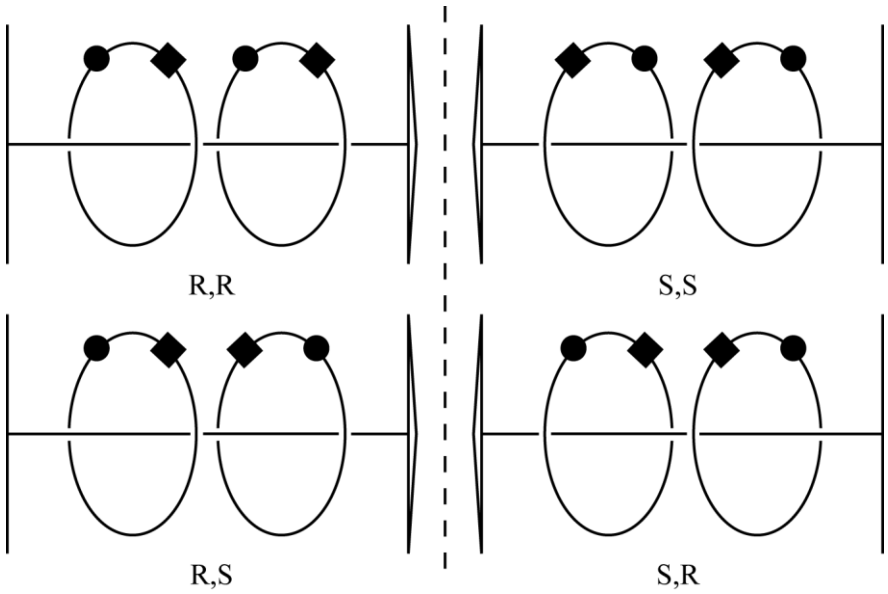

Figure 28: The four possible configurations of a mechanically planar chiral [3]rotaxane.

The relationship between the pair R,R and S,S, and the pair R,S and S,R is that they are pairs of enantiomers. Similarly, the relationship between the pairs R,R and R,S, and the pair S,S and S,R is that they are pairs of diastereomers.

In systems with two or more macrocyclic components it is possible for stereoisomers of a rotaxane to exist, in which the relative orientation of rotationally asymmetric macrocycles *on a symmetric thread* define the stereochemistry arising from the mechanical bonds. Therefore, threading two rotationally unsymmetric macrocycles with a symmetric thread allows for the formation of a pair of enantiomeric rotaxanes, as well as the meso isomer (Figure 29).

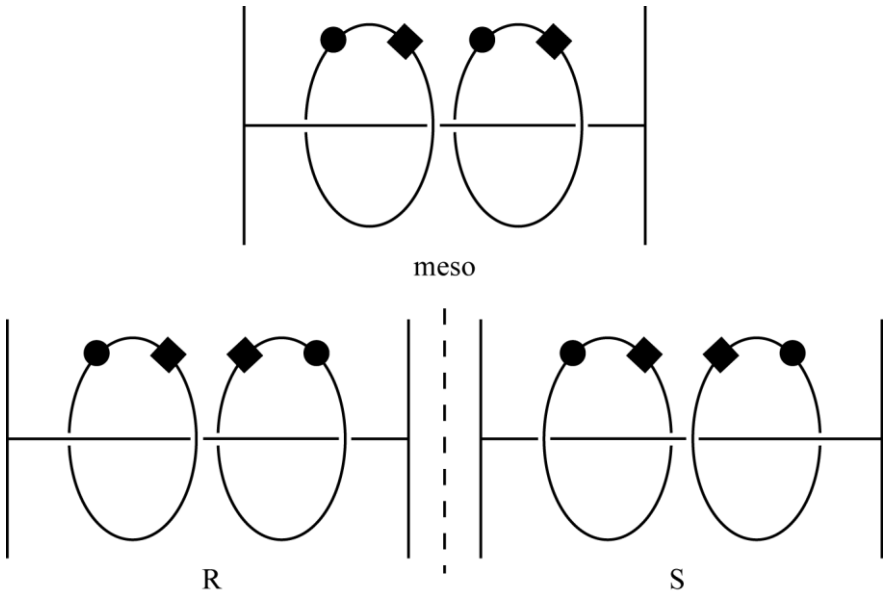

Figure 29: A representation of a mechanically chiral [3]rotaxane consisting of two rotationally asymmetric macrocycles on a symmetric thread.

1.4.1 – Syntheses of mechanically planar chiral rotaxanes.

There are few published examples of mechanically planar chiral rotaxanes in the literature, the prominent ones are discussed below.

The first synthesis and separation of the mechanically planar chiral [2]rotaxane was published by Vögtle in 1997.[30] In this paper he described the synthesis of a racemic mixture of a "cycloenantiomeric" [2]rotaxane (**52**), which was subsequently separated by chiral stationary phase (CSP) HPLC (Figure 30). The term "cyclochiral" was first proposed by Schill, but more correctly refers to the study of rotationally asymmetric cyclic molecules displaying multiple

instances of asymmetry around the ring.[31] Instead we have adopted the planar chiral interpretation as proposed by Takata.[32]

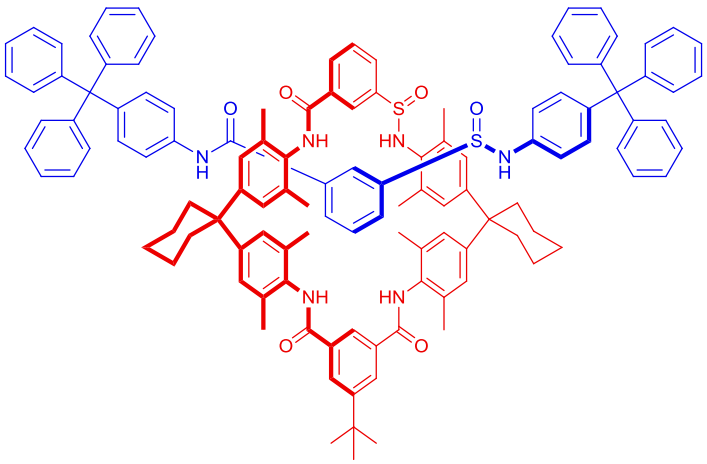

52

Figure 30: One enantiomer of Vögtle's mechanically chiral [2]rotaxane

Vögtle subsequently synthesised examples of mechanically planar chiral rotaxanes which consisted of two rotationally asymmetric macrocycles on a symmetric thread.[33] Partial success was had in separating the three compounds by CSP-HPLC. One enantiomer was isolated, the other eluted as a mixture with the meso-isomer.

Hiratani and co-workers developed a chiral sensor based on a mechanically chiral rotaxane (**54**).[34] A racemic rotaxane composed of an asymmetric thread and an asymmetric macrocycle selectively formed a diastereomer with L-phenylalaninol (**53**, Figure 31). This is *chiral resolution*. The diastereomer and the unbound rotaxane were distinguishable by UV-vis spectroscopy, showing that chiral recognition is possible with mechanically planar chiral rotaxanes. It was proposed that interactions between rotaxanes and chiral molecules may be used in the directional control of molecular motion in similar systems. The enantiomers of the rotaxane were separated by CSP-HPLC.

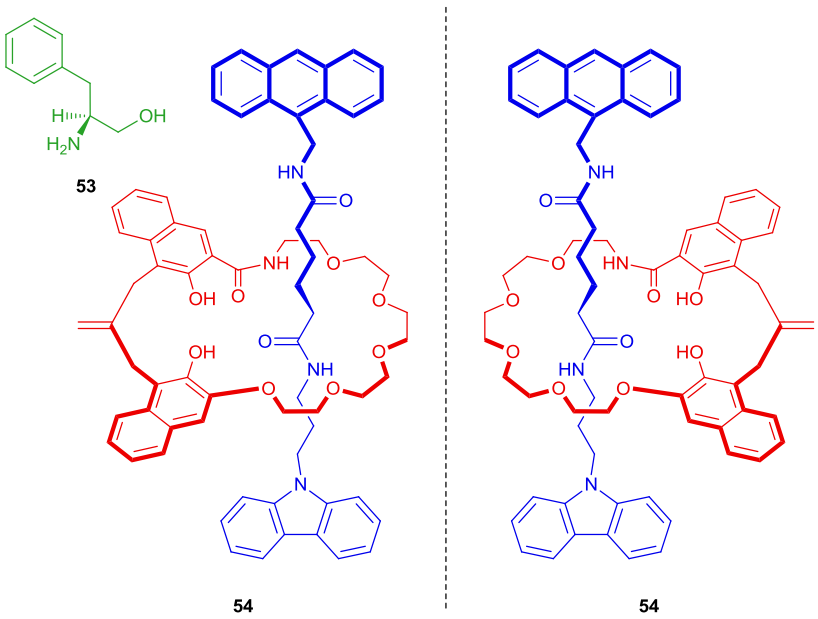

Figure 31: Hiratani's mechanically chiral rotaxane forms a diastereomeric complex with L-phenylalaninol

Lacour reported an attempt towards a diastereoselective synthesis of a mechanically chiral pseudo- rotaxane.[35] This approach relied on the idea of inducing selectivity through matched and mis-matched orientations of a macrocycle and a helicene stopper. Unfortunately the selectivity of the reaction was low and only gave a de of ~8%. As the pseudo-rotaxane was not mechanically bonded it was not possible to separate the two isomers (Figure 32).

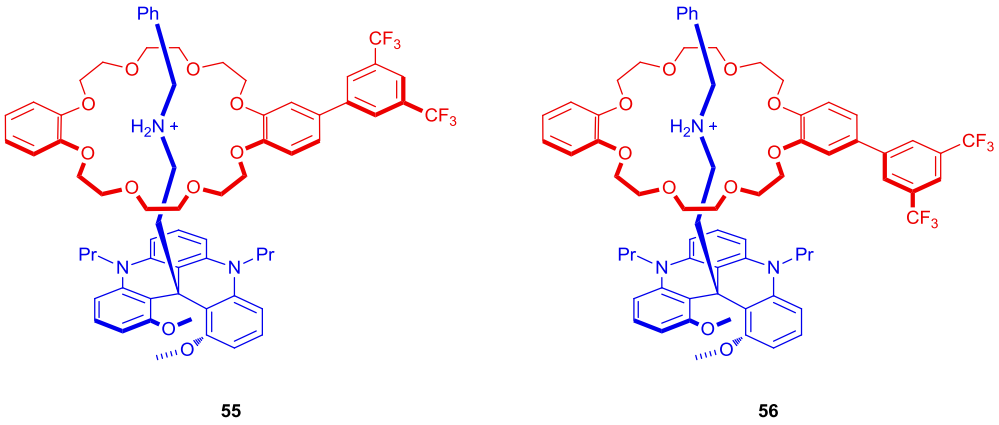

Figure 32: Lacour's diastereomeric synthesis of mechanically planar chiral pseudo-[2]rotaxanes

In 2007, Takata and co-workers published an attempted catalytic asymmetric synthesis of a planar chiral rotaxane sensor, the synthesis of which utilised a chiral trialkylphosphane catalyst in an end-capping acylation reaction of a pseudo-rotaxane.[32] Pleasingly they were able to synthesise the rotaxane (**60**) in a 4% ee in the first demonstration of a catalytic asymmetric

synthesis of a planar chiral rotaxane (Figure 33). However, the mixture of enantiomers still required separation by CSP-HPLC.

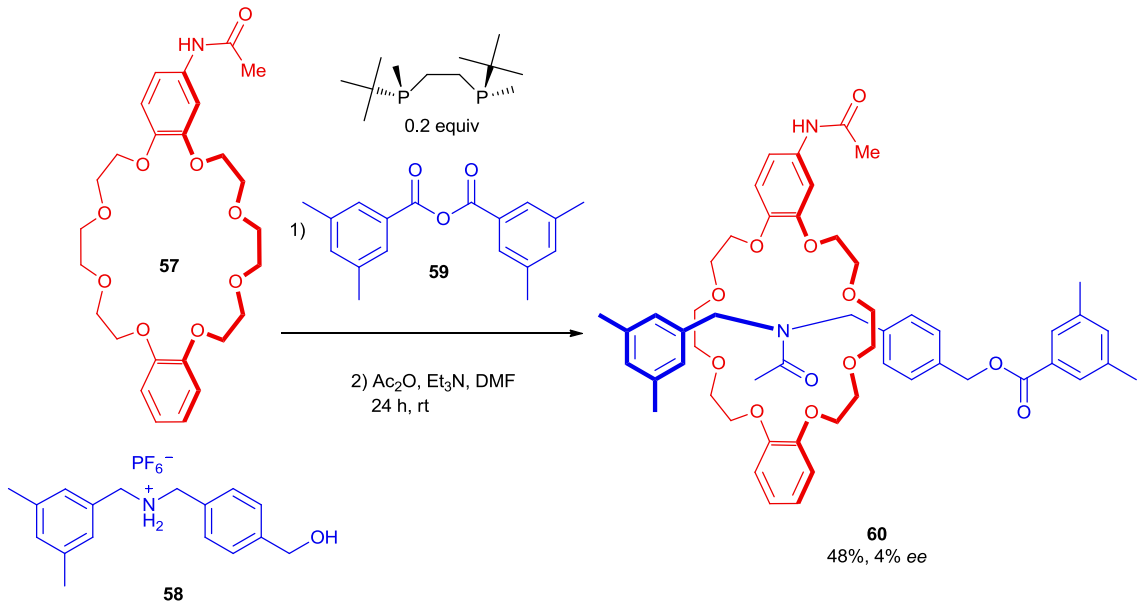

Figure 33: Makita's enantioselective synthesis of a mechanically planar chiral [2] rotaxane

Lee and co-workers subsequently attempted the synthesis of mechanically planar chiral rotaxanes by employing a chiral bis-oxazoline (Box) derived macrocycle (**62**) in a series of active template reactions.[36] Despite extensive optimisation of the reaction conditions they were unable to synthesise the target rotaxanes (including **64**) in all but a trace yield (Figure 34). Lee and co-workers suggested that excessive flexibility in the macrocycle allowed for transannular thread forming reactions to out-compete the mechanical bond forming reaction, and that increasing the rigidity of the macrocycle may have increased the yield of the rotaxanation.

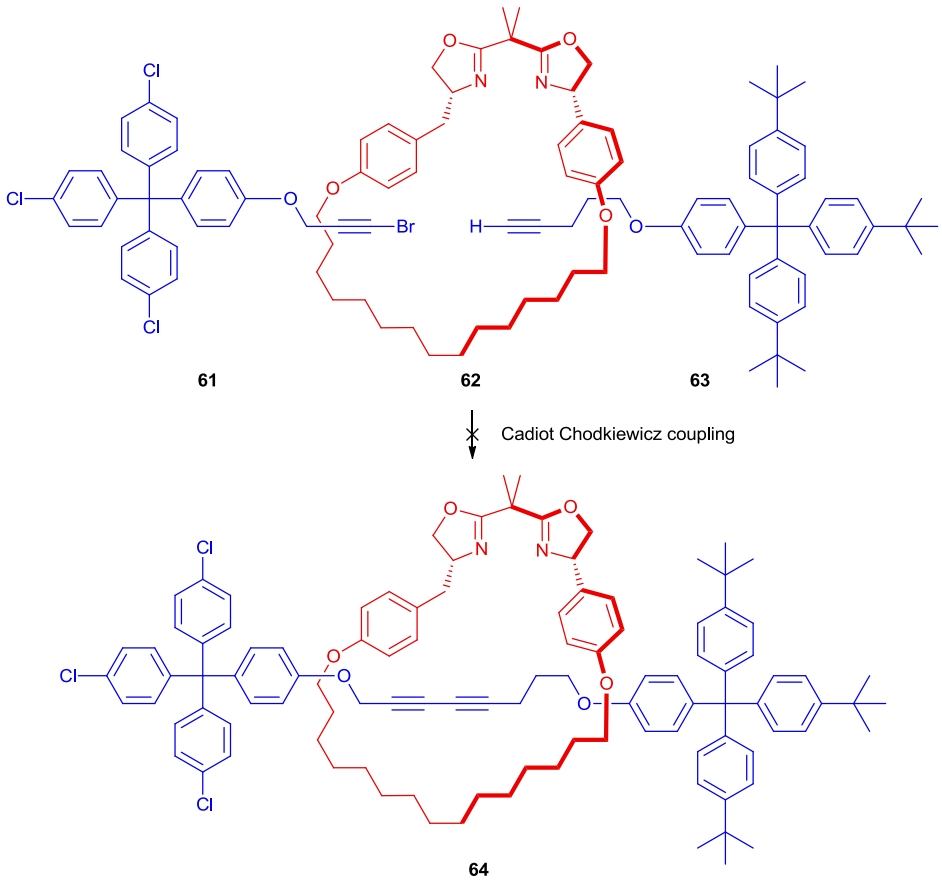

Figure 34: Lee and co-workers's attempted synthesis of a mechanically planar chiral [2]rotaxane using a C1-symmetric Box macrocycle

1.5 – Concluding remarks

At the time of the project's inception it was clear that there was room for improvement in the synthesis of mechanically planar chiral rotaxanes. Despite the attempts of the community it had not been possible to isolate a mechanically planar chiral rotaxane in an enantiopure form without resorting to CSP-HPLC. We proposed a chiral auxiliary approach in which mixed mechanically and covalently chiral rotaxane diastereomers are separated using standard techniques, and the covalent source of chirality subsequently removed. Mixed mechanically and covalently chiral systems have been made but not separated. The reactions used previously to synthesise mechanically planar-chiral rotaxanes were poor in selectivity and we thought a new approach might be needed.

By building on the small macrocycle work of Goldup and co-workers we hoped to be able to facilitate the synthesis of these compounds, as small sterically crowded systems are expected to offer advantages in separation compared to the previously synthesised systems which are less congested. This would therefore allow for easier access to these compounds and therefore investigation of this novel class of materials.

1.6 – References

[1] Frisch, H. L.; Wasserman, E. *J. Am. Chem. Soc.* **1961**, *83*, 3789.

[2] Harrison, I. T.; Harrison, S. *J. Am. Chem. Soc.* **1967**, *89*, 5723.

[3] Schill, G.; Lüttringhaus, A. *Angew. Chemie Int. Ed. English* **1964**, *3*, 546.

[4] Dietrich-Buchecker, C.; Sauvage, J.; Kintzinger, J. *Tetrahedron Lett.* **1983**, *24*, 5095.

[5] Wu, C.; Lecavalier, P. R.; Shen, Y. X.; Gibson, H. W. *Chem. Mater.* **1991**, *3*, 569.

[6] Hogg, L.; Leigh, D. A.; Lusby, P. J.; Morelli, A.; Parsons, S.; Wong, J. K. Y. *Angew. Chem - Int. Ed.* **2004**, *43*, 1218.

[7] Fuller, A. M.; Leigh, D. A.; Lusby, P. J.; Oswald, I. D. H.; Parsons, S.; Walker, D. B. *Angew. Chem - Int. Ed.* **2004**, *43*, 3914.

[8] Ashton, P. R.; Brown, C. L.; Chrystal, E. J. T.; Parry, K. P.; Pietraszkiewicz, M.; Spencer, N.; Stoddart, J. F. *Angew. Chem. Int. Ed.* **1991**, *30*, 1042.

[9] Anelli, P. L.; Ashton, P. R.; Spencer, N.; Slawin, A. M. Z.; Stoddart, J. F.; Williams, D. J. *Angew. Chem. Int. Ed.* **1991**, *30*, 1036.

[10] Ashton, P. R.; Grognuz, M.; Slawin, A. M. Z.; Fraser Stoddart, J.; Williams, D. J. *Tetrahedron Lett.* **1991**, *32*, 6235.

[11] Martínez-Díaz, M.-V.; Spencer, N.; Stoddart, J. F. *Angew. Chem. Int. Ed. English* **1997**, *36*, 1904.

[12] Cantrill, S. J.; Rowan, S. J.; Stoddart, J. F. *Org. Lett.* **1999**, *1* (9), 1363.

[13] Aucagne, V.; Hänni, K. D.; Leigh, D. A.; Lusby, P. J.; Walker, D. B. *J. Am. Chem. Soc.* **2006**, *128*, 2186.

[14] Berná, J.; Crowley, J. D.; Goldup, S. M.; Hänni, K. D.; Lee, A. L.; Leigh, D. A. *Angew. Chem. Int. Ed.* **2007**, *46*, 5709.

[15] Goldup, S. M.; Leigh, D. A.; Long, T.; McGonigal, P. R.; Symes, M. D.; Wu, J. *J. Am. Chem. Soc.* **2009**, *131*, 15924.

[16] Langton, M. J.; Matichak, J. D.; Thompson, A. L.; Anderson, H. L. *Chem. Sci.* **2011**, *2*, 1897.

[17] Goldup, S. M.; Leigh, D. A.; McGonigal, P. R.; Ronaldson, V. E.; Slawin, A. M. Z. *J. Am. Chem. Soc.* **2010**, *132*, 315.

[18] Aucagne, V.; Berná, J.; Crowley, J. D.; Goldup, S. M.; Hänni, K. D.; Leigh, D. A.; Lusby, P. J.; Ronaldson, V. E.; Slawin, A. M. Z.; Viterisi, A.; Walker, D. B. *J. Am. Chem. Soc.* **2007**, *129*, 11950.

[19] Barran, P. E.; Cole, H. L.; Goldup, S. M.; Leigh, D. A.; McGonigal, P. R.; Symes, M. D.; Wu, J.; Zengerle, M. *Angew. Chem. Int. Ed.* **2011**, *50*, 12280.

[20] Lahlali, H.; Jobe, K.; Watkinson, M.; Goldup, S. M. *Angew. Chem. Int. Ed.* **2011**, *50*, 4151.

[21] Ruble, J. C.; Latham, H. a.; Fu, G. C. *J. Am. Chem. Soc.* **1997**, *119*, 1492.

[22] Asakawa, M.; Brancato, G.; Fanti, M.; Leigh, D. A.; Shimizu, T.; Slawin, A. M. Z.; Wong, J. K. Y.; Zerbetto, F.; Zhang, S. *J. Am. Chem. Soc.* **2002**, *124*, 2939.

[23] Bottari, G.; Leigh, D. A.; Pérez, E. M. *J. Am. Chem. Soc.* **2003**, *125*, 13360.

[24] Blanco, V.; Leigh, D. A.; Marcos, V.; Morales-Serna, J. a.; Nussbaumer, A. L. *J. Am. Chem. Soc.* **2014**, *136*, 4905.

[25] Hattori, G.; Hori, T.; Miyake, Y.; Nishibayashi, Y. *J. Am. Chem. Soc.* **2007**, *129*, 12930.

[26] Ogoshi, T.; Yamafuji, D.; Aoki, T.; Kitajima, K.; Yamagishi, T. A.; Hayashi, Y.; Kawauchi, S. *Chem. - A Eur. J.* **2012**, *18*, 7493.

[27] Ogoshi, T.; Kanai, S.; Fujinami, S.; Yamagishi, T. A.; Nakamoto, Y. *J. Am. Chem. Soc.* **2008**, *130*, 5022.

[28] Frisch, H. L.; Wasserman, E. **1961**, *83* (18), 3789.

[29] Schill, G. *Catenanes, Rotaxanes and Knots*; Academic Press: New York, **1971**.

[30] Yamamoto, C.; Okamoto, Y.; Schmidt, T.; Jager, R.; Vogtle, F. *J. Am. Chem. Soc.* **1997**, *119*, 10547.

[31] Eliel, E.; Wilen, S.; Mander, L. *Stereochemistry of Organic Compounds*; John Wiley and Sons: New York, 1994.

[32] Makita, Y.; Kihara, N.; Nakakoji, N.; Takata, T.; Inagaki, S.; Yamamoto, C.; Okamoto, Y. *Chem. Lett.* **2007**, *36*, 162.

[33] Schmieder, R.; Hübner, G.; Seel, C.; Vögtle, F. *Angew. Chemie - Int. Ed.* **1999**, *38*, 3528.

[34] Kameta, N.; Nagawa, Y.; Karikomi, M.; Hiratani, K. *Chem. Commun. (Camb).* **2006**, 3714.

[35] Mobian, P.; Banerji, N.; Bernardinelli, G.; Lacour, J. *Org. Biomol. Chem.* **2006**, *4*, 224.

[36] Glen, P. E.; O'Neill, J. a T.; Lee, A. L. *Tetrahedron* **2013**, *69*, 57.

Chapter 2 – Synthesis of mechanically planar-chiral [2]rotaxanes

2.1 – Introduction

In their 2011 paper, Goldup and co-workers found that a small chiral half-thread desymmetrised the macrocycle of the parent rotaxane (**65**).[20] It appeared that efficient chiral information transfer between the two rotaxane components was possible, and this initial observation that chiral information can be transferred between two mechanically interlocked molecules yielded a vital clue as to how to approach the synthesis of mechanically planar rotaxanes. The strong induction of asymmetry into the symmetric macrocycle inspired us to develop a system in which this attribute of small mechanically interlocked molecules would allow us to synthesise (and isolate) mechanically chiral isomers of a [2]rotaxane.

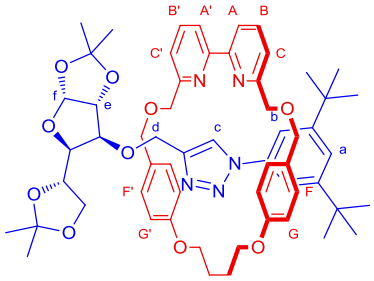

65

Figure 35: Goldup's small sterically congested rotaxane

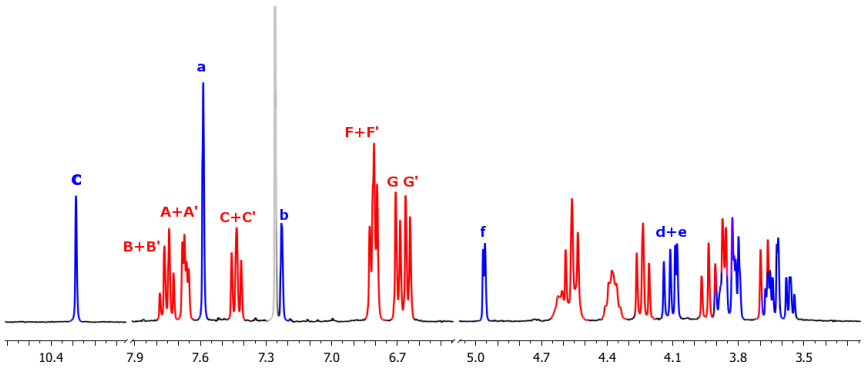

Figure 36: Sections of the ^{1}H NMR plot of rotaxane 65 with selected atom labels (axis shows δ ppm)

Based on the knowledge that the combination of a rotationally unsymmetric macrocycle and a chiral thread would form a pair of diastereoisomeric [2]rotaxanes we propose that inclusion of a cleavable chiral moiety in the thread would allow for the subsequent displacement of the chiral unit. We describe this as a chiral-auxiliary approach to the synthesis of mechanically planar-chiral rotaxanes. Separation of the diastereomers and subsequent replacement the chiral unit with an achiral substitute then furnishes us with separate enantiomers of a mechanically planar chiral rotaxane, without resorting to CSP-HPLC methods during isolation (Figure 37).

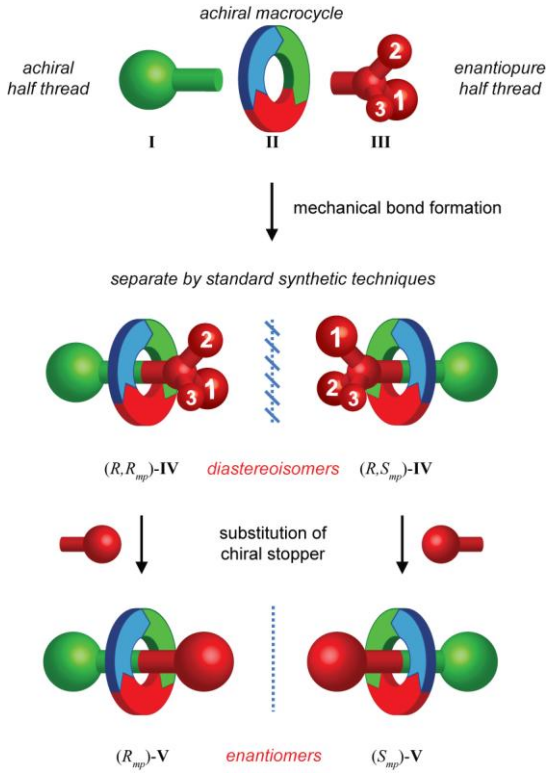

Figure 37: Scheme for the proposed synthesis of enantiopure mechanically chiral [2]rotaxanes

The high yielding AT-CuAAC rotaxanation method developed by Goldup and co-workers provides a robust route for the synthesis of these small, sterically congested and chiral systems and should enable us to synthesise our target diastereomers in good yields. In order to synthesise the diastereomers we first need to synthesise both a cleavable chiral half-thread and a rotationally asymmetrical macrocycle. The thread of the rotaxane must be translationally asymmetric, and while the triazole moiety of the thread satisfies this condition, we propose that two end groups with different functionality exaggerate this property which may aid in the separation of the diastereomers.

It seemed unlikely that our initial reaction conditions would be selective for one diastereomer, as such our ability to separate these diastereomers is important if we want to avoid using CSP-HPLC at any stage. However, we were confident that a suitable combination of macrocycle and chiral auxiliary would allow for the separation of the diastereomers. Our motive for avoiding CSP-HPLC for separation is that in order to investigate the properties of these materials, a scalable procedure is required. Separation by normal-phase column chromatography is therefore desirable as it allows for the synthesis and separation of these targets on a large scale.

The cleavage of the chiral auxiliary is one of the last important steps in the synthesis, and therefore a labile chiral group must be included in the thread. The reactivity of the cleavable

unit may be altered by the presence of the macrocycle and so it may be that we have to probe the conditions of the cleavage reaction.

2.2 – Results and discussion

As reported by Goldup and co-workers a ‘small’ rotaxane was shown to exhibit strong chiral information transfer from a centrochiral thread into the macrocycle, which was observed as desymmetrisation of signals in the ^{1}H NMR spectra. We concluded that modification of this basic structure should serve as the basis for further investigation into mechanically chiral rotaxanes (Figure 38).

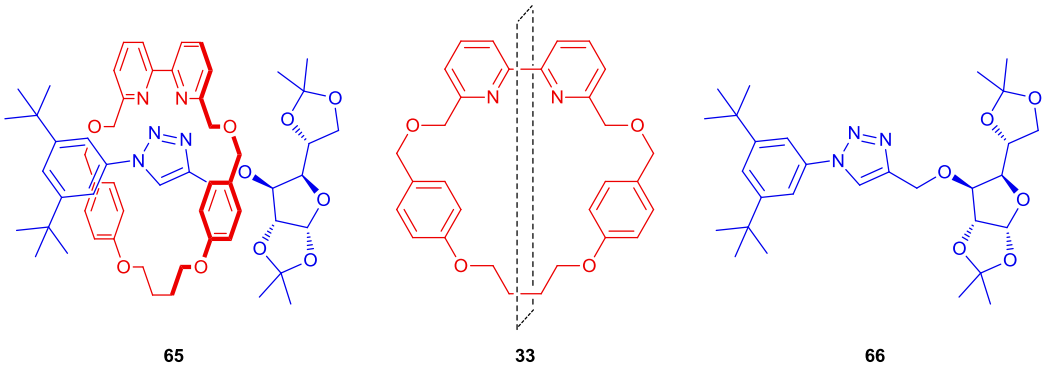

Figure 38: Structures of rotaxane 65, and its two components (33 and 66). The plane of symmetry perpendicular to the plane of macrocycle 33 is marked with a dotted line

In order to generate a mechanically diastereomeric rotaxane through modification of this design it was necessary to remove the plane of symmetry bisecting the macrocycle through the bipyridine group perpendicular to the plane of the macrocycle (as shown in Figure 38). Any new macrocycle needed to be structurally similar to **33** as we wanted to closely mimic the chemical properties of this macrocycle. The 2,2’-bipyridine moiety was necessary as it is the centrepoint for the high yielding CuAAC-AT mechanical bond forming reaction we planned to exploit.

Thus, we proposed that any new macrocycle must, (a) contain a 2,2’-bipyridine moiety, (b) be approximately the same ring size as **33**, and (c) be synthetically accessible in a chemically useful number of steps. We predicted that if the macrocycle was approximately the same size we could expect it to behave in a similar manner to **33**, allowing for high yielding rotaxanation reactions. We defined the ring size by counting the number of atoms around the inside of the macrocycle; in the case of **33** there are 26 atoms around the inside of the ring. Macrocycle **33** is

accessible in good yield in 7 steps from commercial reagents and by following a similar synthetic sequence we predicted that a new macrocycle would also be obtained in a good yield.

2.2.1 – 1st generation macrocycle

Based on the synthetic route to **33** we envisioned exchanging the order of functionality in the ring to generate a new species, macrocycle **67** (as shown in Figure 39). The three atoms in the 'arm' of the macrocycle (in green) were moved into the alkyl chain (in red) at the bottom of the macrocycle, while replacing the extra oxygen atom with carbon for synthetic ease. The flanking aromatic on this side (in blue) was then directly attached to the pyridine.

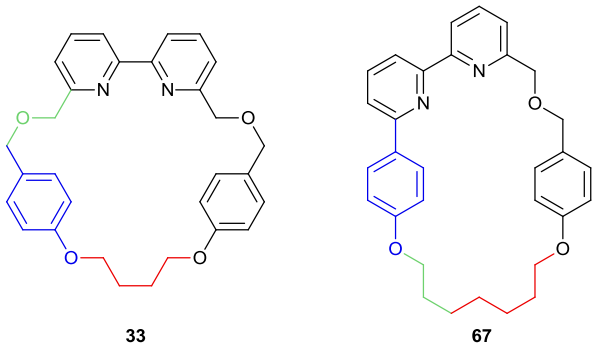

Figure 39: Goldup and co-workers original macrocycle (33) and the modified macrocycle (67)

We expected this macrocycle to behave in a similar manner to **33** although we had concerns about how the steric bulk of the flanking aromatic ring might affect the ability of the bipyridine to bind to Cu(I).

2.2.1.1 – Retrosynthesis of macrocycle 67

A retrosynthesis of macrocycle **67** was carried out which follows an analogous route to the original synthesis of macrocycle **33** (Figure 40). Following this route would require bisphenol **69** which could be synthesised from the allyl-protected precursor **69**. Retrosynthesis of **69** via cleavage of the bipyridine gives two bromopyridine species, **70** and **71**.

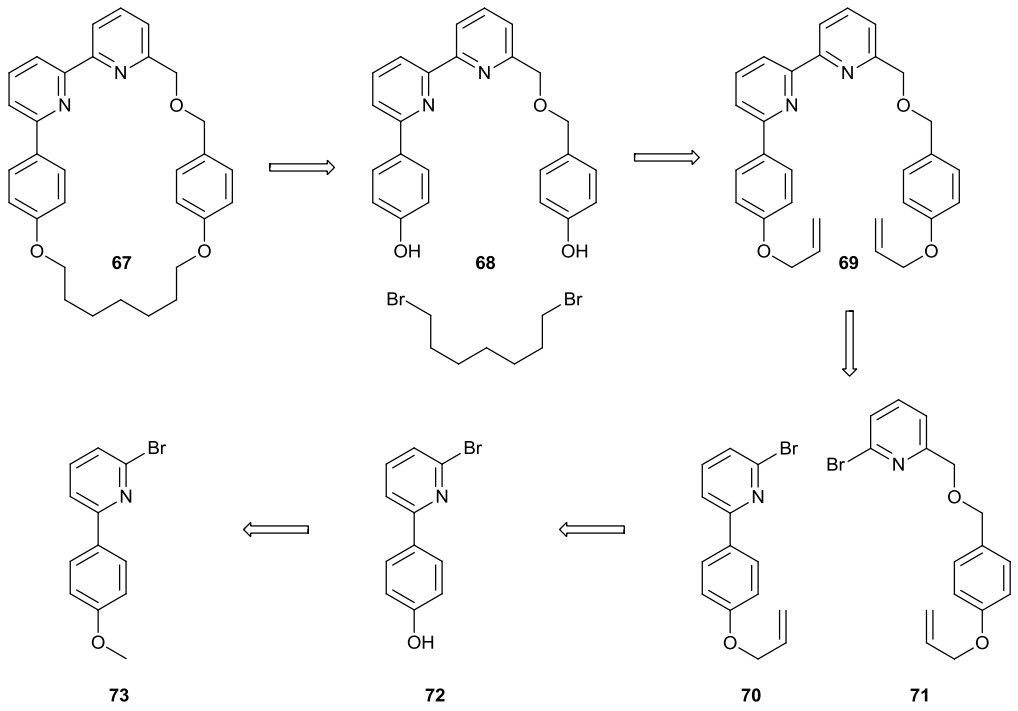

Figure 40: Retrosynthesis of asymmetric macrocycle 67

Unlike the synthesis of **33** in which a nickel-mediated dimerization of **71** was utilised to synthesise an allyl-protected macrocycle precursor we now needed to couple together two different 'halves' of a macrocycle precursor. The nickel-mediated aryl-aryl coupling of **70** and **71** would theoretically only produce a statistical mixture of products and therefore a maximum 50% yield of the target compound **69** (Figure 41). To counter this, we instead investigated cross-coupling reactions.

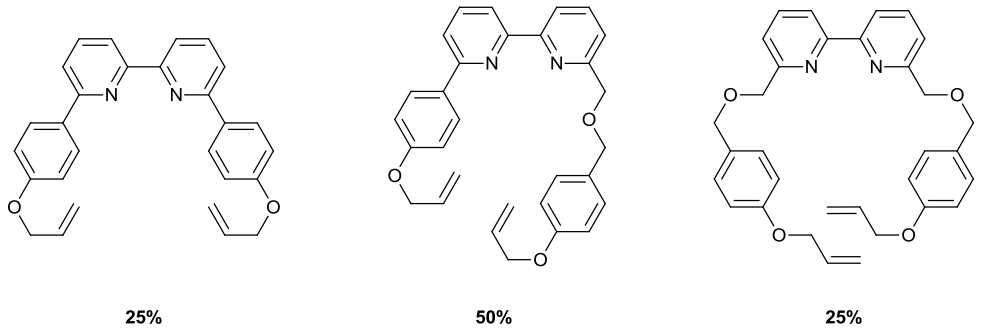

Figure 41: Theoretical statistical distribution of the products of a nickel mediated coupling of two bromo-pyridine macrocycle precursors, 70 and 71

At this time it became apparent that the choice of the allyl protecting group caused us some difficulty. Attempts at performing a palladium-mediated cross-coupling resulted in cleavage of the allyl-protecting group under the reaction conditions which subsequently interfered with the reaction through allylation of the pyridine.

We proposed that we could improve the synthesis of the macrocycle by making a minor modification to the structure.

2.2.2 – 2nd generation macrocycle

Substitution of the remaining benzylic-ether oxygen atom in macrocycle **67** with a carbon atom should improve the stability of the intermediate compounds and allow for a simplified protecting group strategy to be employed (Figure 42).

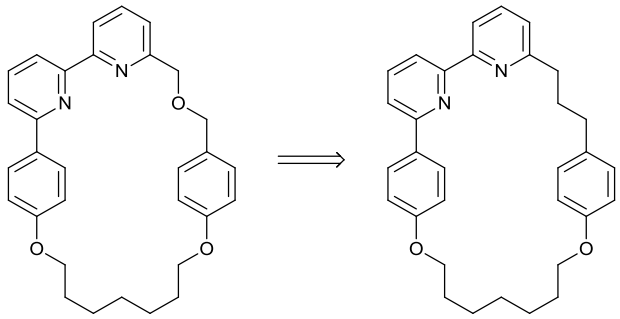

67 **74**

Figure 42: 1st generation target macrocycle 68 and new target macrocycle 74

A retrosynthesis of macrocycle **74** gave a different bromopyridine intermediate (**77**, Figure 43). Similarly to arylpyridine **73**, alkylpyridine **77** incorporates a methylether as a masked phenol and should be readily accessible from commerically available materials. Coupling of compounds **73** and **77** would allow us to avoid using allyl protecting groups and instead perform a double demethylation on bipyridine intermediate **76** to generate macrocycle precursor **75** (Figure 43). The synthesis of aryl-pyridine **73** is possible in one step from commercial reagents, and alkyl-pyridine **77** can be synthesised in two steps in a single one-pot reaction.

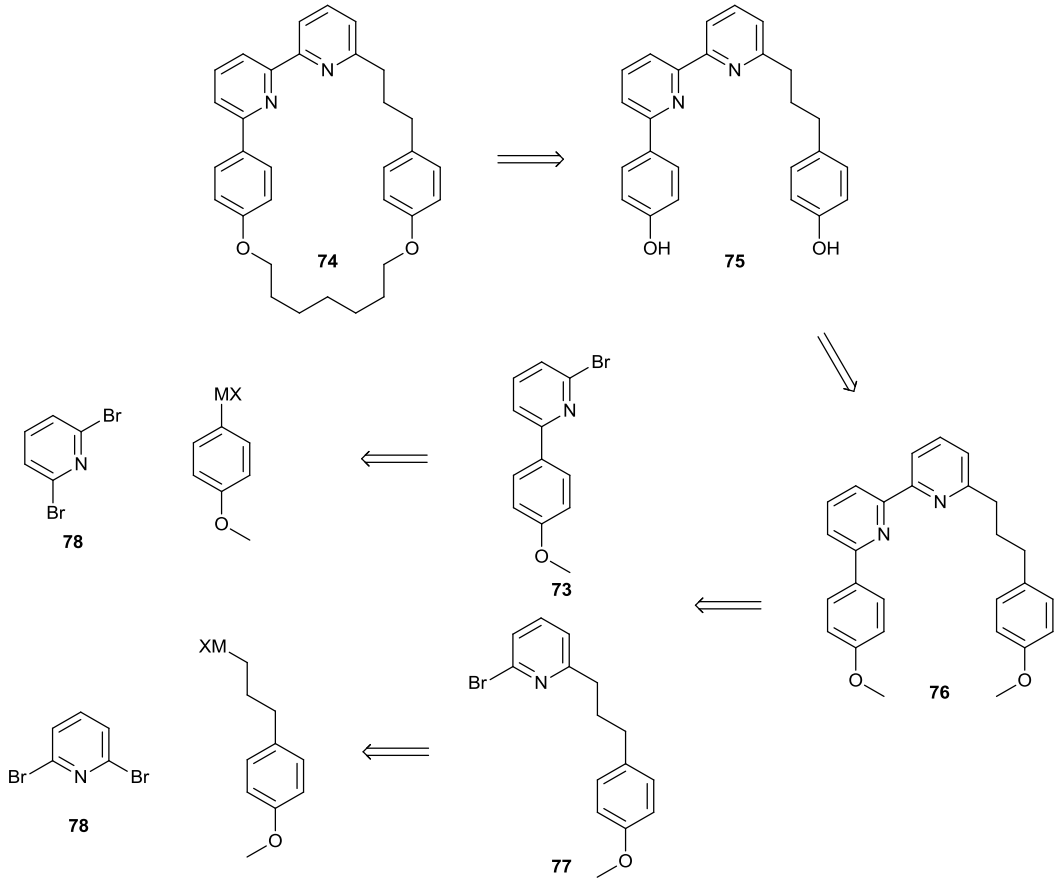

Figure 43: Retrosynthesis of macrocycle 74

2.2.2.1 – Synthesis of arylpyridine derivative 73

Initial synthesis of arylbromopyridine **73** was achieved through a Kumada coupling of 2,6-dibromopyridine (**78**) and (4-methoxyphenyl)magnesium bromide (**79**, Figure 44). Unfortunately this reaction also yielded a significant amount of biaryl **80** which was formed by the homocoupling of the Grignard reagent. We were able to separate this material via column chromatography but upon scale-up this purification quickly became undesirable as the reaction would often be run on ten or more grams of **78**. The subsequent chromatography therefore required large quantities of silica and solvent. Purification of bromopyridine **73** from this mixture was possible through recrystallisation but resulted in the loss of some product, reducing the yield from 56% (by NMR) to 33% isolated yield. The reaction also produced triaryl **81** in small quantities which could also be removed though crystallisation from diethyl ether.

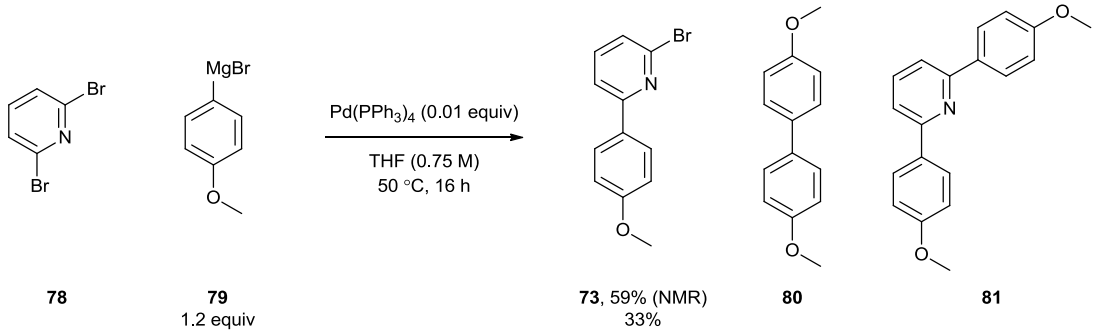

Figure 44: Synthesis of bromopyridine 73

To try and improve the synthesis of **73** we decided to instead try a Suzuki coupling reaction. We thought that relative stability of boronic acid **82** in comparison to the organometallic species would help with the purification, as the low solubility of any residual boronic acid in common organic solvents should improve the yields of recrystallization and would potentially allow us to avoid column chromatography at this step.

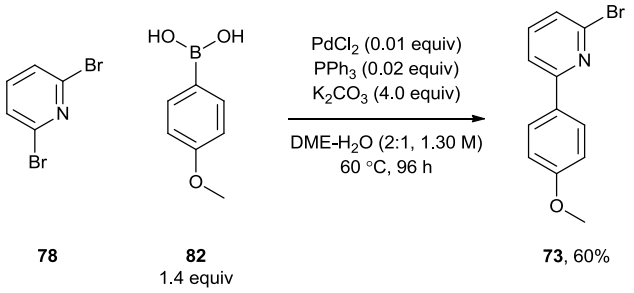

Figure 45: Alternative synthesis of bipyridine precursor 73

Pleasingly the reaction occurred smoothly in the presence of palladium (II) chloride and triphenylphosphine which also allowed us to avoid use of the more expensive tetrakis(triphenylphosphine)palladium(0) catalyst used previously. The procedure was simpler and the reaction conditions much less sensitive than those required for the Kumada coupling. The reaction could be conducted under air and then purged with nitrogen just before the solvent was added and the reaction initiated (Figure 45). Pleasingly, the cross-coupling was more efficient and reduced the amounts of biaryl **80** and triaryl **81** produced, which simplified the purification. Compound **73** was isolated in good yield (60%).

2.2.2.2 – Synthesis of alkylpyridine derivative 77

Alkylbromopyridine **77** was also synthesised via a Suzuki coupling reaction. Following the *in situ* hydroboration reaction of 1-allyl-4-methoxybenzene (**83**) with 9-borabicyclo[3.3.1]-nonane

(9-BBN) to form the trialkylborane (**84**), the borane was stirred with 2,6-dibromopyridine, potassium carbonate, palladium (II) chloride and triphenylphosphine, successfully producing compound **77** in good yield (73% over two steps) (Figure 46).

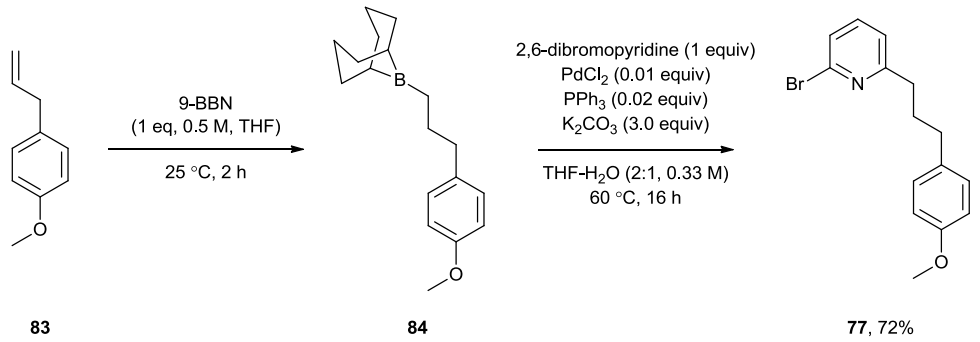

Figure 46: Synthesis of bromopyridine 77

The reaction also formed one equivalent of 9-borabicyclo[3.3.1]nonan-9-ol but attempts to separate this material via chromatography were unsuccessful. Acidification of crude **77** with a solution of HBr in methanol allowed us – on removal of methanol *in vacuo* – to triturate the viscous residue with petrol and ether enabling us to extract the 9-borabicyclo[3.3.1]nonan-9-ol, as well as any unreacted **83**. The residue from the trituration was then dissolved in dichloromethane and neutralised with sodium hydroxide allowing for the recovery of **77** in a 72% yield, which also eliminated the need for chromatography after this reaction sequence.

With the two half-macrocycle precursors (compounds **73** and **77**) in hand the next step was to find a suitable coupling reaction for the formation of the bipyridine.

2.2.2.3 – Synthesis of the protected macrocycle precursor 76

In preparation for a Kumada coupling, direct magnesiation of arylbromide **73** was attempted with ^{i}PrMgCl.LiCl in THF. Disappointingly the reaction gave less than 5% conversion at ambient temperatures over 16 hours as assessed by ^{1}H NMR. In parallel, lithiation of the arylbromide **73** and subsequent transmetallation to $ZnCl_2$ was attempted in preparation for a Negishi coupling. Lithiation with *n*-BuLi occurred smoothly at -78 °C in under an hour, and subsequent transmetallation to $ZnCl_2$ (as a 1 M solution in THF) was achieved within one further hour by allowing the reaction to warm to room temperature (Figure 47).

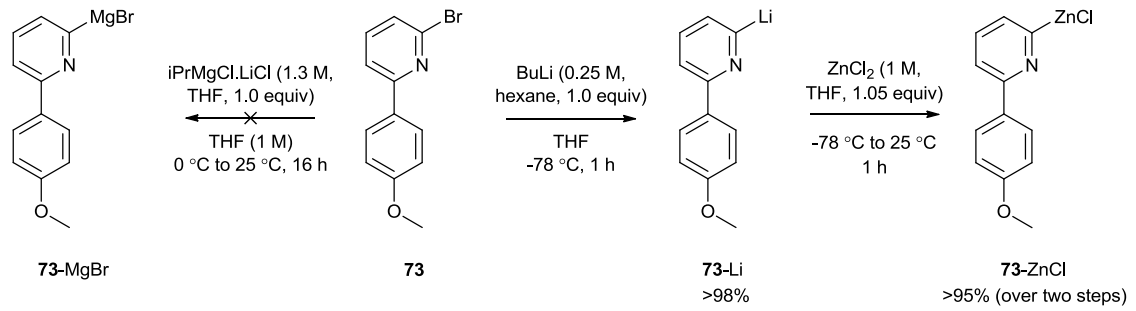

Figure 47: Metallation of arylpyridine 73

The success of each step of the metalation was quantified by quenching an aliquot of the reaction separately with MeOD and MeOH and analysing the ^{1}H NMR spectra of the resulting solutions. Typical conversion to the aryllithium species was greater than 99%, and the overall conversion to the organo-zinc species was greater than 95%.

Following a typical procedure for a Negishi coupling, the pre-formed organo-zinc species (**73**-ZnCl) was subsequently cannulated into a reaction vessel containing a stirred solution of the second coupling partner (bromopyridine **77**), palladium (II) chloride, and triphenylphosphine in THF. The reaction was heated at 60 °C and stirred for 6 hours. This reaction gave protected macrocycle precursor **76** in good yield (55%).

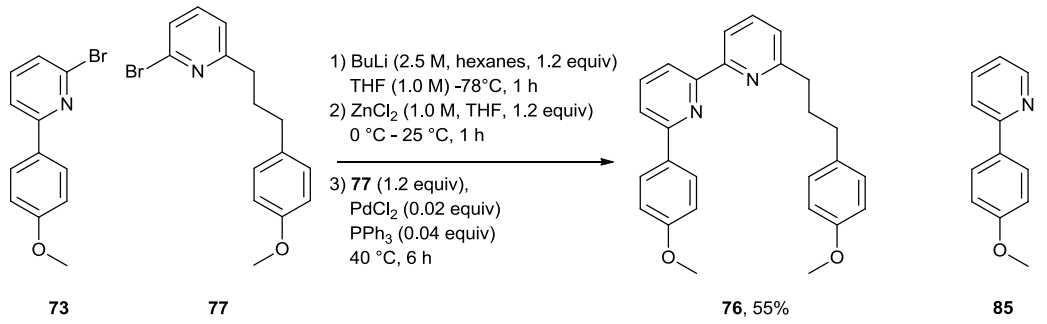

Figure 48: Synthesis of protected macrocycle precursor 76

We subsequently found that the reaction required 1.2 equivalents of **73**-ZnCl to ensure full conversion of pyridine **77** to precursor **76**. While initially isolated via column chromatography, we subsequently found that the protodehalogenated material left over from the quenching of **73**-ZnCl (compound **85**) could be extracted by refluxing the crude material in petrol and decanting the mother liquor. This removed the contaminant and allowed the product to be recrystallized from diethyl ether to give **76** in excellent purity and good yield.

2.2.2.4 – Demethylation of protected macrocycle precursor 76

Model reactions were run to assess the viability of the demethylation of compound **76** using bromopyridine **73** as an analogue (Figure 49).

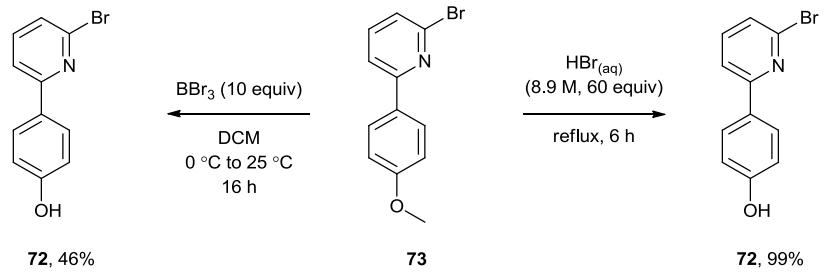

Figure 49: Deprotection of phenylmethylether 73

Initial attempts at the deprotection were undertaken with boron tribromide.[37] Despite literature precedent the reaction gave a low yield of the product which therefore required separation from the crude mixture. Methyl ether **73** was instead subjected to an alternative procedure with refluxing aqueous hydrogen bromide solution (55% w/w aq.). Pleasingly this gave the demethylated arylpyridine in quantitative yield. Following an identical procedure but using bis-methylether **76** gave the macrocycle precursor **75** in excellent yield (Figure 50). The material was recoverable either through an aqueous workup or could be isolated as the hydrogen bromide salt through evaporation of the reaction mixture.

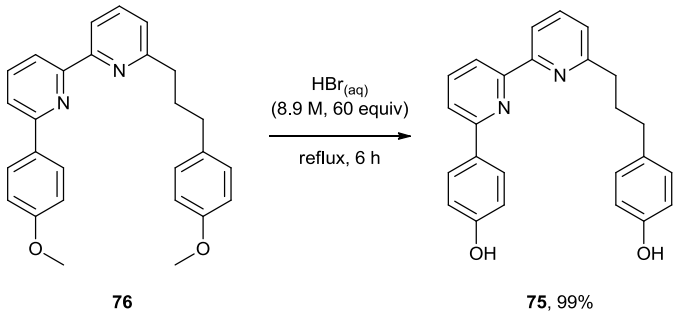

Figure 50: Deprotection of protected macrocycle intermediate 76

2.2.2.5 – Macrocyclisation of precursor 75

The macrocycle precursor **75** was subjected to a double Williamson-ether macrocyclisation reaction with 1,7-dibromoheptane (**86**) in DMF in the presence of potassium carbonate according to the group's previous macrocyclisation reactions (Figure 51).[20] The reaction was deemed complete after 72 hours on observation of the disappearance of the ^{1}H NMR signals

corresponding to the alkyl bromide. The crude macrocycle was isolated by removal of the DMF *in vacuo* followed by an aqueous workup of the residue to remove the potassium carbonate.

The crude ^{1}H NMR indicated approximately 10% conversion to a macrocyclic product, based on the integration of aromatic signals shifted to lower ppm and the shift to higher ppm of signals corresponding to the alkyl chain in the arm of the macrocycle. Initial attempts at purification via column chromatography were somewhat unsuccessful but latter attempts after modification of the gradient gave reasonable separation allowing isolation of the macrocycle in 5% yield. This is lower than that for macrocycle **33** (12%) but enabled us to isolate enough of macrocycle **74** such that we could use it in a rotaxanation reaction.

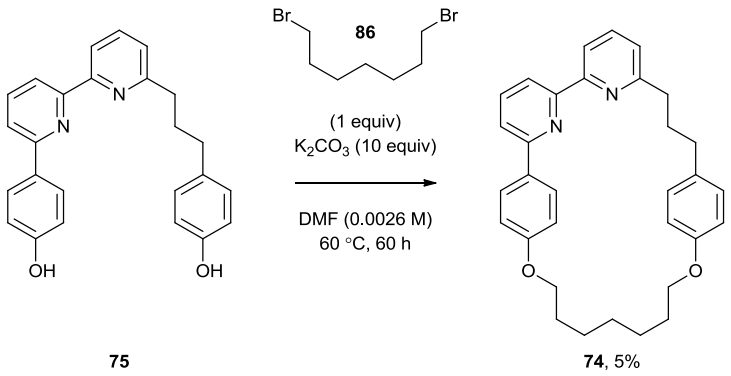

Figure 51: Synthesis of macrocycle 74

2.2.2.6 – AT-CuAAC rotaxanation with macrocycle 74

We carried out a simple test reaction with two half threads, 1-ethynyl-3,5-di-*tert*-butylbenzene (**34**) and 1-azido-3,5-di-*tert*-butylbenzene (**32**). Pleasingly, the reaction proceeded cleanly and in similar yields to the previously reported reactions with macrocycle **74**, the reaction giving rotaxane **87** in 40% yield (Figure 52).[20]

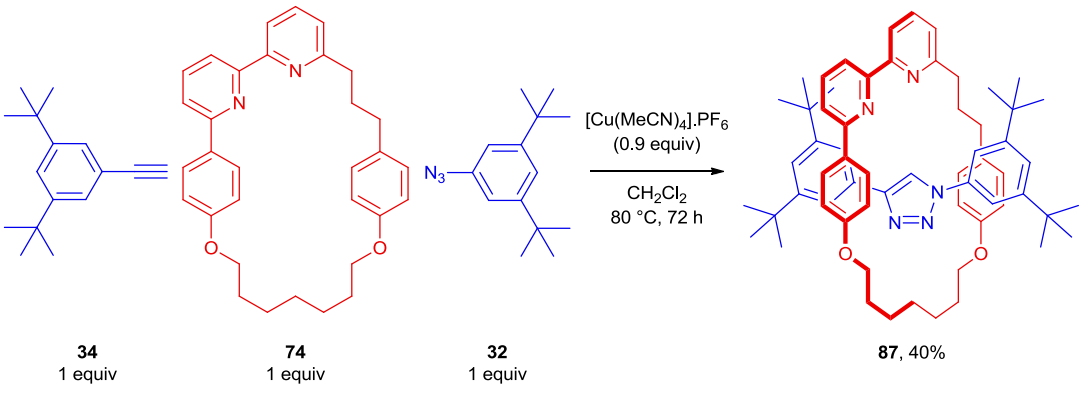

Figure 52: Synthesis of a rotaxane incorporating macrocycle 74

Having demonstrated the ability of the new macrocycle to undergo a rotaxane forming reaction we then were able to continue the project with the synthesis of the cleavable half-threads.

2.2.3 – Synthesis of a cleavable chiral half-thread

Having successfully synthesised a rotationally unsymmetrical macrocycle we then aimed to synthesise and isolate the first enantiopure mechanically planar chiral rotaxane using a chiral auxiliary approach. As previously proposed, we require a half-thread containing a cleavable chiral moiety that would then allow us to displace the chiral auxiliary and replace it with an achiral stopper. The displacement must be S_N2 in nature as removal of one stopper before the addition of its replacement would result in the potential dethreading of the macrocycle. By ensuring that the incoming stopper is added before the cleaving of the bulky chiral moiety we ensure the mechanical bond is maintained throughout the transformation.

2.2.3.1 – Half-thread structure

Taking our cue from the structure of rotaxane **65**, in which chiral information transfer between rotaxane components was observed by Goldup and co-workers,[20] we proposed to develop a cleavable chiral half-thread based on the 1,2:5,6-di-O-isopropylidene-α-D-glucofuranose (**92**) moiety of that rotaxane (Figure 53).

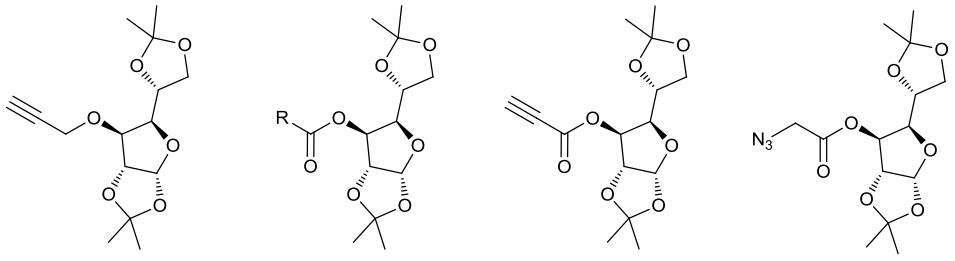

Figure 53: α-D-glucofuranose derived half-threads

We considered that as the point of cleavage should be stable under a variety of mild conditions, yet susceptible to a number of substitution reactions, that therefore that the addition of an ester group to the original thread would provide this functionality. The most obvious candidate to us was half-thread **89** as the product seemed accessible via a Steiglich esterification with the corresponding alkyne, dicyclohexylcarbodiimide and 4-dimethylaminopyridine (Figure 54).[38]

However, despite a number of attempts we were unable to synthesise the target compound, observing that no reaction was taking place.

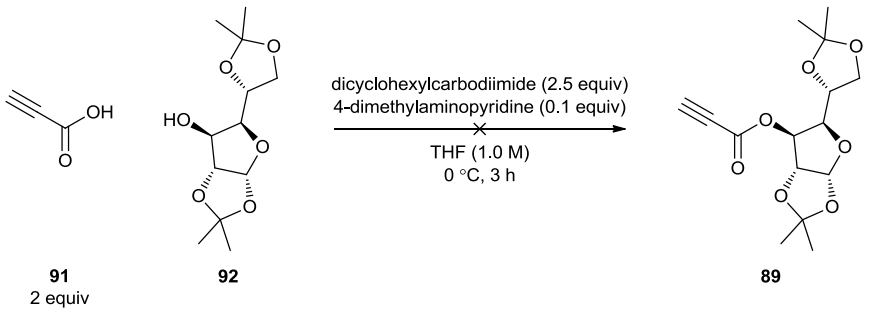

Figure 54: Attempted synthesis of ethynyl half-thread 89

At this stage we noted that the internal arrangement of the triazole is not integral to the reaction or the final compound meaning that the groups bearing the azide and alkyne moieties could be exchanged to facilitate an easier synthetic route. As direct replacement of the ethynyl group with an azide moiety at the position adjacent to the carbonyl carbon is difficult, an additional carbon atom was added into the design of the half-thread in order to aid the synthesis of azide **90**. Taking this approach would allow us to use two readily accessible half-threads, the alkyne **34** and the azide **90** (both available in two steps from commercial reagents).

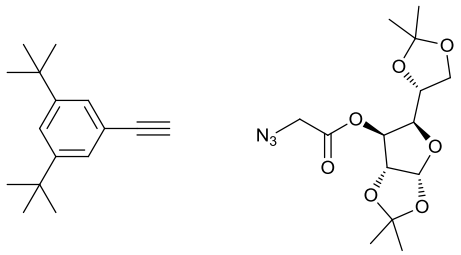

Figure 55: Half-threads 34 and 90

2.2.3.2 – Synthesis of 90

A review of the literature suggested a variety of conditions would allow for the synthesis of this α-azido ester, some of which were employed in a brief screening. Concurrent reactions were set up with different bases; basic alumina,[39] triethylamine, pyridine,[40] DMAP, and potassium carbonate. All reactions but the one containing basic alumina gave some conversion to the ester, and of the others the reaction containing pyridine gave almost quantitative conversion, the highest observed.

The reaction was then scaled up and the esterification of the glucose-di-acetonide (**92**) with α-chloroacetylchloride (**93**) in the presence of pyridine was carried out at 25 °C for 16 hours. The initial reaction proceeded cleanly and the product was isolated by flash column chromatography using diethyl ether and petrol, in 93% yield. However, the workup for this reaction typically yielded material of high enough purity to carry through into the next reaction.

The azidification of the α-chloro ester **94** with sodium azide in DMF at 25 °C for 6 hours occurred smoothly. The target compound, **90**, was purified from the crude material recovered from the workup by flash column chromatography, eluting in petrol and Et_2O, and gave the isolated material in excellent yield. The azide was isolated as a viscous and colourless oil that solidified on standing.

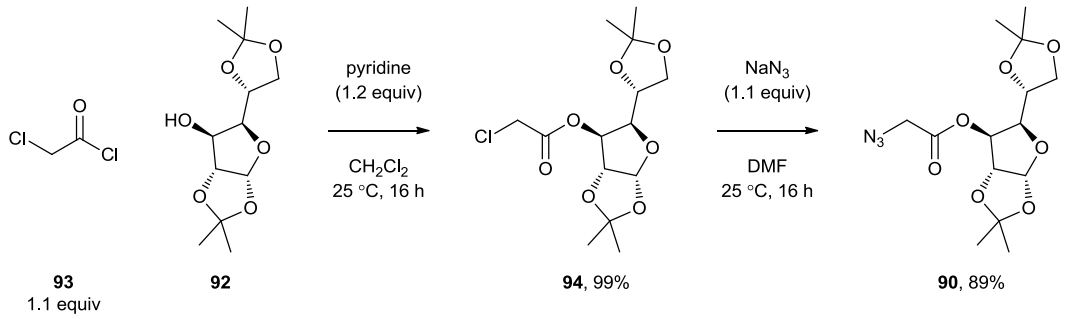

Figure 56: Synthesis of cleavable chiral half-thread 90

In preparation for the synthesis and analysis of the rotaxane, the corresponding thread was synthesised from the azide half-thread **90** and alkyne **34** via a CuAAC coupling protocol which produced the thread in quantitative yield (Figure 57). Thread **95** was purified via column chromatography and was isolated as a colourless solid.

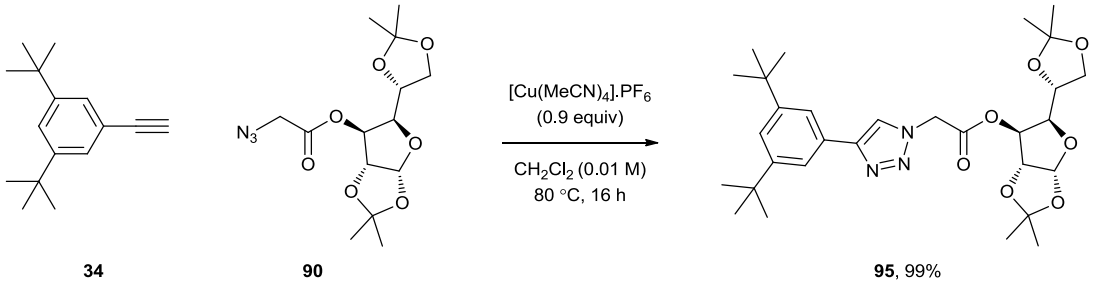

Figure 57: Synthesis of thread 95

2.2.4 – Synthesis of mechanically diastereomeric [2]rotaxanes

With macrocycle **74** and half threads **34** and **90** in hand we attempted the synthesis of a pair of diastereomeric rotaxanes (Figure 58).

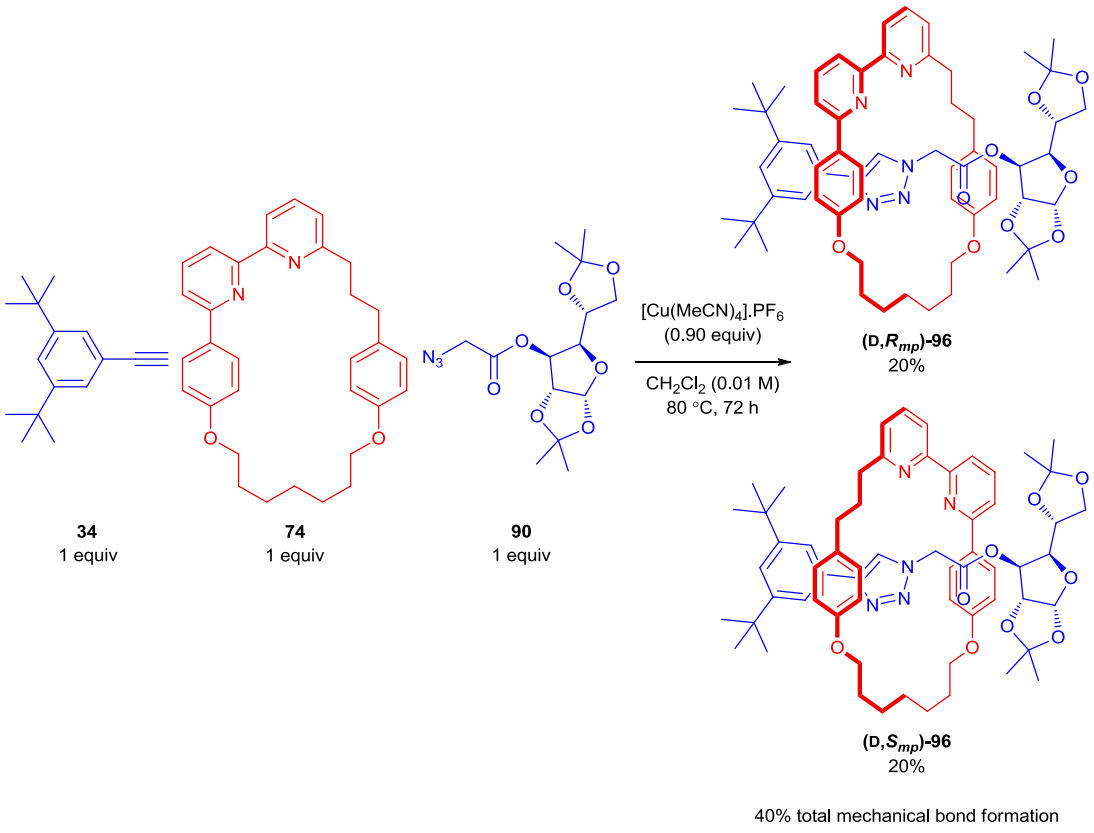

Figure 58: Synthesis of rotaxanes (D,R_{mp})-96 and (D,S_{mp})-96[†]

One equivalent each of the half-threads **34** and **90**, the rotationally asymmetric macrocycle **74** and the Cu(I) catalyst were heated in dichloromethane at 80 °C for 72 hours. At this time an aliquot was worked up to assess the extent of the reaction's progress. From analysis of the ^{1}H NMR of the aliquot this reaction appeared to give two rotaxane species. The spectrum was complex and we observed at least two new sets of aromatic signals, in an approximate 1:1 ratio. The consumption of **74** to form rotaxanes **96** was approximately 40%, meaning the individual NMR yields of each rotaxane were approximately 20%. The rest of the half-threads had been consumed and converted to thread.

As all the half-threads had been consumed the reaction could not continue and so the material was worked up in a solution of Na_4-EDTA in aqueous ammonia. The crude reaction was purified via column chromatography and eluted in 1:1 petrol-dichloromethane and a gradient of

[†] The stereochemical labelling of the rotaxane is explained in section 2.2.5

acetonitrile. Unfortunately, despite attempts at modifying the gradient of the column we were unable to perfectly separate the two rotaxanes. However, we were able to isolate enough clean material for each rotaxane to assign the signals in the crude NMR, allowing us to confirm the 1:1 ratio of the two diastereomeric rotaxanes in the crude reaction product.

2.2.4.1 – Optimisation of the rotaxane forming reaction

Altering the reaction conditions allowed us to ensure full consumption of the macrocycle, simply increasing the stoichiometry of the half-threads ensured that the macrocycle was fully captured (Figure 59). A second reaction was run with five equivalents of each of the half-threads resulting in approximately 90% conversion of macrocycle **74** to rotaxanes **96**.

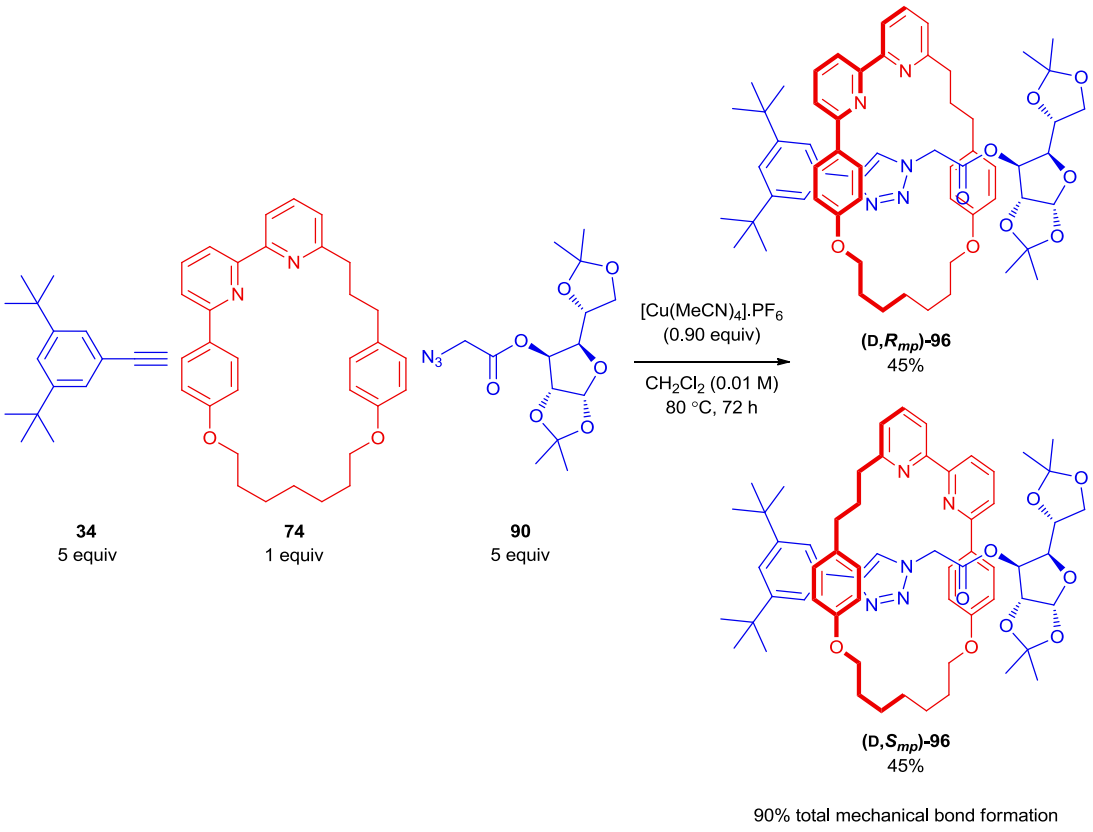

Figure 59: Synthesis of rotaxanes (D,R_{mp})-96 and **(D,S_{mp})-96**

We observed that the percentage conversion of the macrocycle directly matched the number of equivalents of copper catalyst in the reaction. We proposed that the reaction was limited by the amount of copper available in the reaction and that copper remains bound to the rotaxane once the CuAAC-click reaction was complete. If this were the case our maximum yield would be 90%. We ran a further reaction with 0.96 equivalents of tetrakis(acetonitrile)copper(I) hexafluorophosphate and pleasingly the reaction proceeded to ~95% conversion to the

rotaxanes (as ascertained by ^{1}H NMR analysis). Attempts were made to run the reaction with one equivalent of the Cu(I) catalyst, but it was found that even a small excess of Cu(I) was detrimental to the yield of rotaxane. To ensure maximum yields were obtained all future reactions were run with 0.96 equivalents of Cu(I).

2.2.4.2 – Isolation of the diastereoisomeric rotaxanes

Isolation of the rotaxanes from the reaction in which five equivalents of half-threads were used proved troublesome. Near complete consumption of the macrocycle resulted in less contamination of the initial fractions of the first diastereomer by residual macrocycle **74**. However, the excess equivalents of half-threads resulted in a large amount of thread forming during the reaction. This meant that a large percentage of the second rotaxane isomer then co-eluted with the thread, lowering the isolated yield of the second rotaxane diastereomer. Following extensive attempts to optimise the purification we were able to separate the macrocycle, the two rotaxanes, and the thread through careful control of the gradient and by lengthening the column of silica used.

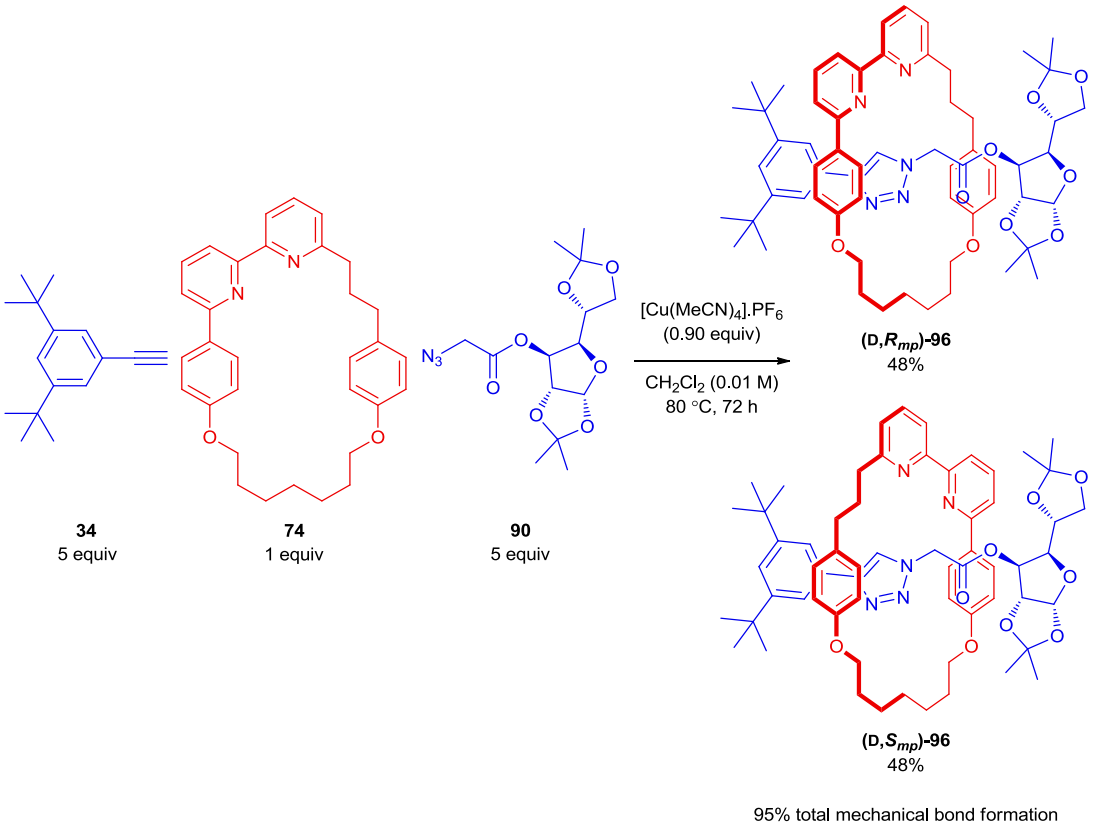

Figure 60: Optimised synthesis of rotaxanes 96

2.2.5 – Detailed structural analysis of (D,R_{mp})-96 and (D,S_{mp})-96

In order to assign the stereochemistry of the rotaxanes we required the crystal structure. Analysis of the crystal structure in comparison to the NMR spectra is given below.

2.2.5.1 – Crystal structure and stereochemical assignment

Single crystal X-ray diffraction analysis of rotaxanes **96** allowed us to directly observe the relative orientation of macrocycle and thread and therefore assign the absolute stereochemistry of the mechanical bond (Figure 61).

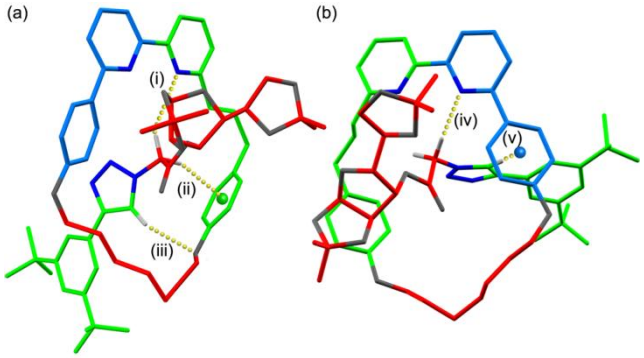

Figure 61: X-ray crystal structures of (a) (D,R_{mp})-96 and (b) (D,S_{mp})-96. Selected distances (Å): (i) 2.9, (ii) 2.5, (iii) 2.5, (iv) 2.3, and (v) 2.6

In order to differentiate the mechanical sources of chirality from other sources of molecular asymmetry we use the suffix "mp" to indicate the mechanically planar chiral nature of the bond.

To determine the mechanical stereochemistry we assign atom priorities A→D based on the Cahn-Ingold-Prelog system as shown for (D,R_{mp})-**96** (Figure 62); A is the highest priority atom in the thread and B is the highest priority point of difference in its substituents; atoms C and D are assigned similarly in the macrocycle. The molecule is then viewed along the A→B axis: if atoms C and D are disposed clockwise the stereochemistry is assigned as *R*; if atoms C and D are disposed anticlockwise the stereochemistry is assigned as *S*. Thus, the late eluting diastereoisomer is assigned as (D,R_{mp})-**96** and the early-eluting diastereoisomer as (D,S_{mp})-**96**, where "D" refers to the covalent stereochemistry of the glucose unit and R_{mp}/S_{mp} refers to the mechanical planar chirality resulting from the orientation of the ring.

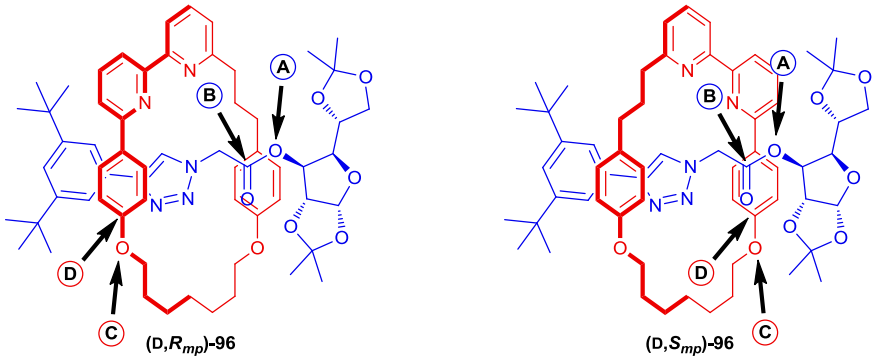

Figure 62: Diagram showing atom labels for assignment of mechanical stereochemistry

2.2.5.2 – NMR spectra

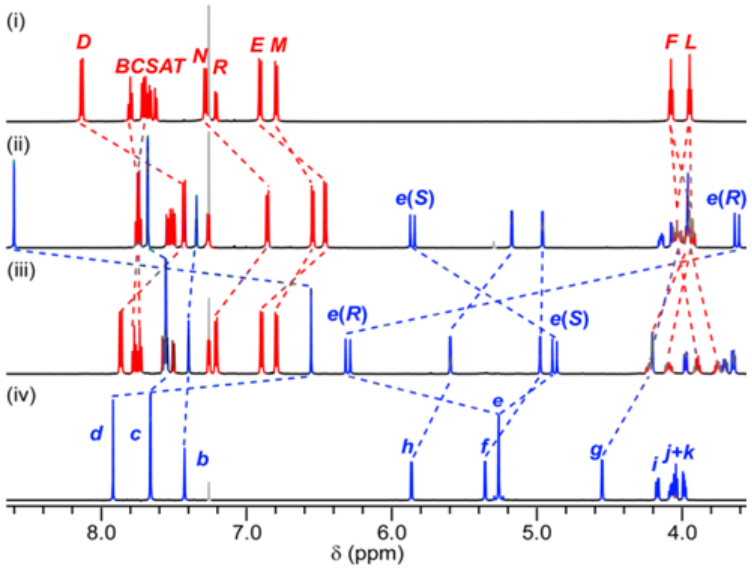

Figure 63: Partial ^{1}H NMR with selected signals assigned, of (i) macrocycle 74, (ii) (D,R_{mp})-96, (iii) (D,S_{mp})-96, and (iv) thread 95

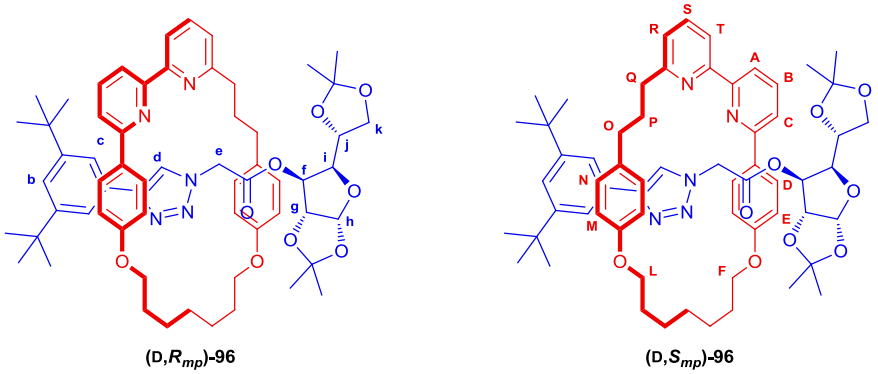

Figure 64: Structure of rotaxanes 96 with corresponding NMR atom labels

The ^{1}H NMR (Figure 63) spectra of rotaxanes **96** are significantly different, reflecting the expected strong interplay of the mechanical and covalent sources of chirality. Furthermore, with the caveat that solid-state structures are not necessarily representative of solution-state co-conformations, the non-covalent interactions observed by X-ray crystallography (Figure 61) provide surprisingly good explanations for some of the key differences in the ^{1}H NMR spectra of rotaxanes **96**.[41] Most strikingly, the signals corresponding to H_e appear as well separated doublets in 5.86 and 3.63 ppm in the R_{mp} isomer and 6.31 and 4.88 ppm in the S_{mp} compound. In both cases, their X-ray structures suggests that one of H_e is engaged in a CH-N hydrogen bond with a bipyridine nitrogen, with the CH-N contact in (D,S_{mp})-**96** (2.3 Å) is significantly shorter than for (D,R_{mp})-**96** (2.9 Å), which correlates with the larger relative deshielding of H_e in the S_{mp} diastereoisomer. Similarly, the large relative shielding of one of H_e in (D,R_{mp})-**96** ($\Delta\delta$ = 1.65 ppm) compared with the non-interlocked thread can be tentatively attributed to a close CH-π contact (2.5 Å) with the flanking aromatic ring that is not present in the X-ray structure of the S_{mp} isomer ($\Delta\delta$ = 0.37 ppm). The X-ray structures also indicate that the deshielded H_e, which participates in the CH-N hydrogen bond with the bipyridine nitrogen is H_e(*S*) in (D,R_{mp})-**96** but H_e(*R*) in (D,S_{mp})-**96**. Thus the relative shift of the diastereotopic protons H_e in the two mechanical diastereoisomers is large; $\Delta\delta$ = 2.68 ppm and 0.98 ppm for H_e(*R*) and H_e(*S*) respectively.

The signal corresponding to the triazole proton (H_c) undergoes a marked shift from 7.93 to 6.53 ppm in (D,S_{mp})-**96** and to 8.60 ppm in (D,R_{mp})-**96**. Instead of the shielding CH-π interaction of H_e as seen in (D,R_{mp})-**96** it is the triazole proton H_c which points directly into the π-system, thus being significantly shielded.

2.2.5.3 – Circular dichroism

The CD spectra of rotaxanes (D,R_{mp})-**96** and (D,S_{mp})-**96** are given in Figure 65. Both compounds exhibit similar intensity of molar CD over the same range of wavelengths, and also share some similar features in their shape, such as a local minimum at 295 nm and a shoulder/local maximum at 280 nm. The most apparent difference in phase is observed below 280 nm. We have been unable to attribute these differences to any specific structural feature, but the fact that the two CD spectra are different, and that the thread itself has a CD of zero intensity across the measured spectrum, indicates that the mechanical bond between macrocycle and thread plays a large role in the appearance of the CD spectrum.

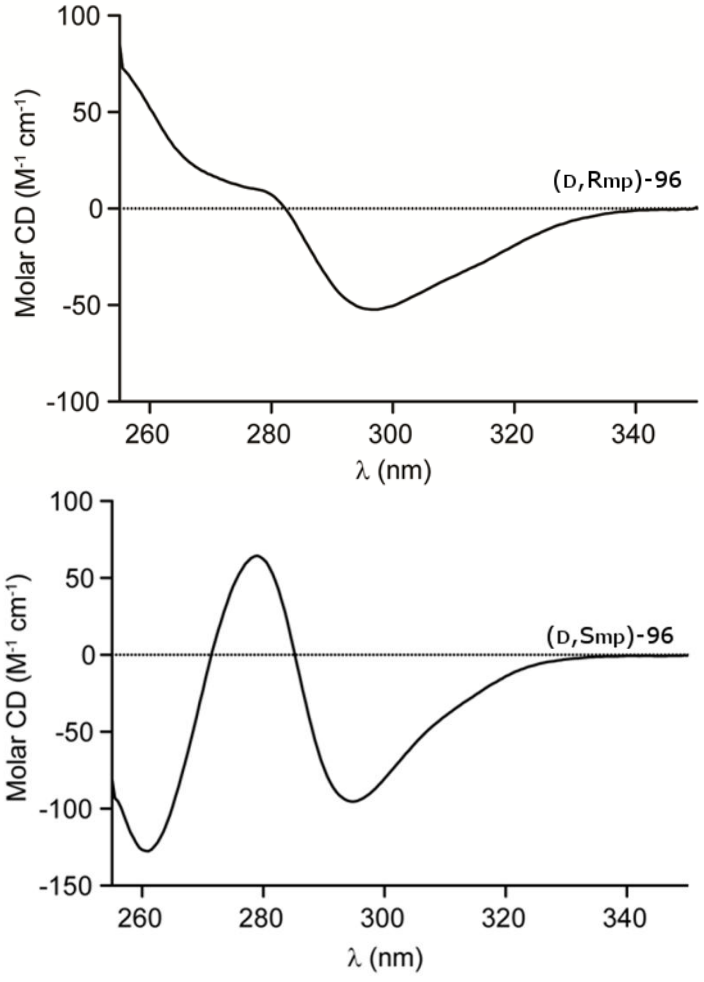

Figure 65: CD spectra of rotaxanes (D,R_{mp})-96 and (D,S_{mp})-96

2.2.6 – Synthesis of mechanically enantiomeric [2]rotaxanes

2.2.6.1 – Nucleophile selection and auxiliary cleavage

With both (D,R_{mp})-**96** and (D,S_{mp})-**96** in hand we set about attempting the cleavage of the chiral moiety of the thread. Mild conditions would of course be preferred but the steric congestion around the ester suggested that the reaction could be hindered. We were aware that the requirement to use a bulky nucleophile that also acts as a stopper in the product rotaxane may limit the ability of the nucleophile to access the carbonyl of the ester.

A number of nucleophilic candidates were proposed for the cleavage of the diastereomeric intermediates which included amine and organometallic reagents (Figure 66). We found examples of nucleophilic substitution reactions in rotaxanes in the literature, but the particularly sterically congested nature of the diastereomers made us consider that these same conditions may not be as successful in the case of (D,R_{mp})-**96** and (D,S_{mp})-**96**.

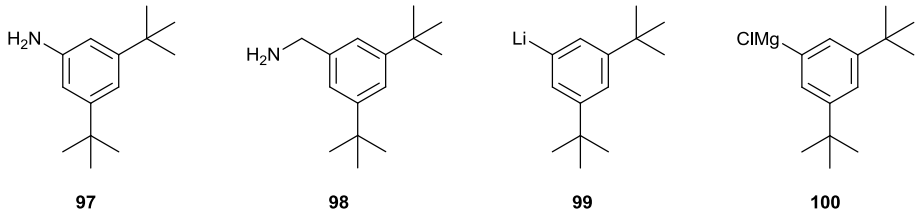

Figure 66: Nucleophiles screened for the cleavage of diastereomeric rotaxanes

The amines **97** and **98** were synthesised from commercial reagents according to literature procedures (Figure 67).[42,43]

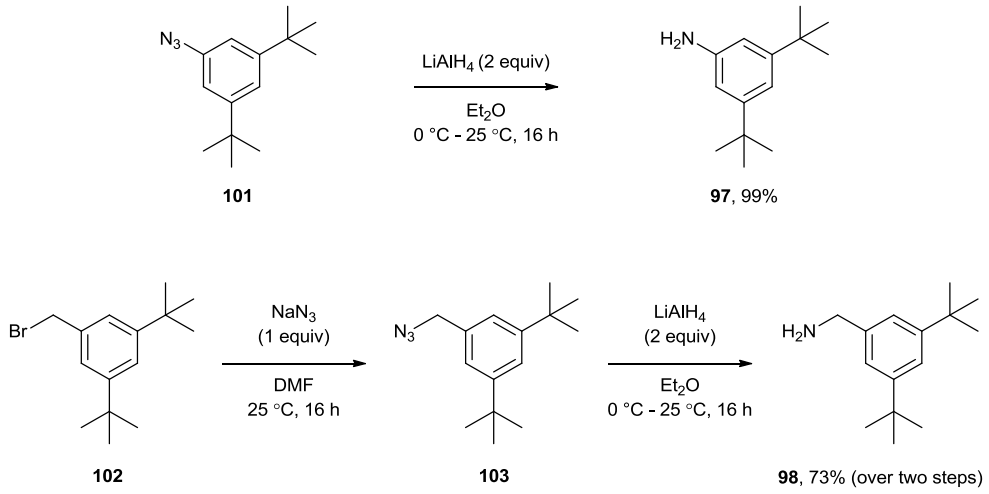

Figure 67: Synthesis of amine nucleophiles

Concurrently we attempted the displacement of the sugar moiety with both an active organolithium species **99** and the equivalent organomagnesium species **100**. The organometallic reagents were prepared *in situ* from the corresponding aryl bromide **104** (Figure 68).

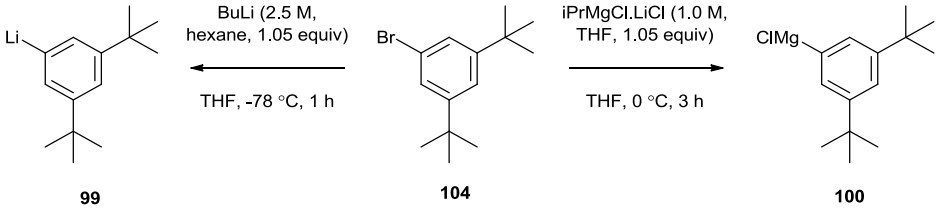

Figure 68: Synthesis of organometallic nucleophiles

Unfortunately, in both cases, instead of the organometallic nucleophiles attacking the carbonyl carbon of rotaxane **96**, they seemed to destroy the sugar moiety resulting in de-threading of the rotaxane as determined by the observation of significant amounts of the macrocycle in the ^{1}H NMR spectra.

For simplicity, the diagrams in this section show only the reactions performed using (D,R_{mp})-**96.**

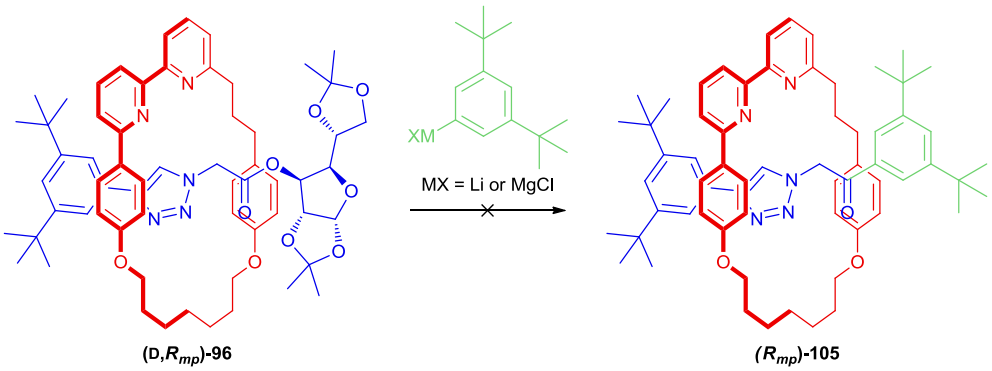

Figure 69: Unsuccesful cleavage of the chiral moiety

Next we investigated aminolysis of the thread. Pre-activation of the amines with trimethylaluminium was found to be effective when attempting to cleave **95**.

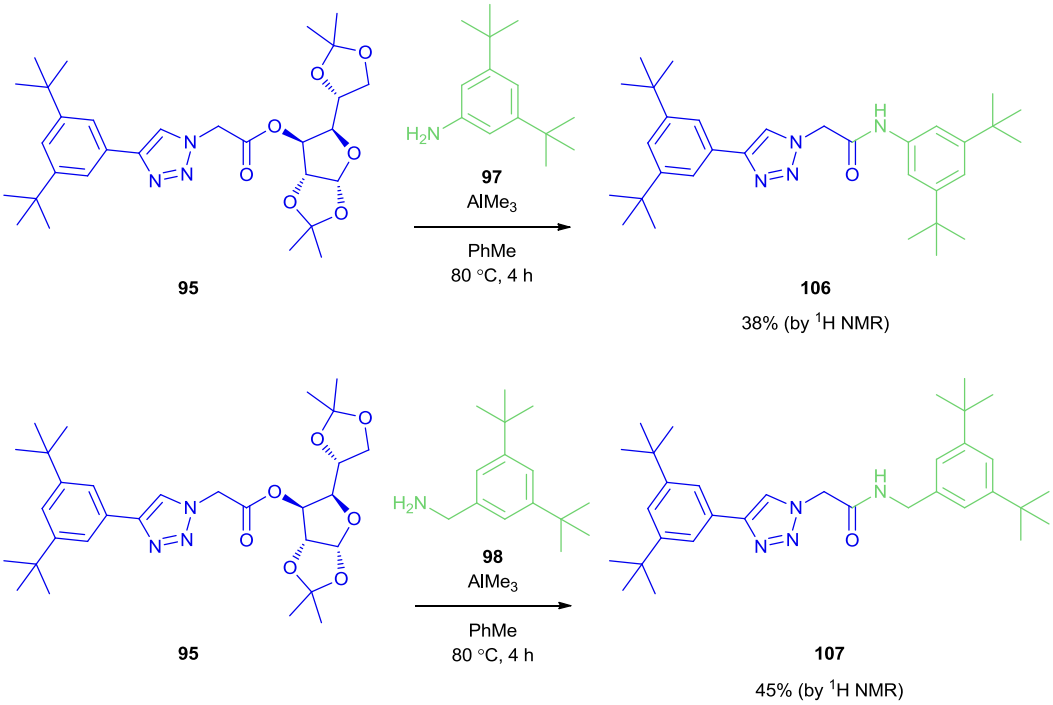

Figure 70: Aminolysis of 95

The reaction conditions were then applied to (D,R_{mp})-**96.** Pleasingly, both the aminolyses were successful to some extent but the benzylamine derivative was more effective than its aniline counterpart (Figure 71). This increase in reactivity can be attributed to the extra carbon atom in the benzylamine providing a less sterically hindered nucleophile. Repeating the aminolysis with 2.5 equivalents of the amine gave excellent conversion to the enantiomeric rotaxane product.

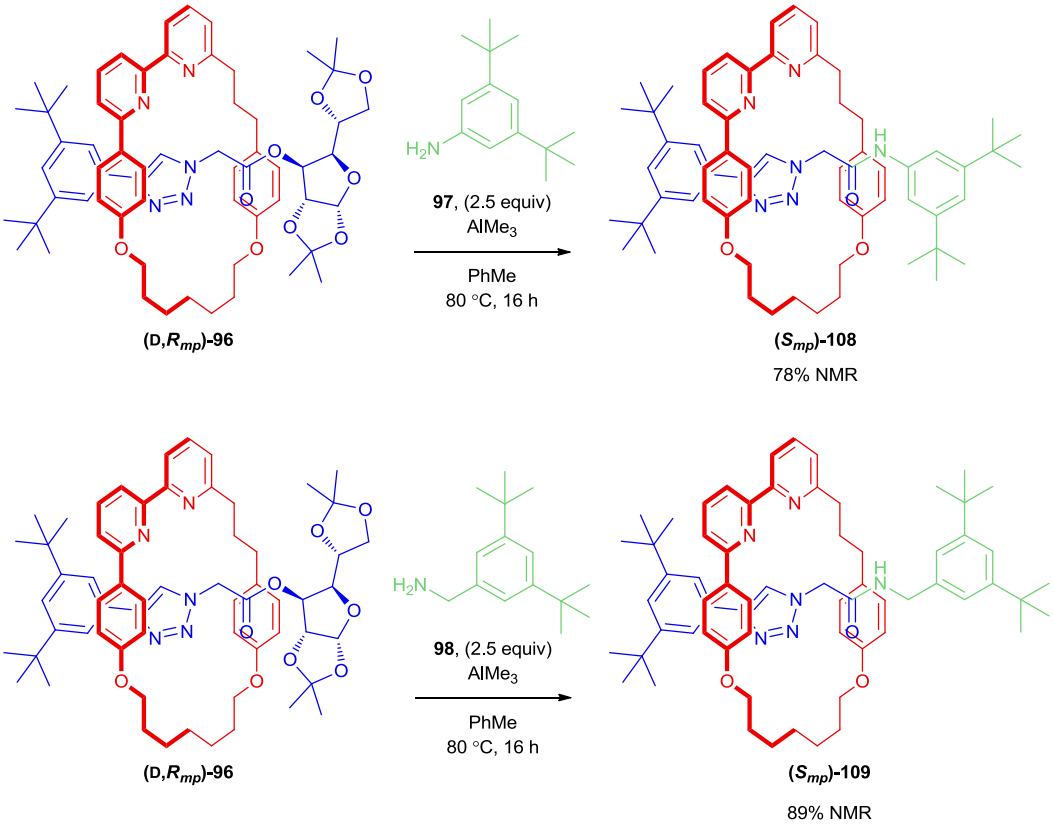

Figure 71: Aminolysis of rotaxanes 96

The same conditions were applied to (D,S_{mp})-**96** which successfully generated the opposite enantiomer of the S_{mp}- isomer of rotaxane **109**. Optimal conversion was achieved by employing 2.5 equivalents of the activated amine and heating the reaction for 16 hours (Figure 72).

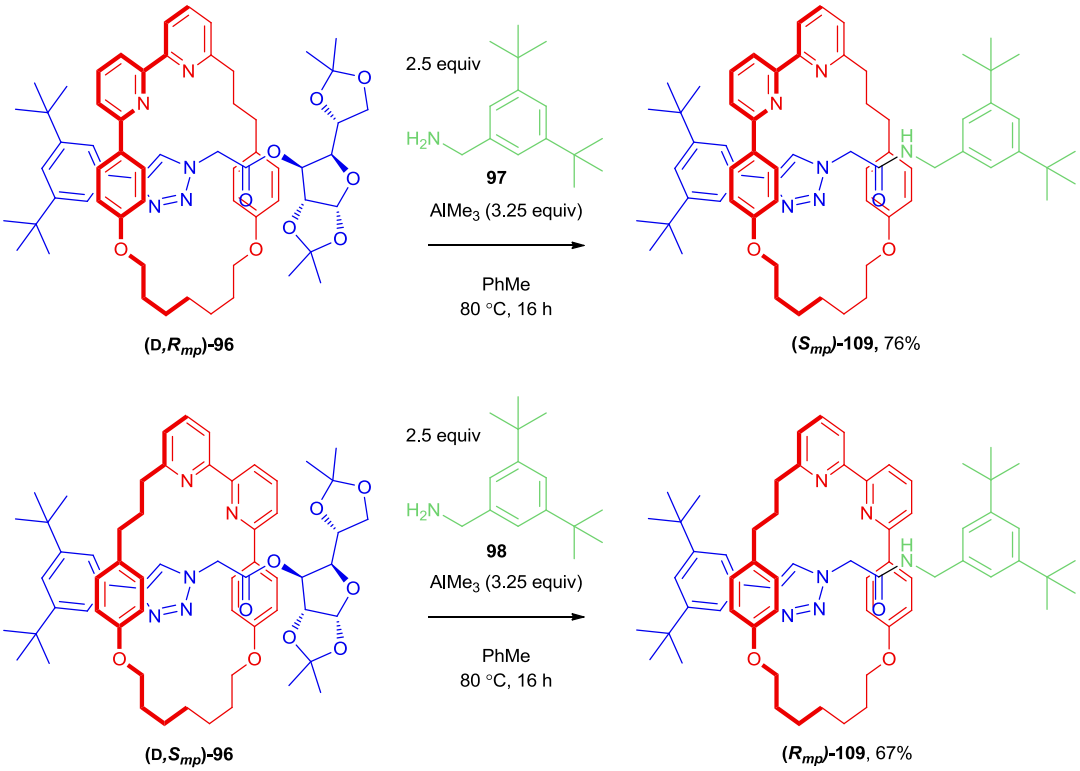

Figure 72: Aminolysis of rotaxanes 96

The purification of each enantiomer was achieved via column chromatography, successfully separating the rotaxane from the cleaved α-D-glucofuranose and a small amount of macrocycle (approximately 0.1 equivalents with respect to the rotaxanes). In both cases we observed that the reaction also produced approximately 0.1 equivalents of the amide bearing thread. This implies that the reaction in which the amine approaches from the opposite face of the macrocycle as the α-D-glucofuranose moiety accounts for around 10% of the successful substitution reactions.

2.2.6.2 – Synthesis of rac-109

In order to allow analysis by CSP-HPLC racemic rotaxane **109** was synthesised through a click reaction of the corresponding half-threads (**34** and **111**) and macrocycle **74**. The amide containing half thread (**111**) was synthesised according to the following sequence (Figure 73). The 2-chloroacetamide derived half thread intermediate **110** was synthesised from **98** and 2-chloroacetylchloride (**93**). The 2-azidoacetamide derived half-thread **111** was synthesised by stirring **110** and sodium azide in DMF overnight.

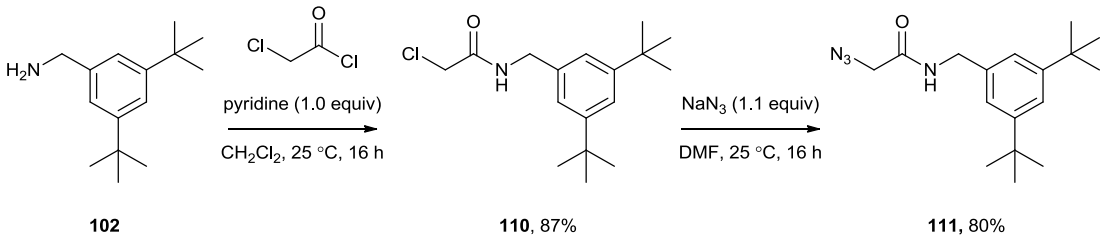

Figure 73: Synthesis of amide half-thread 111

The half threads were combined with macrocycle **74** and following identical conditions as employed in the synthesis of rotaxanes **96,** successfully formed racemic rotaxanes **109** (denoted **rac-109**) were isolated in excellent yield (89%).

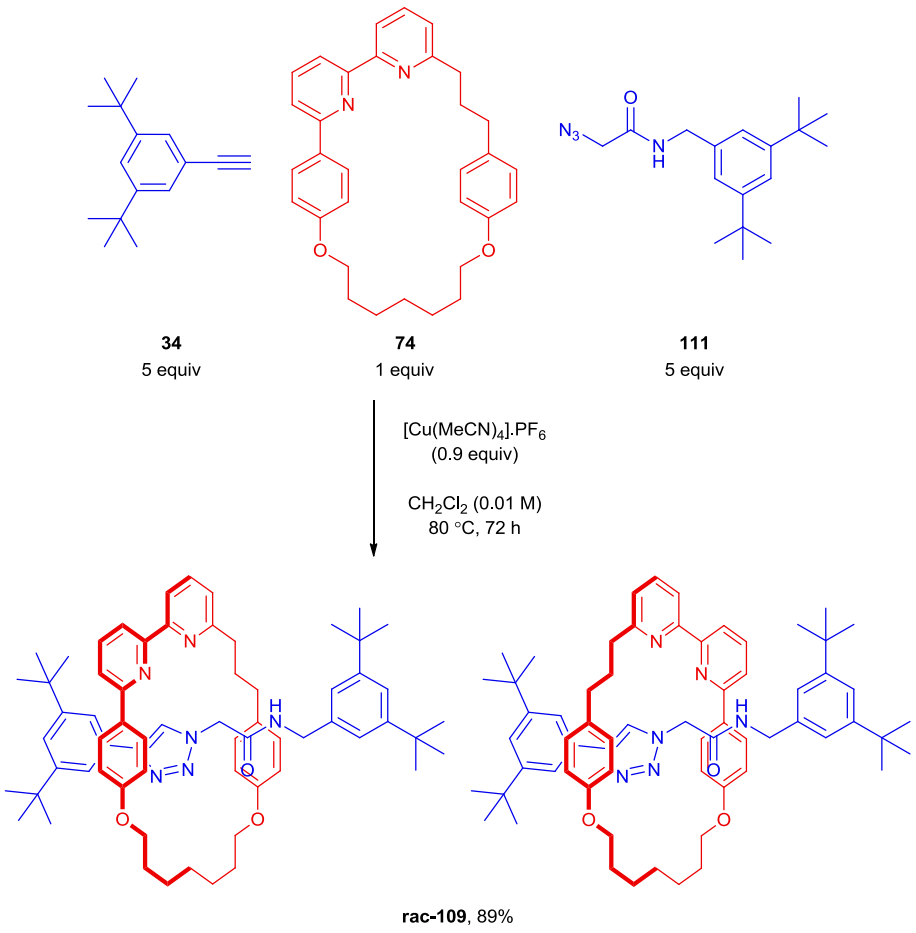

Figure 74: Synthesis of racemic rotaxanes 109

2.2.7 – Analysis of rotaxanes 109

Samples of the enantiomers were characterised by mass spectrometry, ^{1}H and ^{13}C NMR, CD spectroscopy, and the optical purity of rotaxanes **109** was confirmed by chiral stationary phase HPLC.

2.2.7.1 – CSP-HPLC analysis

The aminolysis of (D,R_{mp})-**96** gave rise to one enantiomer of rotaxane **109** in an er of 99.3:0.7 while reaction of (D,S_{mp})-**96** gave the other as a single diastereomer (>99.5:<0.5).

As the substitution of the glucose moiety doesn't affect the relative orientation of the macrocycle and thread components the configuration of the mechanical bond in rotaxanes **96** can be assigned unambiguously. Thus, (D,R_{mp})-**96** and (D,S_{mp})-**96** give rise to rotaxanes (S_{mp})-**109** and (R_{mp})-**109** in 98.6 and >99% ee respectively (Figure 75 and Figure 76). The inversion of the stereochemical label is due to a formal inversion of the thread axis as a result of the aminolysis reaction (Figure 77).

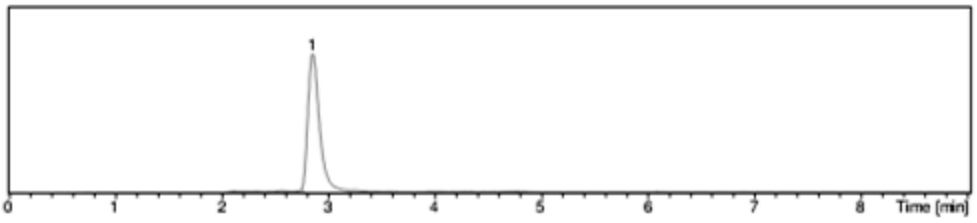

#	RT [min]	Area	Chromatogram	Intens.	Max. m/z	Area Frac. %
1	2.9	3630.0	UV Chromatogram, 190-900 nm	293	995.4	100.0

Figure 75: CSP-HPLC trace of rotaxane (R_{mp})-109

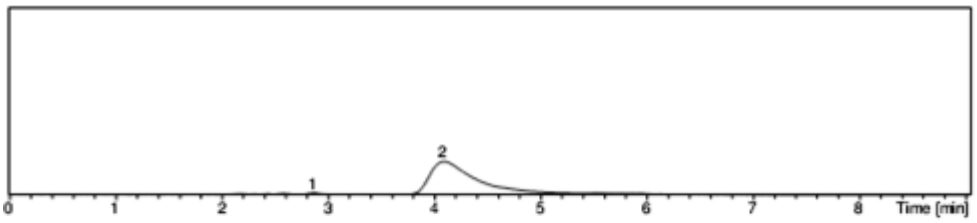

#	RT [min]	Area	Chromatogram	Intens.	Max. m/z	Area Frac. %
1	2.9	14.872	UV Chromatogram, 190-900 nm	3	995.6	0.7
2	4.1	2110.513	UV Chromatogram, 190-900 nm	69	995.5	99.3

Figure 76: CSP-HPLC trace of rotaxane (S_{mp})-109

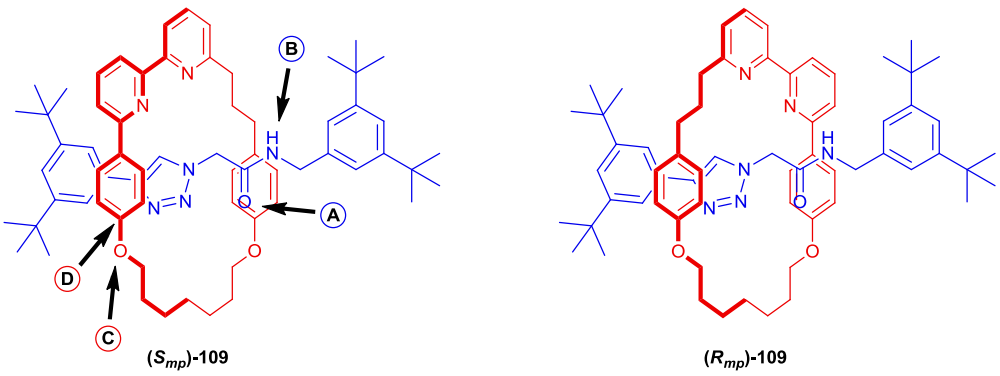

Figure 77: Assignment of mechanical stereochemistry for rotaxanes 109

2.2.7.2 – NMR spectra

The ^{1}H NMR spectra of the enantiomers of rotaxane **109** are identical, and comparison with the corresponding achiral, non-interlocked thread clearly demonstrates the chiral environment of the mechanical bond. H_e and H_g, which are enantiotopic in the thread, are diastereotopic in rotaxane **109** and both are split into two widely separated signals. The significant deshielding of H_f in rotaxanes **109** compared to the non-interlocked thread is tentatively assigned to a hydrogen bond between the amide NH and the bipyridine unit.

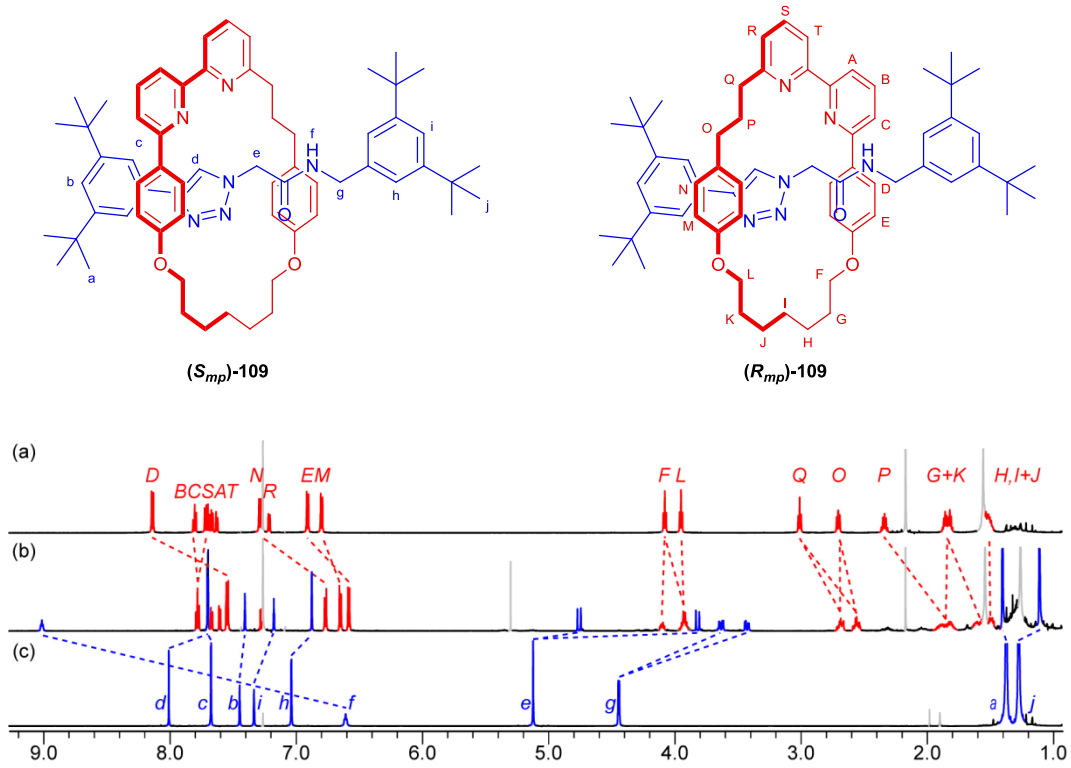

Figure 78: Diagrams of rotaxanes 109 showing NMR atom labels (top), and stacked ^{1}H NMR spectra (bottom) for rotaxane 109 showing (a) the macrocycle, (b) the rotaxane and (c) thread

2.2.7.3 – Circular dichroism

CD spectroscopy confirmed the enantiomeric nature of the two rotaxanes as the spectra were indeed mirror images of each other. We also formed the 1:1 complex of the rotaxane with tetrakis(acetonitrile)copper(I) hexafluorophosphate in chloroform. Reintroduction of Cu(I) into the rotaxane gave samples with more complex CD spectra in which the sign of the CD effect inverts at λ = 266 nm and 295 nm. In both cases the amplitude of the CD effect observed is relatively large.[44]

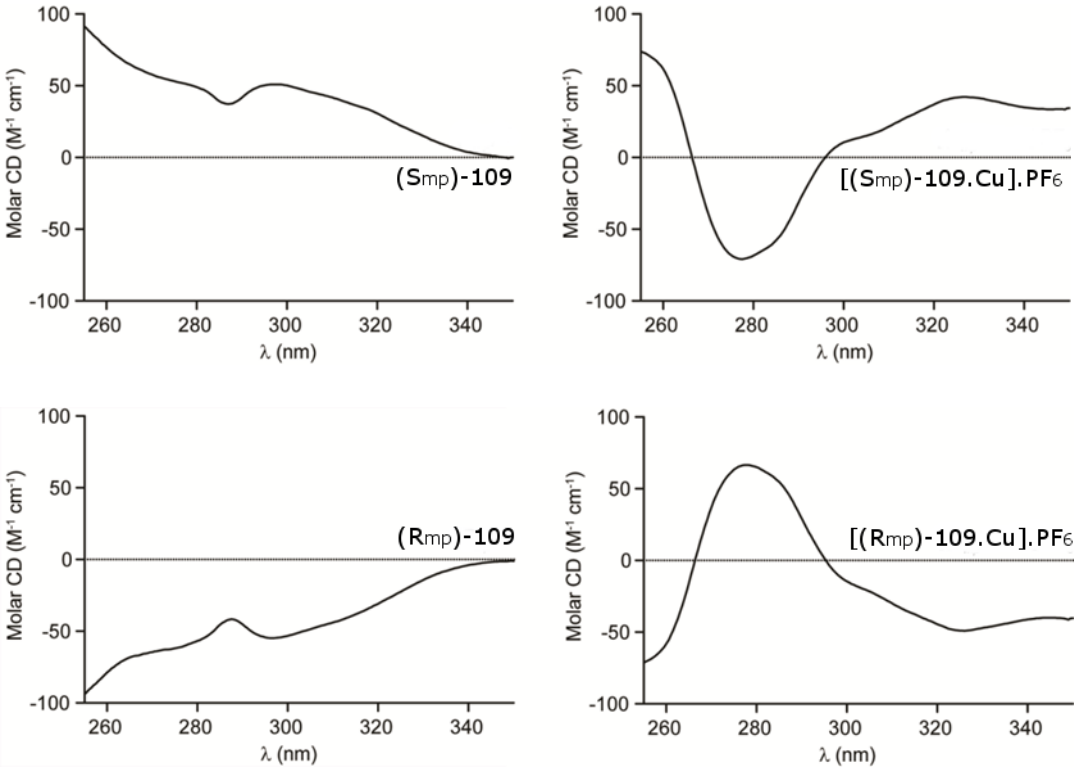

Figure 79: CD Spectra of rotaxanes 109 and their Cu(I) complexes

2.3 – Concluding remarks

In conclusion, we have succeeded in synthesising the first mechanically planar chiral rotaxanes in high enantiopurity without the need for chiral separation techniques. Our approach also allowed us to unambiguously assign the absolute stereochemistry of the mechanical bond which had also not previously been achieved. Given the synthetic utility of the active template method for the synthesis of rotaxanes, this approach may prove general and, by avoiding the need for CSP-HPLC, scalable. Thus, these proof-of-concept studies open up this under-explored form of molecular asymmetry for study, and we anticipate that this will lead to exciting developments across a range of areas including materials, sensing and catalysis. Ultimately, by combining mechanical chirality with the well-developed chemistry of rotaxane molecular shuttles, it may prove possible to realise molecular machines that display dynamic control over chiral space, such as switchable catalysts which can produce either hand of a desired product in response to external stimuli.

2.4 – References

[37] Hayes, M. A.; Meckel, C.; Schatz, E.; Ward, M. D. *Dalton Transactions*, **1992**, 703.

[38] Neises, B.; Steglich, W. *Angew. Chemie Int. Ed. English* **1978**, *17*, 522.

[39] Tiwari, P.; Misra, A. K. *Carbohydrate Research*, **2006**, *341*, 339

[40] Venuti, M. C.; Alvarez, R.; Bruno, J. J.; Strosberg, A. M.; Gu, L.; Chiang, H. S.; Massey, I. J.; Chu N.; Fried, J. H.; *Journal of Medicinal Chemistry*, **1988**, *31*, 2145

[41] The key intercomponent interactions observed using ROESY spectroscopy in rotaxanes 100 are also in agreement with the solid state structure.

[42] Gassensmith, J. J.; Barr, L.; Baumes, J. M.; Paek, A.; Nguyen, A.; Smith, B. D. *Org. Lett.* **2008**, *10*, 3343.

[43] Grunder, S.; Muñoz Torres, D.; Marquardt, C.; Bałaszczyk, A.; Krupke, R.; Mayor, M. *Eur. J. Org. Chem.* **2011**, 478.

[44] Grimme, S.; Harren, J.; Sobanski, A.; Vögtle, F. *Eur. J. Org. Chem.*, **1998**, 1491.

Chapter 3 – Diastereoselective synthesis of mechanically planar-chiral [2]rotaxanes

3.1 – Introduction

Despite our success in synthesising a pair of enantiomerically pure mechanically chiral rotaxanes, our current reagents and conditions gave no selectivity between the diastereomers, a problem that we thought needed addressing. In the next chapter we outline our efforts towards a diastereoselective synthesis of mechanically planar chiral rotaxanes. The chiral auxiliary employed in combination with our asymmetric macrocycle afforded only a 1:1 mix of diastereomeric rotaxanes and more accurately acts as a chiral derivitising agent. This 1:1 ratio limited us to a theoretical maximum 50% yield of each specific enantiomer. Here we describe successful studies towards a diastereoselective synthesis of mechanically chiral rotaxanes.

3.2 – Results and Discussion:

In order to improve the diastereomeric ratio there were a number of modifications to the reaction that we could make; this included changing the temperature, solvent, or additives in the reaction. We could also make changes to the structure of the chiral auxiliary or the macrocycle employed in the reaction.

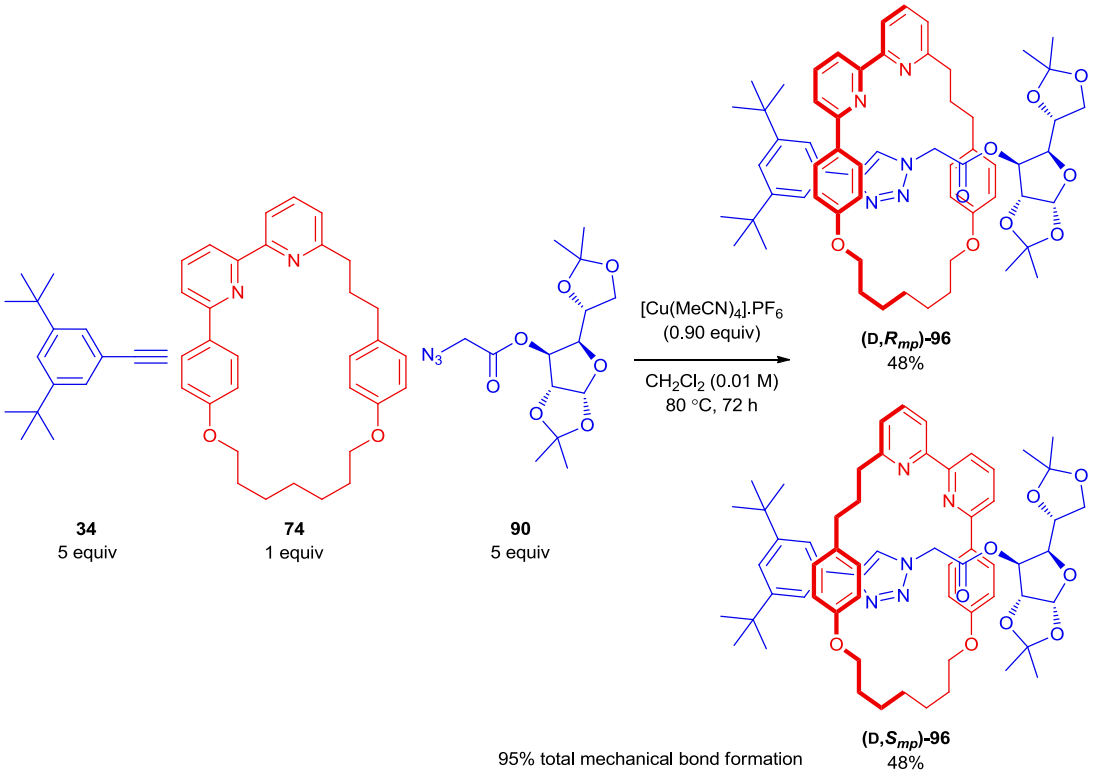

Figure 80: Optimised conditions for the synthesis of rotaxanes 96

3.2.1 – Modification of the existing reaction conditions

We thought that the simplest way to introduce diastereoselectivity to the reaction was through modification of the reaction conditions, which would allow for a rapid screening without resorting to synthesising new reagents.

3.2.1.1 – Effect of temperature on diastereoselectivity

Initial attempts at improving the selectivity of the rotaxanation focused on running the reaction at a lower temperature. Standardised reactions were run at 80 °C and 25 °C by taking a common reaction mixture and splitting it between two CEM vials to run the reactions concurrently (Figure 81). The reaction run at 80 °C was a standard and pleasingly the reaction completed as expected after 72 hours. The reaction at 25 °C was significantly slower and on aliquoting after five days the reaction was only 50% complete (as observed by ^{1}H NMR). The reaction was left for a further three days at which time the reaction was 80% complete. Despite not achieving full conversion of the macrocycle we were able to observe that the ratio between diastereomers was still 1:1. Given that there was no change in the diastereomeric ratio despite a drop in temperature of 55 °C – as well as the fact that the reaction was incomplete after eight days – we decided to halt this avenue of investigation.

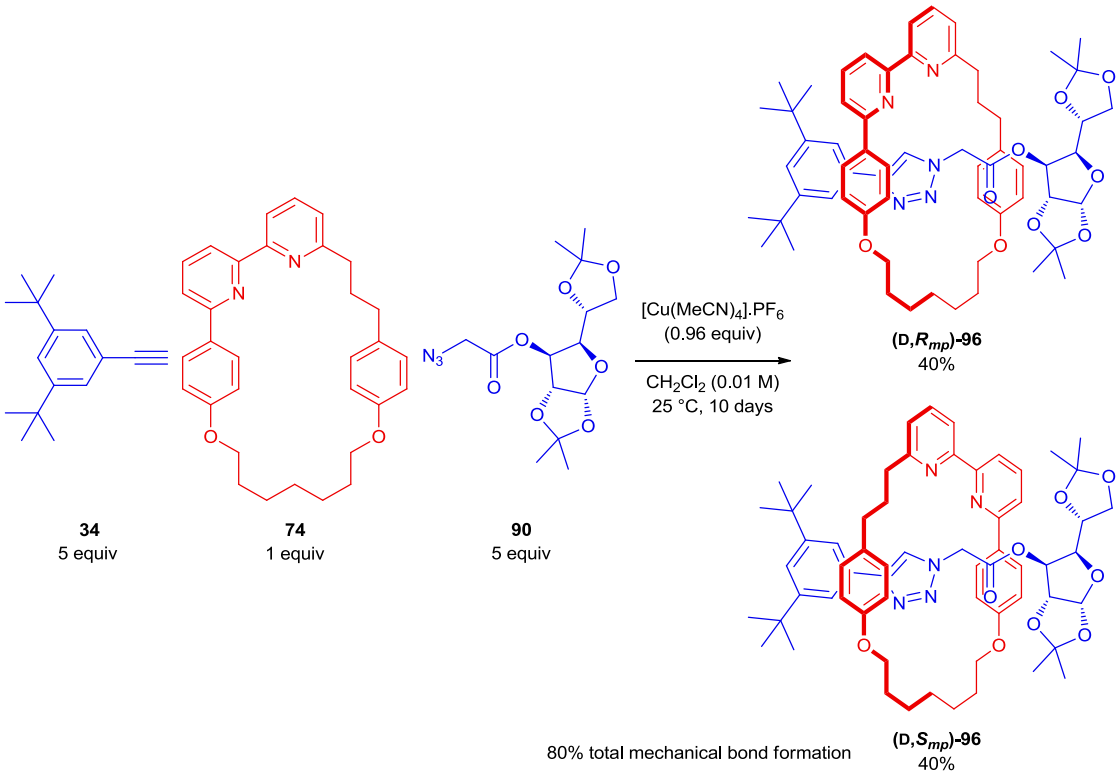

Figure 81: Room temperature rotaxane formation

3.2.1.2 – Effect of solvent on diastereoselectivity

We undertook a solvent screen to assess the effect on the dr of the reaction. Five solvents were selected – THF, DMF, acetonitrile, toluene and ether – and five identical reactions were set up under the standard procedure with the solvent added last before heating the reactions for 72 hours (Figure 82).

The reactions were set up under identical conditions but on addition of the solvent the reactions prepared in acetonitrile and ether both showed signs of reagent insolubility. On heating, the reagents in acetonitrile fully dissolved while in ether a solid persisted and the reaction remained cloudy. After 72 hours each reaction was aliquoted and the sample analysed by ^{1}H NMR. Despite some minor variation in the yield of rotaxane formation, none of the reactions gave any increase in selectivity.

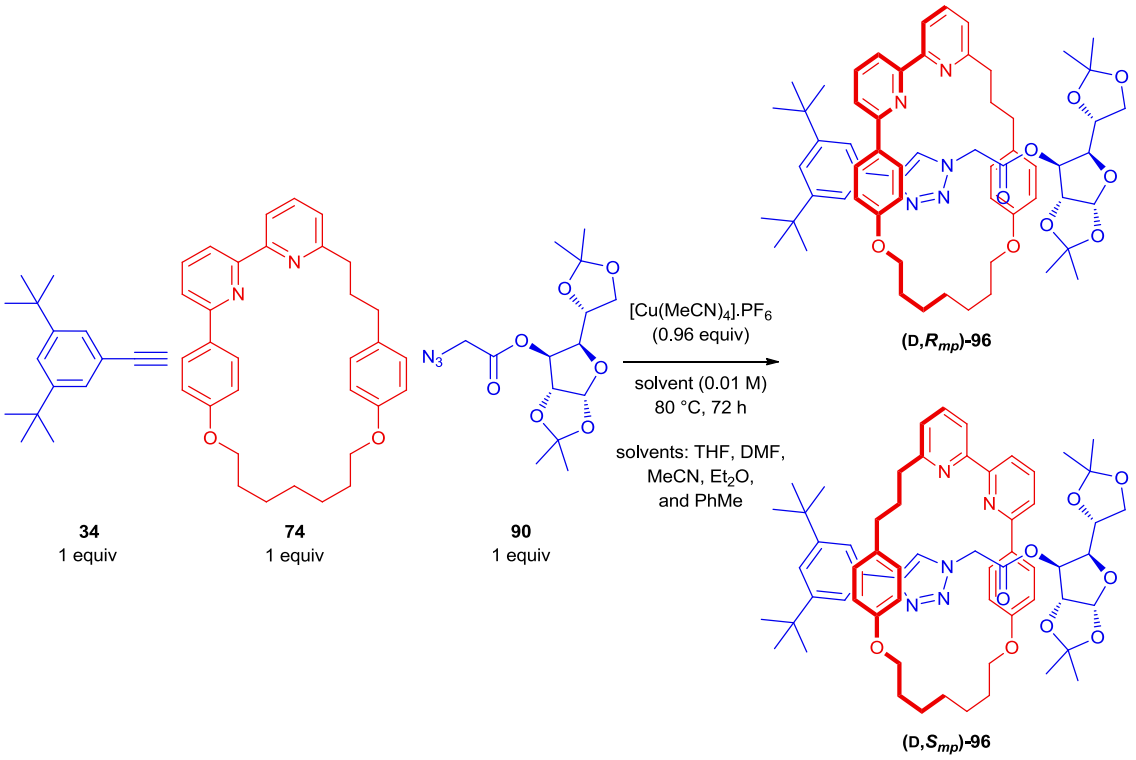

Figure 82: Effects of solvent on diastereoselectivity

3.2.1.3 – Effect of half-thread structure on diastereoselectivity

Our first attempt at narrowing down a suitable target to act as our chiral auxiliary came from the original half-thread that inspired the project, the propargylated sugar **39**. Using our pre-existing reagents and conditions we were quickly able to ascertain that this combination of half-threads didn't give any selectivity in the rotaxanation reaction, again giving an apparent dr of 1:1 according to analysis of the NMR spectra (Figure 83). Disappointingly we were unable to separate rotaxanes **110** by column chromatography.

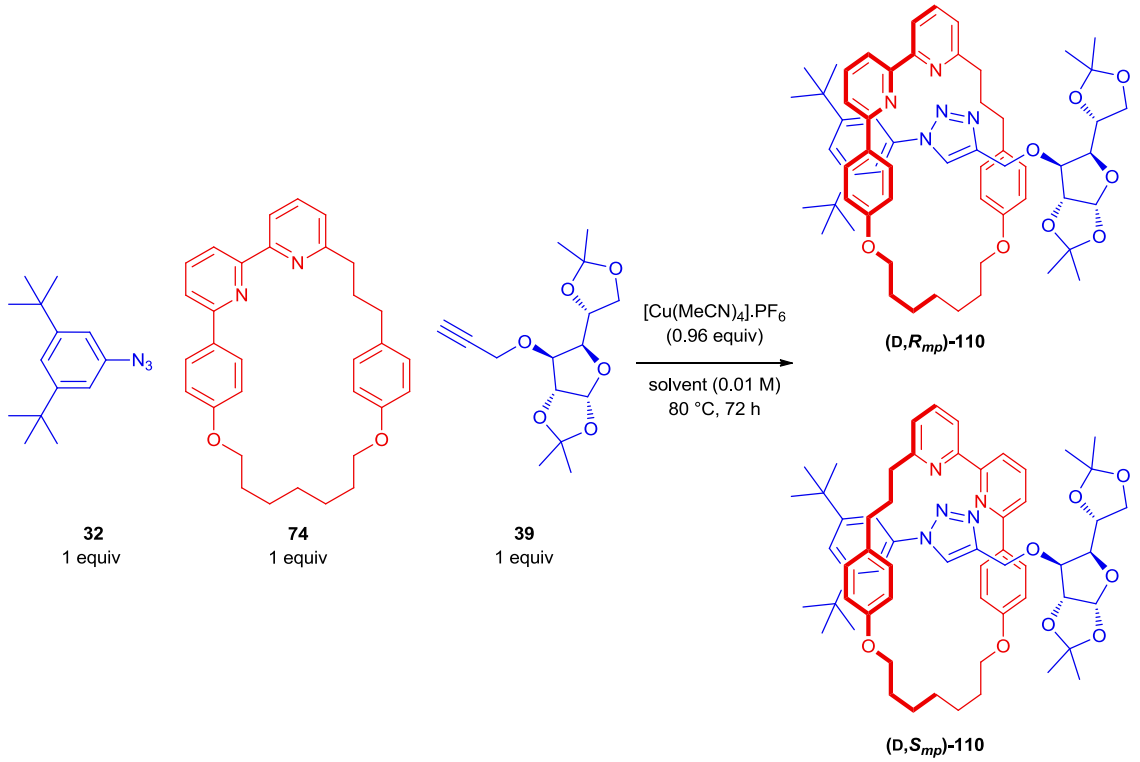

Figure 83**: Synthesis of diastereomeric rotaxanes half-threads 32 and 39**

We investigated other small, chiral and commercially available compounds and settled on a bulky oxazolidinone as our chiral source material (**111**, Figure 84). On building the space-filling model of the target rotaxane we were pleased to find that the diphenylmethyl moiety appeared to act as a stopper for the macrocycle. Following literature precedent we successfully synthesised the 2-chloroacetyl oxazolidinone **112** in good yield.[45] The intermediate chloride was converted to azide **113** via the established protocol using sodium azide in DMF and was also isolated in good yield (51% over two steps) (Figure 84).

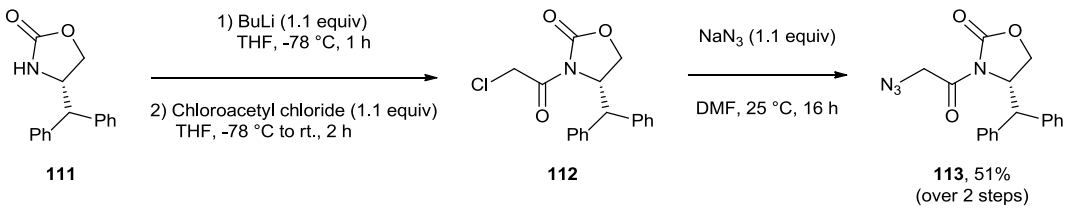

Figure 84: Synthesis of new oxazolidinone half-thread 117

A reaction of oxazolidinone half-thread **113** with alkyne half-thread **34**, and macrocycle **74** was undertaken, which gave rotaxane **114** in good yield (40% mechanical bond formation) (Figure 85). Disappointingly the reaction wasn't selective for either of the diastereomers (as ascertained by ^{1}H NMR analysis of the mixture of the two diasteromers) nor were we able to isolate the diastereomers from each other.

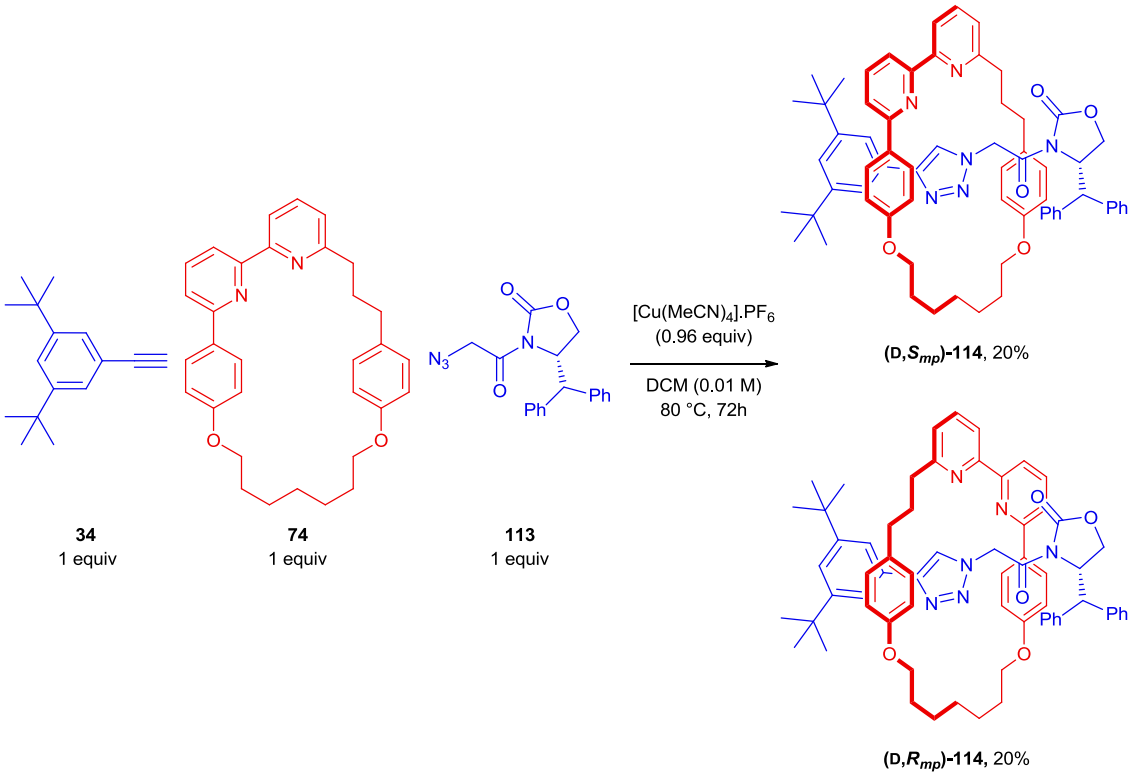

Figure 85: Rotaxanation with oxazolidinone half-thread 113

3.2.1.4 – Effect of the addition of base on diastereoselectivity

Subsequently to the previously described reactions, a discovery in our group provided us with another avenue of investigation. It was found that the presence of an organic base in a similar AT-CuAAC rotaxanation increased the rate of the CuAAC reaction and resulted in complete consumption of the macrocycle in less than 16 hours at 25 °C. We considered that as the addition of a base changes the kinetics of the reaction not only could the addition of base improve the reaction rate, but that it could potentially accelerate the formation of one of the diastereomers over the other, thereby increasing the selectivity. A rotaxanation with one equivalent of the half-threads and one equivalent of diisopropylethylamine (DIPEA) was run at 25 °C. Pleasingly the reaction completed within 6 hours, but unfortunately the reaction was not selective and gave a dr of 1:1 for the rotaxanes.

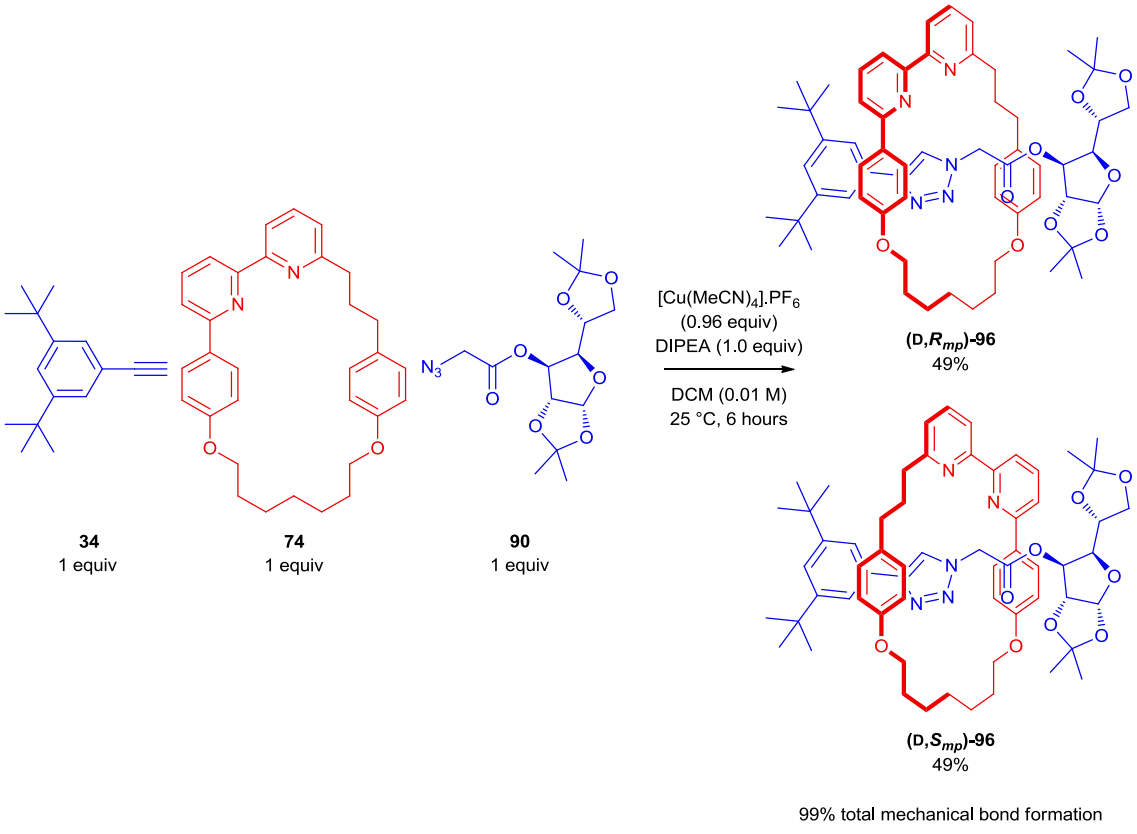

Figure 86**: Rotaxane synthesis in the presence of DIPEA**

3.2.2 – Synthesis of a new macrocycle

Despite attempts to improve the selectivity of the reaction through varying the reaction conditions, we did not observe any change in the selectivity of the rotaxane forming reaction. It was at this time that we considered alternate macrocycle structures. In order to avoid starting an entirely new synthesis it was obvious that the most expedient modification to our macrocycle structure would be through changing the dibromide used in the macrocyclisation step.

We proposed that reducing the conformational freedom of the macrocycle might improve the selectivity of the AT-CuAAC reaction. By restricting the conformational freedom of the pre-rotaxane complex we hoped to increase the difference in energy between the two diastereomeric transition states. This restriction in conformation would be made possible by replacing the flexible alkyl chain with a rigid unit; a number of candidates were proposed (Figure 87).

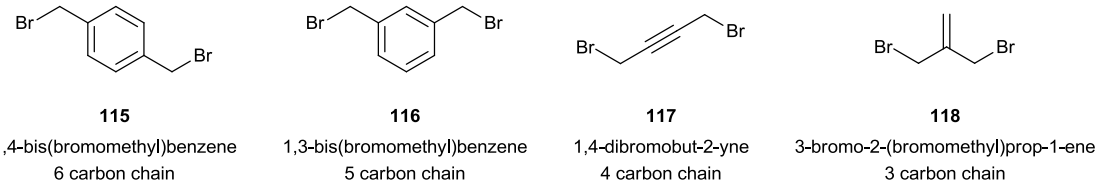

115
1,4-bis(bromomethyl)benzene
6 carbon chain

116
1,3-bis(bromomethyl)benzene
5 carbon chain

117
1,4-dibromobut-2-yne
4 carbon chain

118
3-bromo-2-(bromomethyl)prop-1-ene
3 carbon chain

Figure 87: Proposed reagents for screening in macrocyclization.

While rigidity of the macrocycle is desirable for the rotaxanation reaction it potentially complicates the synthesis of the macrocycle; the viable dibromide candidates for the ring-closing double Williamson ether reaction are smaller in length and more rigid than 1,7-dibromoheptane and therefore carry a penalty in that they may less easily undergo ring closure than in the case of macrocycle **74**. A macrocycle based on **115** has only one less carbon atom in the ring than macrocycle **74** and is potentially more readily accessible than the other options. Macrocycle precursor **75** was subjected to Williamson-ether macrocyclisation conditions with **115** (Figure 88).

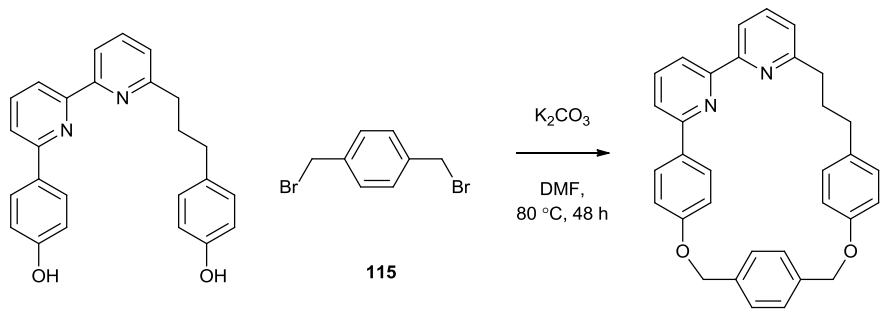

75

115

119, 6%

Figure 88: Macrocyclisation of precursor 75 and dibromide 115

An aliquot of the reaction mixture was worked up under our standard conditions and was analysed by ^{1}H NMR. Pleasingly the reaction appeared to have worked; the characteristic benzylic signals in the NMR attributed to the dibromide were no longer apparent indicating full consumption of the starting material. Optimisation of the column conditions allowed us to isolate macrocycle **119** in a 6% yield.

3.2.3 – Diastereomeric rotaxane synthesis with macrocycle 119

A rotaxanation reaction was run with macrocycle **119**, alkyne half-thread **34** and azide half-thread **90** (Figure 89). Pleasingly this reaction proceeded smoothly and captured approximately 50% of the macrocycle as rotaxane **120**. To our delight the reaction appeared to be somewhat selective for one diastereoisomer of rotaxanes **120**, as ^{1}H NMR analysis of the mixture allowed us to observe a dr of (D,S_{mp})-**120** to (D,R_{mp})-**120** of approximately 2.3:1.

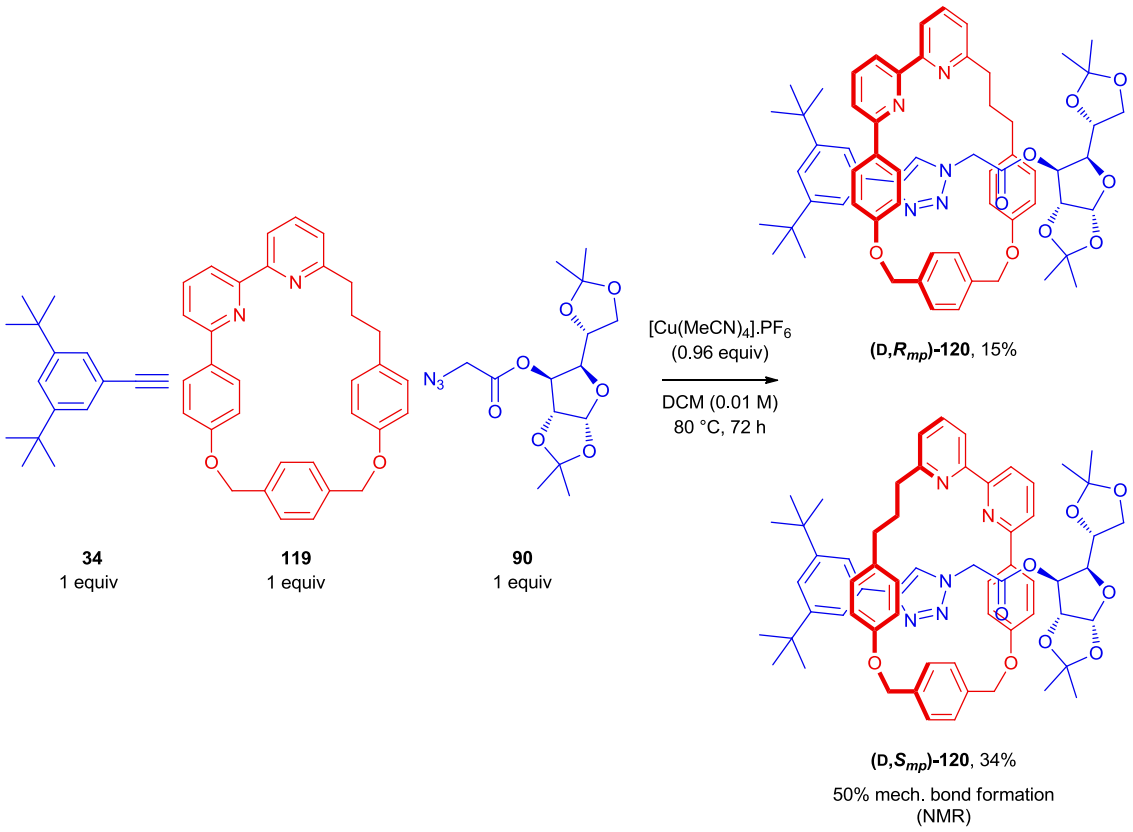

Figure 89: Rotaxanation with macrocycle 119

In order to improve the yield of the reaction we increased the stoichiometry of the half-threads to 5 equivalents which resulted in full conversion of macrocycle **119** to rotaxane **120**, while the diastereomers occurred in the same dr of 2.3:1.

We then repeated the same reaction at room temperature in the presence of DIPEA which gave a similar increase in reaction rate as was observed with the synthesis of rotaxane **96**, and increased the dr to approximately 3:1. We were subsequently able to reduce the stoichiometry of the half-threads to 3 equivalents which allowed the reaction to complete in 16 hours (Figure 90).

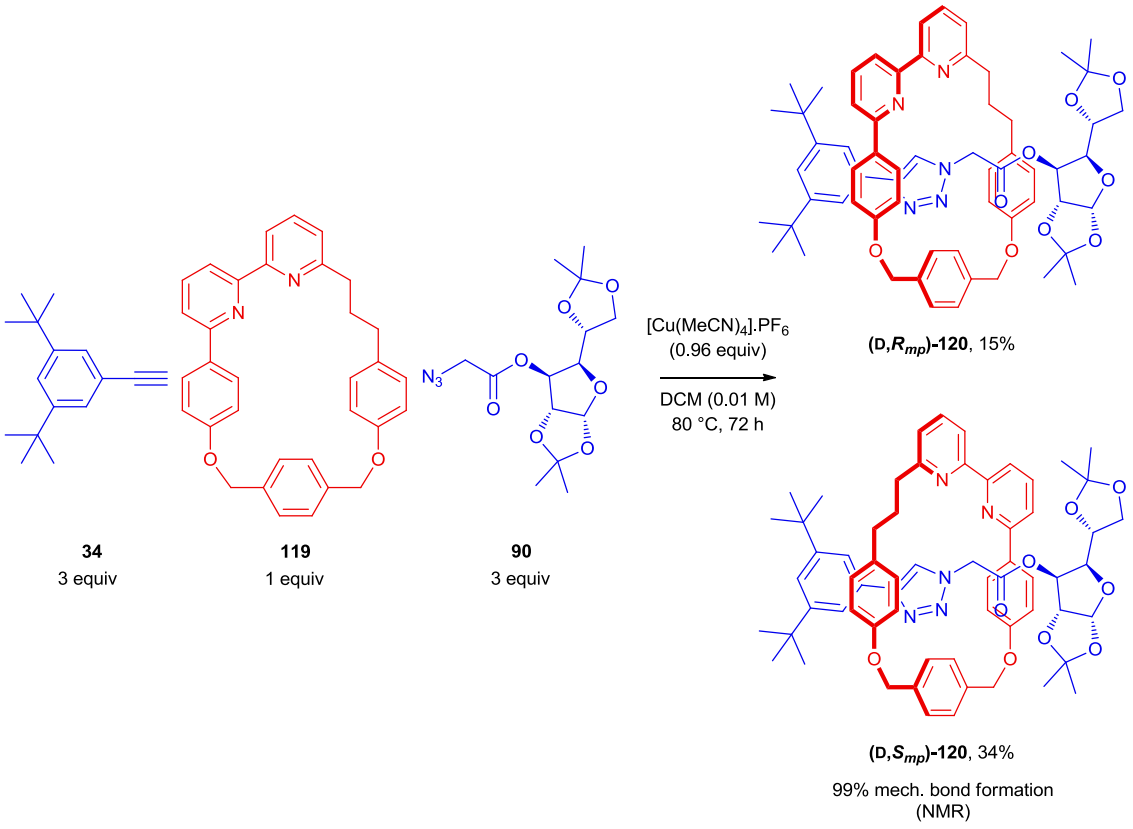

Figure 90: Rotaxanation of macrocycle 119 in the presence of DIPEA

3.2.3.1 – Stability of rotaxanes 120

While performing a series of experiments to improve the dr of the rotaxanation with the new macrocycle we observed significant variation in the dr of the rotaxanes. On multiple repeats of the rotaxanation with 3 equivalents of half-threads we observed differences in the dr from 2.1:1 up to 5.9:1 under seemingly identical conditions.

On examination of the reactions we observed the appearance of signals in the ^{1}H NMR that corresponded to diacetone-D-glucose (**92**). After examining the starting materials to ensure they were not contaminated we concluded that the source of **92** was from decomposition of the rotaxanes. At this time we did not observe large quantities of free macrocycle **119** and we concluded that the excess half-threads were able to re-capture the macrocycle to form more of rotaxanes **120**

While trying to understand the cause of the decomposition we found that the workup of the reactions affected the observed diastereomeric ratio. We found that splitting a reaction mixture and separately working up the two portions resulted in samples with varying dr values, even while following identical protocols. Furthermore, when attempting the separation of the two diastereoisomers we found that rotaxanes **120** would decompose during column chromatography. Rotaxanes **120** were much more polar than rotaxanes **96** and we resorted to a 9:1 mixture of dichloromethane and methanol to elute them from the column. Once the solvent was evaporated and the rotaxanes analysed by ^{1}H NMR we found that they were both contaminated with both macrocycle **119** and the protected sugar **92**.

In order to probe the stability of the rotaxanes an NMR experiment was performed. The rotaxanes were taken up in deuterated chloroform and methanol was added. It was observed that in the presence of methanol-d_4 the minor isomer was fully consumed over 90 minutes and was converted to macrocycle **119**, diacetone-D-glucose and the methyl ester of the thread. The major isomer was also consumed but at a slower rate. By performing an analogous experiment on the thread we subsequently found the free thread was stable to the presence of methanol in deuterated chloroform.

Given the instability of the rotaxanes which complicated the optimisation of the reaction, we decided instead to focus on the isolation and characterisation of the rotaxanes.

3.2.3.2 – Isolation of rotaxanes 120

The decomposition of rotaxane 120 proved troublesome during their purification. From the decomposition observed in the presence of methanol it was apparent that the rotaxanes were susceptible to small nucleophiles. In order to prevent further rotaxane decomposition a new solvent system was developed. A mixture of 3:1 chloroform-hexane was selected as the apolar phase as it allowed the thread and any unconsumed macrocycle to elute well before the rotaxanes, and ether was chosen as the polar solvent as it was effective in eluting the rotaxanes from the column in relatively narrow bands. Acetonitrile was briefly employed as the polar eluent but was also found (through an NMR experiment) to increase the rate of decomposition of the rotaxanes. It was thought that in this case the decomposition was driven by hydrolysis of the ester by trace water present in the acetonitrile.

Despite appearing to eliminate sources of nucleophiles from our solvent system we were still experiencing small amounts of decomposition of the minor diastereomer. After a period of purifying the rotaxanes under a new chloroform-petrol-ether system it was found that the chloroform was stabilised with approximately 0.7% ethanol. Ethanol free chloroform was obtained and the purification attempted again. However, the alcohol free solvent was much less effective at eluting the rotaxanes, which caused streaking and caused more mixed fractions to be collected. After observing the effect of doping the chloroform with different amounts of ethanol we found that adding 0.8% ethanol to the chloroform gave the optimum separation. To avoid decomposition of the diastereomers we developed a procedure that involved extracting the column fractions with water to remove residual ethanol before drying over sodium sulphate. The subsequent evaporation of chloroform and ether allowed the isolation of rotaxanes **120** in good yield. This procedure allowed us to isolate clean samples of both diastereomers for characterisation.

3.2.4 – Structural analysis of rotaxanes 120

Despite attempts to obtain the crystal structure of the diastereomeric rotaxanes we were unable to grow crystals of sufficient size and quality to obtain a good diffraction. For ease of discussion, we give these two enantiomers an arbitrary assignment. From here on we shall denote the first eluting (major) diastereomer of rotaxane **120** as (D,S_{mp})-**120**, and the second eluting (minor) diastereomer as (D,R_{mp})-**120**.

Samples of rotaxanes **120** were characterised by ^{1}H and ^{13}C NMR, as well as mass spectrometry and UV-vis and CD spectroscopy. To fully assign the absolute stereochemistry of the rotaxanes we required the crystal structure. However, despite numerous attempts it was not possible to prepare any samples of rotaxanes **120** suitable for X-ray crystallography due to decomposition during slow crystallisation.

3.2.4.1 – NMR spectra

Despite the ^{1}H NMR spectra of the two diastereomers showing significant differences, they also share some features of the NMR spectra of the rotaxanes containing macrocycle **74**. The ^{1}H NMR spectrum of rotaxanes **120** provides evidence for the mechanically chiral nature of the rotaxanes; the protons corresponding to H_e are (similarly to the signals in rotaxanes **96**) shifted to lower ppm and split into two widely separated doublets, which also appear to be broadened compared to those of the free thread. The position of the triazole proton H_c is significantly different, being shifted to a higher ppm of ~9.5 in (D,R_{mp})-**120**, and to a lower ppm of ~7.5 ppm in (D,S_{mp})-**120**. The signals from the benzylic protons (H_F and H_I) in the xylyl moiety of the macrocycle are split, from two doublets into two doublets of doublets in the rotaxanes as the thread desymmetrises the two sets of protons through the plane of the macrocycle.

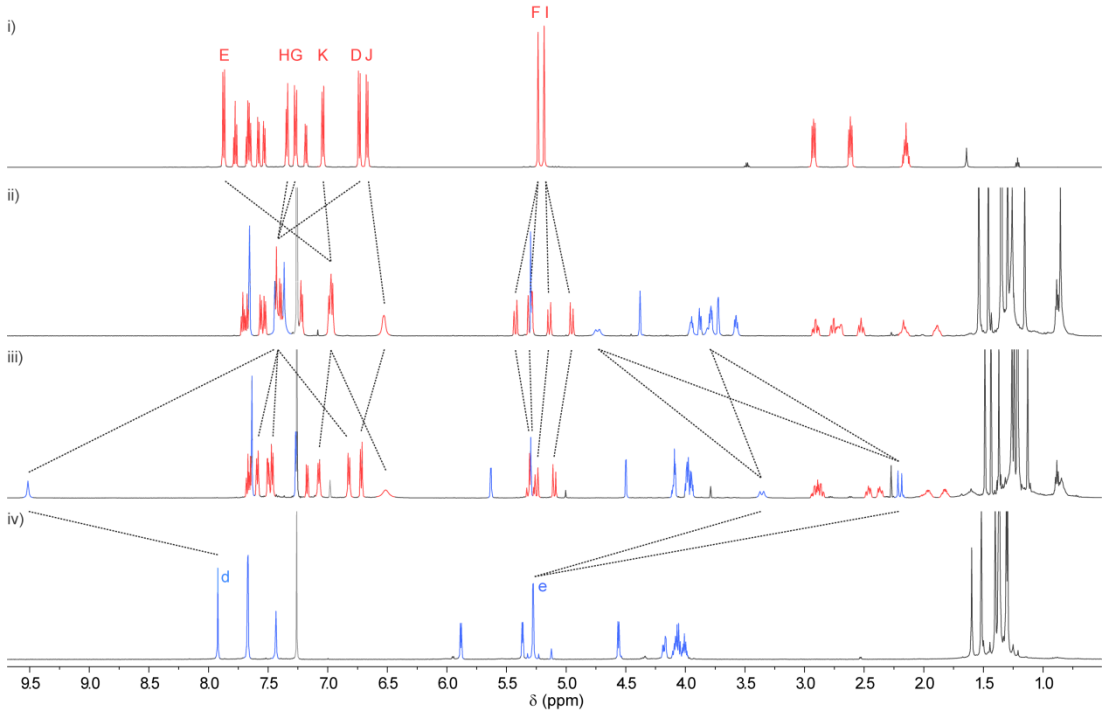

Figure 91: Partial ^{1}H NMR (600 MHz, $CDCl_3$, 300 K) showing i) macrocycle 119, ii) (D,S_{mp})-120, iii) (D,R_{mp})-120 and iv) the thread

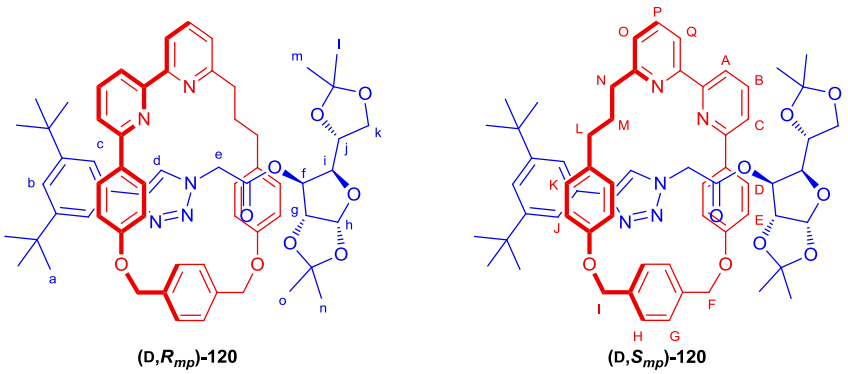

Figure 92: Structures of rotaxanes 120 with corresponding ^{1}H NMR atom labels

3.2.4.2 – Circular dichroism

The CD spectra of (D,S_{mp})-**120** and (D,R_{mp})-**120** were recorded. As with rotaxanes (D,S_{mp})-**96** and (D,S_{mp})-**96**, the spectra are significantly different indicating strong interplay between the mechanical and covalent sources of chirality.

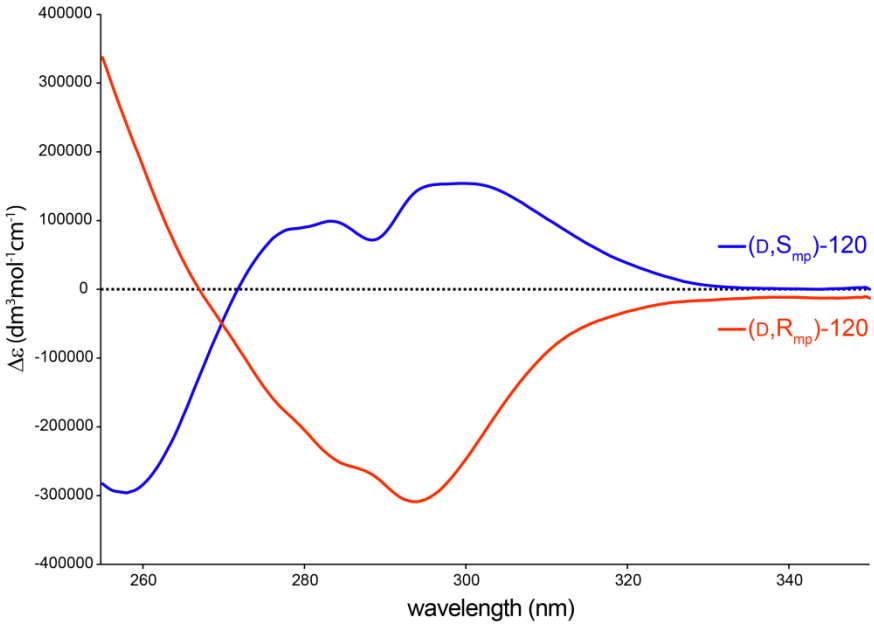

Figure 93: CD spectra of (D,S_{mp})-120 and (D,R_{mp})-120

3.2.5 – Synthesis of mechanically enantiomeric [2]rotaxanes

3.2.5.1 – Aminolysis of (D,S_{mp})-120 and (D,R_{mp})-120

The instability observed in rotaxanes **120** led us believe that they might undergo aminolysis under less forcing conditions than were required for the aminolysis of rotaxanes **96**. An NMR experiment was undertaken in which (D,S_{mp})-**120**, was subjected to the presence of 5 equivalents of 3,5-di-*tert*-butylbenzylamine (**98**) in deuterated chloroform (Figure 94).

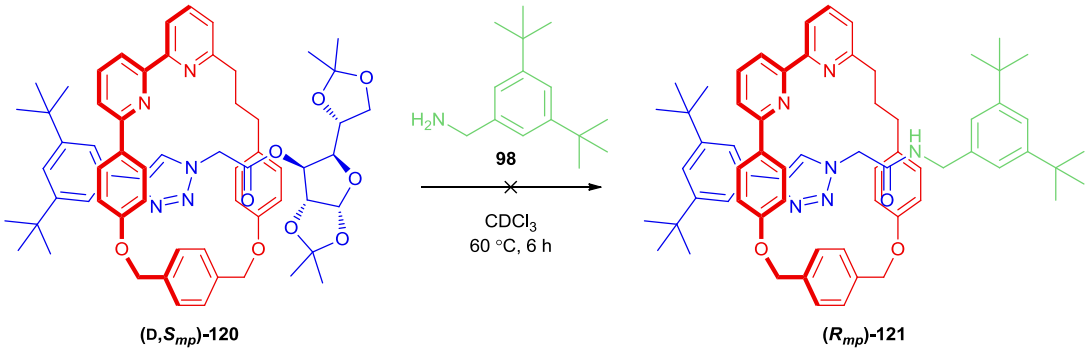

Figure 94: Attempted aminolysis of (D,S_{mp})-120

Despite being left for 16 hours the amine did not cleave the thread, nor did it on heating the reaction mixtures at 60 °C for a further 6 hours. The same reaction was repeated with (D,R_{mp})-**120** which gave the same result – no aminolysis was observed. Having ascertained that rotaxanes **120** required a more activated nucleophile they were then separately subjected to the established aminolysis conditions used in the synthesis of rotaxanes **121**. Pleasingly this reaction proceeded cleanly and in excellent yields (Figure 95).

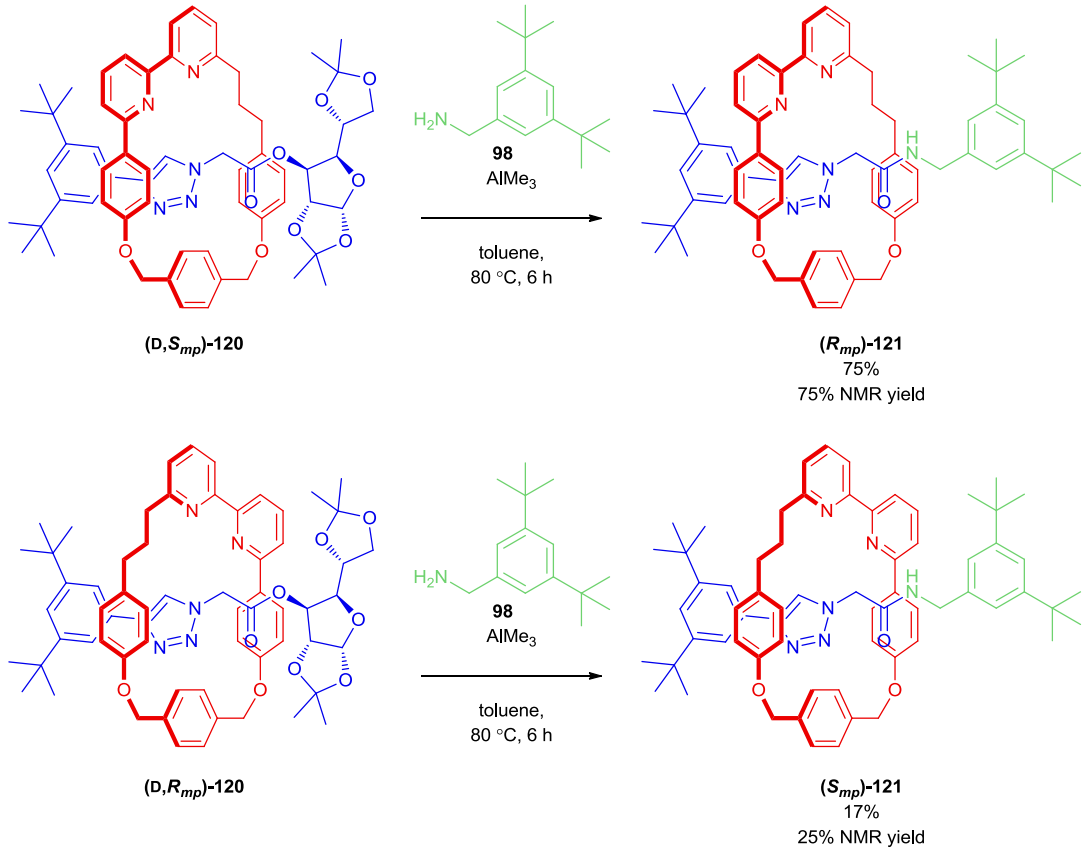

Figure 95: Aminolysis of rotaxanes 120

Purification of the rotaxanes was achieved via column chromatography, allowing the isolation of enantiomerically pure rotaxanes **121** in good yields.

3.2.5.2 – Synthesis of rac-121

A racemic sample of rotaxane **121** was synthesised through an AT-CuAAC coupling reaction between the amide derived azide half-thread **111** and alkyne half-thread **34**. Pleasingly the reaction completed in good yield with 3 equivalents of the half-threads.

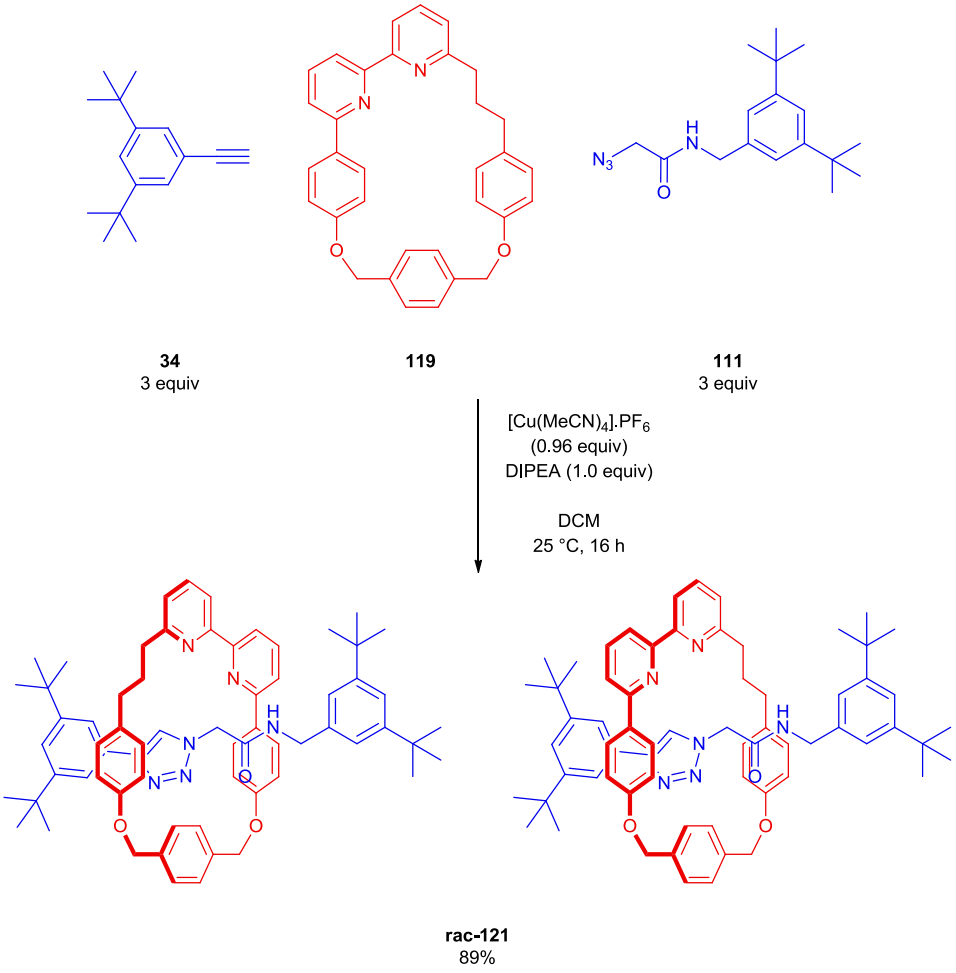

Figure 96: Synthesis of racemic rotaxanes 121

As expected, the NMR data for this compound matches the enantiopure material. The CD spectrum showed no chiral response as was expected for the racemic mixture. The mass spectrum isotope pattern matched both the predicted pattern and the spectra observed for the enantiopure samples.

3.2.6 – Characterisation of rotaxanes 121

Rotaxanes **125** were characterised by NMR, CD spectroscopy, mass spectroscopy and CSP-HPLC. We also attempted to prepare samples for analysis by X-ray crystallography. Unfortunately we were not able to prepare a crystal of sufficient quality to acquire the crystal structure.

3.2.6.1 – NMR spectra

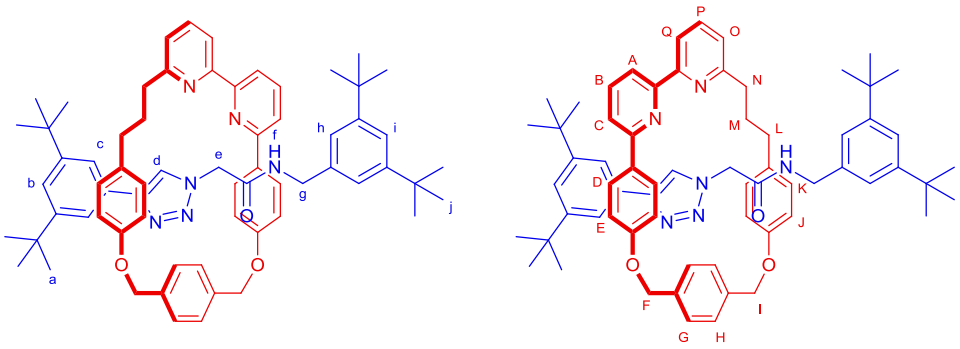

Figure 97: Digram of rotaxanes (R_{mp})-121 and (S_{mp})-121 with NMR atom labels

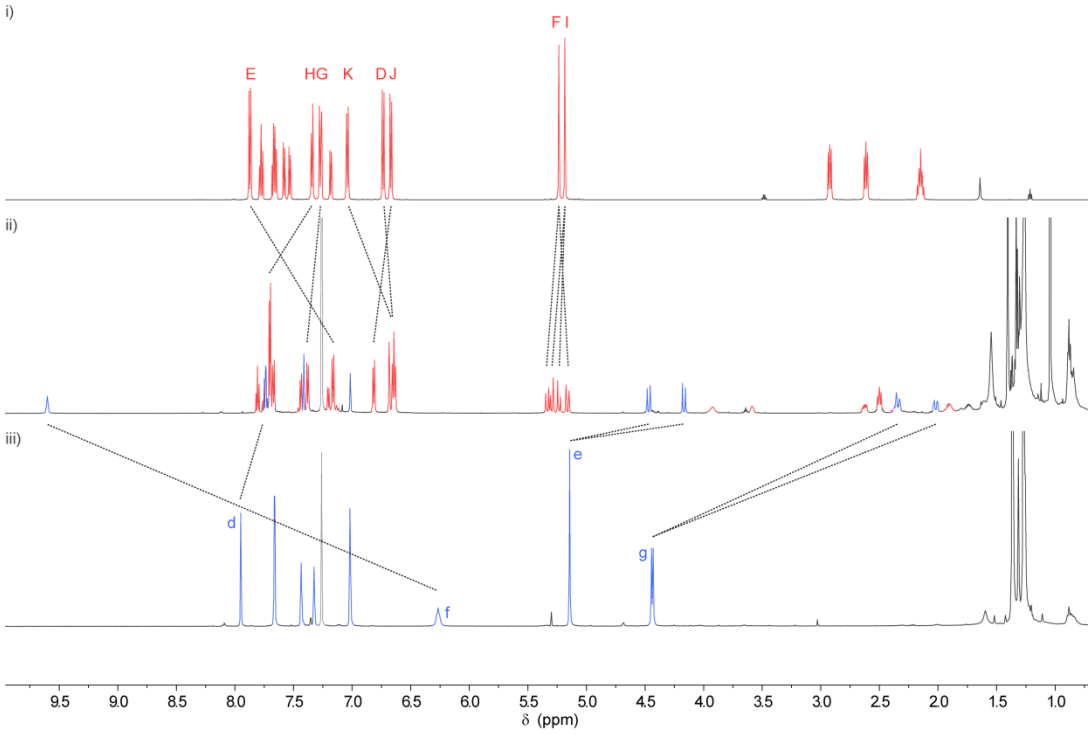

Figure 98: NMR (600 MHz, $CDCl_3$, 300 K) of i) macrocycle 119, ii) rotaxane 121 and iii) thread

Protons H_e and H_g, which are enantiotopic in the thread, are diastereotopic in the rotaxane and their signals are shifted to lower ppm. Both signals appear as pairs of doublets, where H_e moves from 5.14 ppm in the thread to 4.47 and 4.17 ppm in the rotaxane, and H_g moves from 4.43 ppm in the thread to 2.34 and 2.02 ppm in the rotaxane.

The signal for the amide proton, H_f, moves from 6.27 ppm in the free thread up to 9.60 ppm in the rotaxane, which is tentatively assigned to a hydrogen bond with the macrocycle. This assignment is corroborated by the lack of a significant change in the chemical shift of H_d. Signals for protons H_F and H_I are also desymmetrised but experience relatively small changes in chemical shift.

3.2.6.2 – Circular dichroism

As expected, the CD spectra of rotaxanes **121** are mirror images of each other, indicating their enantiomeric nature. Similarly to rotaxanes **109** the enantiomers do not invert in phase across the observed spectrum.

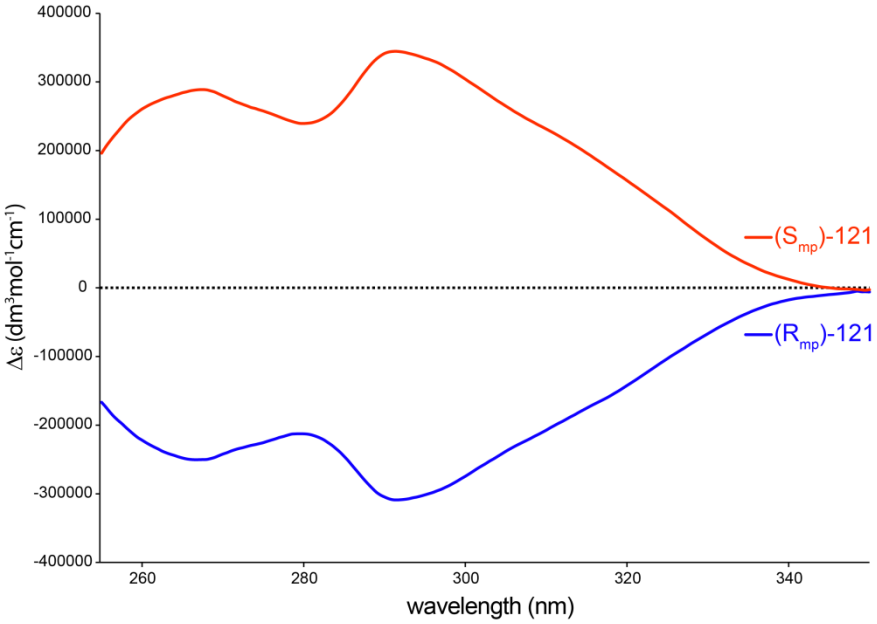

Figure 99: CD spectra of (S_{mp})-121 and (R_{mp})-121

3.2.6.3 – CSP-HPLC

HPLC data for both enantiomers and the racemate of **121** was acquired by Regis Technologies Inc. The data show that the enantiomers isolated were enantiomerically pure and that the racemate sample corresponds to the same compounds (in alignment with the NMR and mass spectral data).

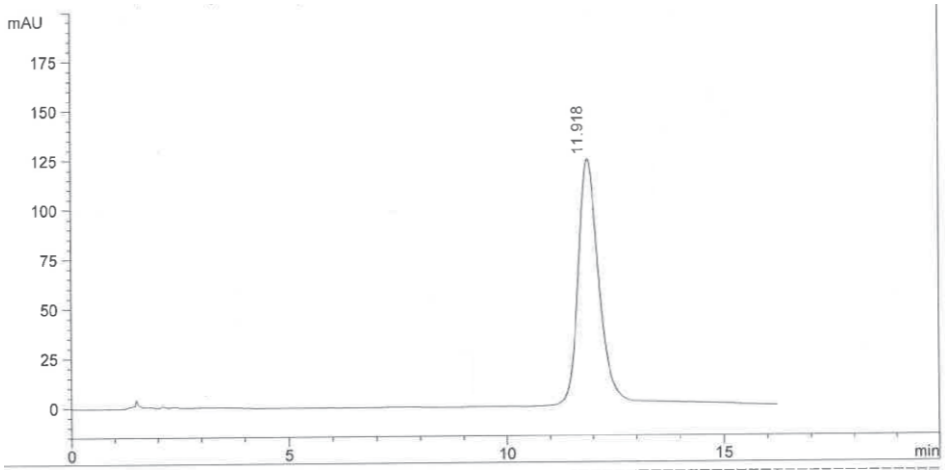

Figure 100: CSP-HPLC trace of (R_{mp})-121

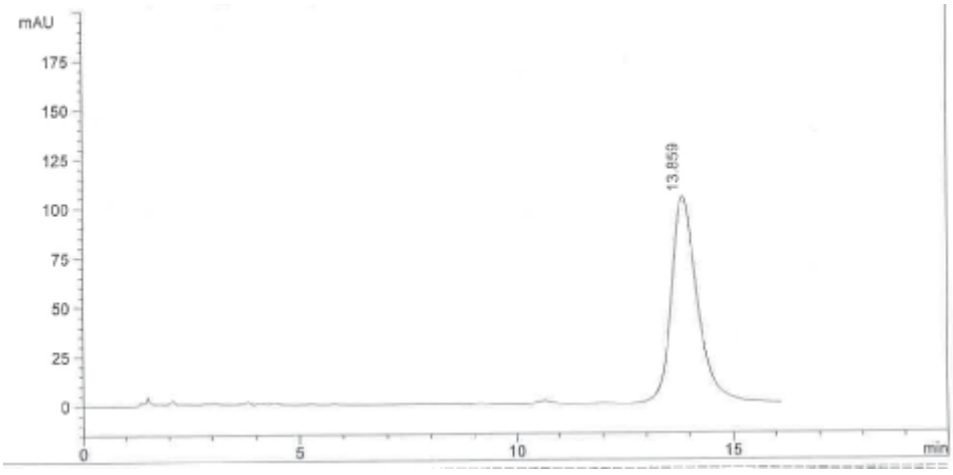

Figure 101: CSP-HPLC trace of (S_{mp})-121

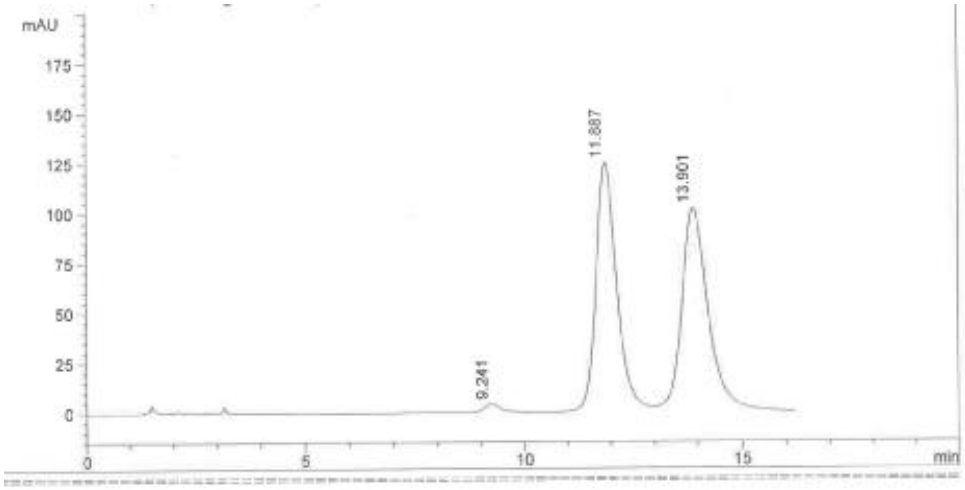

Figure 102: CSP-HPLC trace of rac-121

3.2 – Concluding remarks

Here we have successfully demonstrated the diastereoselective synthesis of mechanically planar chiral rotaxanes in a 2.3:1 ratio. The methodology we have developed utilises easily accessible starting materials, and enables the synthesis of mechanically planar chiral rotaxanes in good yields. The methodology could be developed further and we hope that the selectivity of the rotaxane forming reaction could be improved by the further modification of the structure of the macrocycle and half-thread reagents.

We would also like to investigate the properties of these materials, and future areas of research we would like to investigate include employing the chiral rotaxane materials as catalytic reagents in chiral transformations, as well as to investigate the chiral switching properties in bistable mechanically planar chiral rotaxanes.

Further, we would like to determine which of the structural properties of the rotaxane components are key to ensuring high selectivity in the rotaxanation step. This investigation would include screening a selection of different macrocycle structures against the half-threads already investigated, as well as a selection of new, small, chiral half-threads.

We propose the post synthesis modification of rotaxanes **109** and **121** as a way of quickly accessing potentially catalytically active mechanically planar chiral materials, with the potential to screen their catalytic activity.

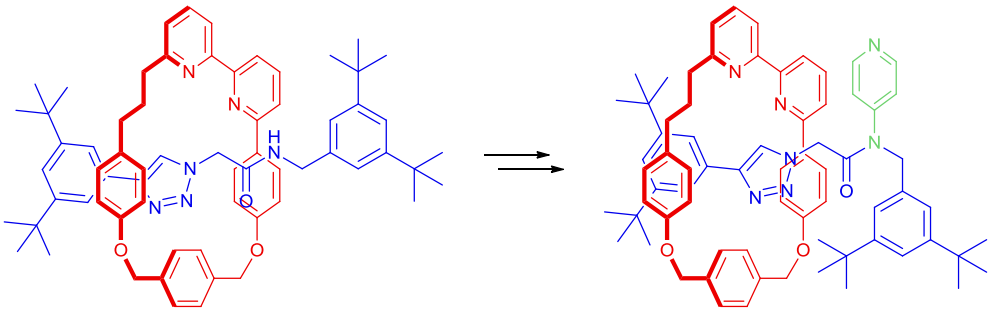

Figure 103: One example for the potential post-synthetic modification of rotaxanes 121

3.3 – References

[45] Tang, J. S.; Verkade, J. G. **1996**, *28*, 8750.

Chapter 4 – Experimental Section

4.1 – General remarks

Unless otherwise stated, all reagents were purchased from commercial sources and used without purification. All reactions were carried out under an atmosphere of N_2 using anhydrous solvents unless otherwise stated. Anhydrous solvents were obtained by passing the solvent through an activated alumina column on an MBRAUN MB SPS-800 solvent purification system. Flash column chromatography was performed using Varian Intelliflash, or Biotage Isolera-4 automated chromatography systems, employing Varian Superflash, or Biotage SNAP or ZIP cartridges. Analytical TLC was performed on pre-coated silica gel plates (0.25 mm thick, 60F254, Merck, Germany) and observed under 254 nm UV light. NMR spectra were recorded on Bruker AV–400, AV3–400 or AV–600 instruments, at a constant temperature of 300 K. Chemical shifts are reported in parts per million from low to high field and referenced to residual solvent. Coupling constants (*J*) are reported in Hertz (Hz). Standard abbreviations indicating multiplicity were used as follows: m = multiplet, quint. = quintet, q = quartet, t = triplet, d = doublet, s = singlet, br = broad, ap = apparent. Melting points were determined using a Sanyo Gallenkamp apparatus and are uncorrected. Low resolution mass spectrometry was carried out by the mass spectrometry services at the Queen Mary University of London. High resolution mass spectrometry was carried out by the EPSRC National Mass Spectrometry Centre in Swansea. Circular dichromism (CD) spectra were acquired on an Applied Photophysics Chirascan spectropolarimeter, recorded using Applied Photophysics software Ver. 4.2.0, in a quartz cell of 0.5 cm path length at a concentration of 10^{-4} M in $CHCl_3$.

4.2 – Reagent preparation

Below are descriptions of the preparation of general reagents and solutions.

1 M HBr in MeOH

MeOH (500 mL) was stirred at 0 °C and acetyl bromide (37.0 mL, 500 mmol) was added slowly via syringe. The mixture was allowed to warm to rt and was used within 1 h.

1 M $ZnCl_2$ in THF

$ZnCl_2$ (35.2 g, 251 mmol) was dried under high vacuum at 160 °C for 16 h. THF (251 mL) was added and the mixture stirred for 6 h until fully dissolved.

1 M EDTA in aqueous NH_3

EDTA-Na_4 (730g, 2.5 mol) was dissolved in a 50:50 mixture of aqueous NH_3 (1.25 L, 35.5% w/w) and tap water (1.25 L).

4.3 – Synthetic procedures

The following compounds were synthesised according to literature procedures: **34**, **94**, **98**.

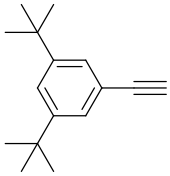

34

Ethynyl-3,5-di-*tert*-butylbenzene (34)[46]**:** 1-bromo-3,5-di-tert-butylbenzene (582 mg, 2.16 mmol) was stirred in THF (10 mL) in a 25mL RBF. To the flask was added TMS-acetylene (0.336 mL, 2.38 mmol) and Et_3N (0.331 mL, 2.38 mmol), followed by careful addition of $Pd(PPh_3)_4$ (125 mg, 0.108 mmol) and CuI (41.2 mg, 0.216 mmol) through a funnel in the neck of the flask. The flask was resealed and re-flushed with N_2, heated to 60°C and stirred for 16 h. The reaction was reduced *in vacuo* and the residue eluted through a silica plug in ethyl acetate (20%) in petrol. The crude material was stirred in MeOH (15 mL) and CH_2Cl_2 (15 mL) with K_2CO_3 (1.0 g, 8.0 mmol) for 2 h before being diluted with diethyl ether (100 mL) and washed with water (2 x 100 mL). The organic extracts were dried over $MgSO_4$ and reduced *in vacuo*. The residue was purified by chromatography in petrol and gave the target as a colourless crystalline solid (388 mg, 84% yield); m.p. 87 – 89 °C; ^{1}H NMR (400 MHz, $CDCl_3$) δ 7.42 (t, *J* = 1.8, 1H), 7.35 (d, *J* = 1.9, 2H), 3.02 (s, 1H), 1.31 (s, 18H); ^{13}C NMR (101 MHz, $CDCl_3$) δ 150.8, 126.3, 123.2, 121.0, 84.8, 75.7, 34.7, 31.2. LRMS (ESI +ve) 215 $[M+H]^+$.

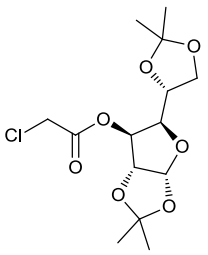

94

Half-thread intermediate 94[47]: α-D-glucofuranose (1.06g, 4.08 mmol) was stirred in CH_2Cl_2 (25 mL) to which pyridine (0.645 mL, 8.16 mmol) was added, followed by the addition of 2-chloroacetyl chloride (0.47 mL, 4.90 mmol) slowly over 5 minutes. The reaction was stirred for 16h, at which time it was diluted with 50 mL CH_2Cl_2, and washed with 3 x 50 mL brine. The extracts were combined, dried over $MgSO_4$ and reduced *in vacuo*. The residue was purified via column chromatography (15% ethyl acetate in petrol) and the target was isolated as a colourless oil (1.25g, 93%). ^{1}H NMR (400 MHz, $CDCl_3$) δ 5.92 (d, *J* = 3.7, 1H), 5.37 (d, *J* = 1.8, 1H), 4.55 (d, *J* = 3.7, 1H), 4.26 – 4.21 (m, 2H), 4.17 – 4.08 (m, 2H), 4.06 – 4.01 (m, 1H), 1.55 (s, 3H), 1.43 (s, 3H), 1.34 (s, 6H); ^{13}C NMR (101 MHz, $CDCl_3$) δ 166.2, 112.7, 109.7, 105.3, 83.3, 80.0, 77.9, 72.5, 67.6, 40.7, 27.0, 26.9, 26.4, 25.4; LRMS (ESI +ve) 337 $[M+H]^+$.

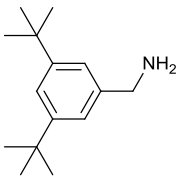

98

3,5-di-*tert*-butylbenzylamine (98)[48]: 3,5-di-*tert*-butylbenzylbromide (103 mg, 0.363 mmol) was stirred in DMF (10 mL) with NaN_3 (26.0 mg, 0.400 mmol) at 25°C for 6 hours. At this time the reaction was diluted with Et_2O (50 mL) and washed with water (3 x 50 mL). The combined aqueous was extracted with Et_2O (50 mL) and the organic extracts were combined and dried over $MgSO_4$ before reducing them *in vacuo*. The extracts were re-dissolved in Et_2O (25 mL) and stirred in an ice bath (at 0°C). To this flask was slowly added $NaBH_4$ (27.5 mg, 0.726 mmol) and the reaction stirred for 1 hour while allowing it to warm to 25°C. The reaction was quenched with MeOH (10 mL) and the organic washed with water (3 x 50 mL). The organic extracts were reduced *in vacuo*, dried over $MgSO_4$, and purified via column chromatography eluting in petrol and CH_2Cl_2. The amine was isolated as a viscous colourless oil which crystallised on standing (72 mg, 0.33 mmol); m.p. 75 – 77 °C; NMR (400 MHz,) 7.33 (t, *J* = 1.7, 1H), 7.16 (d, *J* = 1.8, 2H), 3.86 (s, 2H), 1.33 (s, 18H); ^{13}C NMR (101 MHz, $CDCl_3$) δ 151.4, 134.5, 122.3, 122.3, 55.5, 34.8, 31.4; LRMS (ESI +ve) 220 $[M+H]^+$.

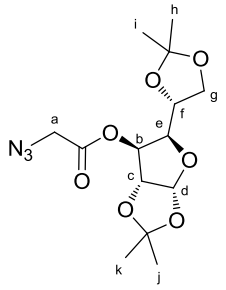

90

(3a*R*,5*R*,6*S*,6a*R*)-5-((*R*)-2,2-Dimethyl-1,3-dioxolan-4-yl)-2,2-dimethyltetrahydrofuro[2,3-*d*][1,3]dioxol-6-yl 2-azidoacetate (90): All operations were conducted under air. A 25 mL round bottomed flask was charged with α-chloroacetate **94**[1] (1.10 g, 3.27 mmol), DMF (10 mL) and NaN_3 (266 mg, 4.09 mmol) and the reaction mixture stirred at 60 °C for 16 h. The reaction was partitioned between CH_2Cl_2 (100 mL) and H_2O (100 mL), the aqueous layer was extracted with CH_2Cl_2 (100 mL) and the combined organic extracts washed with brine (100 mL). The combined organic extracts were dried over $MgSO_4$ and reduced *in vacuo*. Chromatography (15% EtOAc in petrol, R_f = 0.15) afforded azide **90** as a white crystalline solid (1.00 g, 89%); $[\alpha]_D^{20}$ –51.5 (c = 1.0, $CHCl_3$); m.p. 74 – 76 °C; ^{1}H NMR (400 MHz, $CDCl_3$) δ 5.89 (d, *J* = 3.7, 1H, H_d), 5.38 (d, *J* = 2.4, 1H, H_b), 4.54 (d, *J* = 3.7, 1H, H_c), 4.23 – 3.98 (m, 4H, H_e, H_f, and H_g), 3.94 (d, *J* = 17.2, 1H, one of H_a), 3.89 (d, *J* = 17.2, 1H, one of H_a), 1.52 (s, 3H, H_j or H_k), 1.41 (s, 3H, H_j or H_k), 1.31 (s, 6H, H_h and H_i); ^{13}C NMR (101 MHz, $CDCl_3$) 167.1, 112.5, 109.6, 105.1, 83.2, 78.8, 77.4, 72.4, 67.5, 50.3, 26.9, 26.7, 26.2, 25.2; LRMS (ESI +ve) 344 $[M+H]^+$; HRMS (NSI +ve) 366.1270 $[M+Na]^+$ (calc. for $C_{14}H_{21}N_3O_7$ 366.1272 $[M+Na]^+$).

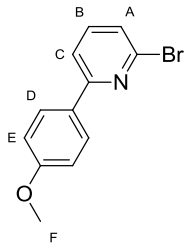

73

2-Bromo-6-(4-methoxyphenyl)pyridine (73); A dry 500 mL round bottomed flask with stirrer bar was charged with 2,6-dibromopyridine (23.6 g, 100 mmol), 4-methoxyphenylboronic acid (21.3 g, 140 mmol), K_2CO_3 (55.4 g, 400 mmol), $PdCl_2$ (173 mg, 0.976 mmol) and PPh_3 (526 mg, 2.01 mmol). Into this flask was cannulated a degassed mixture of DME-H_2O (2:1, 75 mL) and the reaction mixture heated at 60 °C for 96 h. The reaction mixture was partitioned between EtOAc (400 mL) and H_2O (400 mL) and the layers separated. The aqueous layer was extracted with EtOAc (2 × 200 mL) and the combined organic extracts washed with brine (200 mL). The combined organic extracts were dried over $MgSO_4$ and reduced *in vacuo*. The residue was refluxed in petrol (300 mL) for 30 min, allowed to cool, and then filtered. The solid residue was extracted with refluxing Et_2O (300 mL) for 30 min, filtered and the filtrate reduced *in vacuo* to yield pyridine **73** as a pale cream solid (15.9 g, 60%); m.p. 109 – 111 °C (Et_2O), literature[49] 110 °C; ^{1}H NMR (400 MHz, $CDCl_3$) δ 7.95 (d, J = 8.6, 2H, H_D), 7.61 (d, J = 7.7, 1H, H_C), 7.54 (ap t, J = 7.7, 1H, H_B), 7.34 (d, J = 7.7, 1H, H_A), 6.98 (d, J = 8.6, 2H, H_E), 3.87 (s, 3H, H_F); ^{13}C NMR (151 MHz, $CDCl_3$) δ 158.3, 142.1, 138.9, 130.3, 128.4, 127.3, 125.5, 118.1, 114.2, 55.4.

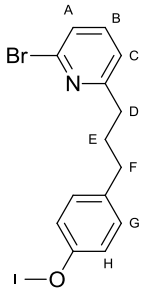

77

2-Bromo-6-(3-(4-methoxyphenyl)propyl)pyridine (77): A dry 500 mL round bottomed flask with stirrer bar was charged with 4-allylanisole (18.5 g, 125 mmol), followed by a solution of 9-borabicyclo[3.3.1]nonane (9-BBN) (250 mL, 0.5 M in THF, 125 mmol) and the mixture stirred at rt for 2 h to give a solution of the corresponding alkyl borane. A second dry 500 mL round bottomed flask with stirrer bar was charged with 2,6-dibromopyridine (29.5 g, 125 mmol), K_2CO_3 (51.8 g, 375 mmol), $PdCl_2$ (221 mg, 1.25 mmol) and PPh_3 (666 mg, 2.50 mmol) and was flushed with N_2. Into this flask was cannulated the solution of the alkyl borane, followed immediately by degassed H_2O (125 mL), and the reaction mixture heated at 60 °C for 16 h. The reaction mixture was partitioned between EtOAc (400 mL) and H_2O (400 mL), and the aqueous layer extracted further with EtOAc (2 × 200 mL). The combined organic extracts were washed with brine (200 mL), dried over $MgSO_4$ and reduced *in vacuo*. The residue was acidified by addition of HBr (1 M in MeOH, 500 mL) and this mixture stirred for 1 h at rt before being reduced *in vacuo*. Petrol (250 mL) was added to the residue, the mixture stirred for 1 h, the solvent decanted and discarded and this operation repeated. The residue was dissolved in EtOAc (200 mL) and washed with 1 M $K_2CO_{3\ (aq.)}$ (200 mL), brine (200 mL), dried over $MgSO_4$ and reduced *in vacuo* to give pyridine **77** as a yellow oil (23.5 g, 72%); b.p. 141 – 143 °C; ^{1}H NMR (400 MHz, $CDCl_3$) δ 7.43 (ap t, *J* = 7.7, 1H, H_B), 7.29 (d, *J* = 7.8, 1H, H_A), 7.10 (d, *J* = 8.6, 2H, H_G), 7.07 (d, *J* = 7.6, 1H, H_C), 6.82 (d, *J* = 8.6, 2H, H_H), 3.78 (s, 3H, H_I), 2.78 (t, *J* = 7.7, 2H, H_D), 2.61 (t, *J* = 7.6, 2H, H_F), 2.01 (ap quint., *J* = 7.7, 2H, H_E); ^{13}C NMR (101 MHz, $CDCl_3$) δ 163.9, 157.9, 141.7, 138.7, 134.1, 129.4, 125.4, 121.7, 113.9, 55.4, 37.6, 34.7, 31.7; LRMS (ESI +ve): 306 $[M+H]^+$; HRMS (EI +ve) 305.0411 $[M]^+$ (calc. for $C_{15}H_{16}{}^{79}BrNO$ 305.0410 $[M]^+$).

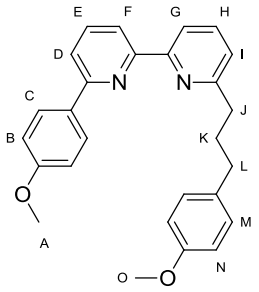

76

6-(4-Methoxyphenyl)-6'-(3-(4-methoxyphenyl)propyl)-2,2'-bipyridine (76): A dry 250 mL round bottomed flask with stirrer bar was charged with 2-bromopyridine **73** (10.6 g, 40.0 mmol) and THF (66 mL) and stirred at –78 °C. *n*-BuLi (17.6 mL, 2.5 M in hexanes, 44.0 mmol) was added slowly down the side of the flask and the mixture stirred at –78 °C for 1 h. $ZnCl_2$ (44.0 mL, 1 M in THF, 44.0 mmol) was added slowly, the reaction mixture allowed to warm to rt and stirred for 1 h to give a solution of the desired 2-pyridyl organozinc. A 250 mL round bottomed flask with stirrer bar was charged with alkyl pyridine **77** (10.2 g, 33.3 mmol), $PdCl_2$ (118 mg, 0.67 mmol), PPh_3 (350 mg, 1.33 mmol) and THF (20 mL). The mixture was allowed to stir for 5 min after which time the 2-pyridyl organozinc reagent was added *via* cannula and the reaction mixture stirred at 40 °C for 16 h. The reaction mixture was filtered through a pad of Celite and the filter washed with EtOAc. The filtrate was partitioned between EtOAc (250 mL) and EDTA-NH_3 solution (250 mL), the layers separated and the aqueous phase extracted with EtOAc (2 × 150 mL). The combined organic extracts were washed with brine (250 mL), dried over $MgSO_4$, and reduced *in vacuo*. The solid residue was recrystallised from EtOH to give bipyridine **78** as fine cream coloured needles (7.12 g, 52%); m.p. 109 – 111 °C (EtOH); ^{1}H NMR (400 MHz, $CDCl_3$) δ 8.43 (d, *J* = 7.6, 1H, H_G), 8.37 (d, *J* = 7.3, 1H, H_F), 8.12 (d, *J* = 8.8, 2H, H_C), 7.84 (ap t, *J* = 7.8, 1H, H_E), 7.74 (ap t, *J* = 7.7, 1H, H_H), 7.70 (d, *J* = 7.8, 1H, H_D), 7.16 (ap d, *J* = 8.3, 3H, H_N and H_I), 7.03 (d, *J* = 8.9, 2H, H_B), 6.85 (d, *J* = 8.6, 2H, H_M), 3.89 (s, 3H, H_A), 3.80 (s, 3H, H_O), 2.91 (t, *J* = 7.6, 2H, H_J), 2.69 (t, *J* = 7.7, 2H, H_L), 2.15 (ap quint., *J* = 7.6, 2H, H_K); ^{13}C NMR (101 MHz, $CDCl_3$) δ 161.7, 160.6, 157.8, 156.2, 156.1, 155.9, 137.6, 137.1, 134.6, 132.3, 129.5, 128.3, 122.9, 119.4, 118.9, 118.6, 114.2, 113.9, 55.5, 55.4, 37.9, 34.7, 31.6; LRMS (ESI +ve) 411 $[M+H]^+$; HRMS (NSI +ve) 411.2066 $[M+Na]^+$ (calc. for $C_{27}H_{26}N_2O_2$ 411.2067 $[M+H]^+$);

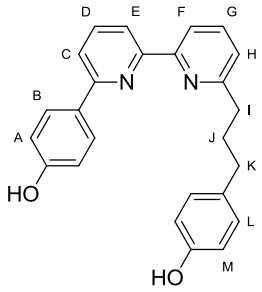

75

4-(3-(6'-(4-Hydroxyphenyl)-[2,2'-bipyridin]-6-yl)propyl)phenol (75): A 100 mL round bottomed flask was charged with bis-methyl ether **76** (7.12 g, 17.3 mmol) and HBr $_{(aq.)}$ (50 mL, 49% w/w, 220 mmol) and the mixture heated under reflux for 6 h. The reaction mixture was allowed to cool and reduced *in vacuo* using a water aspirator. The residue was partitioned between CH_2Cl_2 (100 mL), H_2O (100 mL) and Et_3N (20 mL) added. The aqueous phase was extracted with $CHCl_3$-IPA (3:1, 2 × 100 mL), the combined organic extracts dried over $MgSO_4$ and the solvent removed *in vacuo*. Macrocycle precursor **75** was isolated as an off-white solid (6.56 g, 99%); m.p. 89 – 91 °C (EtOH); ^{1}H NMR (400 MHz, $CDCl_3$) δ 8.35 (d, *J* = 7.8, 1H, H_F), 8.27 (d, *J* = 7.7, 1H, H_E), 8.00 (d, *J* = 8.7, 2H, H_B), 7.80 (ap t, *J* = 7.8, 1H, H_D), 7.71 (ap t, *J* = 7.7, 1H, H_G), 7.65 (d, *J* = 7.8, 1H, H_C), 7.14 (d, *J* = 7.6, 1H, H_H), 7.04 (d, *J* = 8.4, 2H, H_M), 6.92 (d, *J* = 8.6, 2H, H_A), 6.73 (d, *J* = 8.4, 2H, H_L), 2.88 (t, *J* = 7.8, 2H, H_I), 2.62 (t, *J* = 7.2, 2H, H_K), 2.09 (m, 2H, H_J); ^{13}C NMR (101 MHz, $CDCl_3$) δ 161.5, 157.8, 156.4, 156.0, 156.0, 154.4, 137.7, 137.2, 133.9, 131.5, 129.6, 128.5, 122.9, 119.4, 118.8, 118.8, 115.8, 115.3, 37.8, 34.7, 31.7; LRMS (ESI +ve) 383 $[M+H]^+$; HRMS (NSI +ve) 383.1757 $[M+H]^+$ (calc. for $C_{25}H_{22}N_2O_2$ 383.1759 $[M+H]^+$);

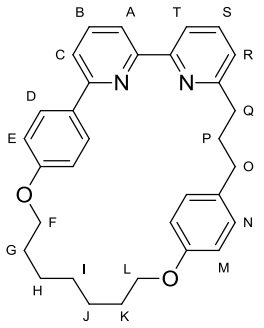

74

Macrocycle 76: A dry 2 L round bottomed flask was charged with bis-phenol **75** (2.01 g, 5.23 mmol), K_2CO_3 (7.23 g, 52.3 mmol), DMF (1.9 L) and 1,7-dibromoheptane (0.893 mL, 5.23 mmol). The reaction mixture was stirred at 80 °C for 72 h after which time the solvent was removed *in vacuo*. The residue was extracted with refluxing Et_2O (3 × 200 mL), the extracts combined and reduced *in vacuo*. The residue was purified by flash chromatography (1st column: 1:1 petrol-CH_2Cl_2 0→10% MeCN; 2nd column: petrol 0→50% Et_2O) and the fractions containing macrocycle **74** were subsequently recrystallised from ^{t}BuOMe to yield macrocycle **74** (100 mg, 4%); m.p. 132 – 134 °C (^{t}BuOMe); ^{1}H NMR (400 MHz, $CDCl_3$) δ 8.14 (d, *J* = 8.6, 2H, H_D), 7.81 (ap t, *J* = 7.7, 1H, H_B), 7.72 – 7.68 (m, 2H, H_C and H_S), 7.66 (dd, *J* = 7.6, 0.7, 1H, H_A), 7.63 (d, *J* = 7.7, 1H, H_T), 7.29 (d, *J* = 8.2, 2H, H_N), 7.21 (d, *J* = 7.2, 1H, H_R), 6.91 (d, *J* = 8.6, 2H, H_E), 6.80 (d, *J* = 8.3, 2H, H_M), 4.07 (t, *J* = 6.4, 2H, H_F), 3.95 (t, *J* = 6.1, 2H, H_L), 3.01 (t, *J* = 6.9, 2H, H_Q), 2.70 (t, *J* = 7.5, 2H, H_O), 2.34 (m, 2H, H_P), 1.90 – 1.77 (m, 4H, H_G and H_K), 1.61 - 1.43 (m, 6H, H_H, H_I and H_J); ^{13}C NMR (151 MHz, $CDCl_3$) δ 162.4 (N=**C**C_R), 160.0 (C_E=**C**-O), 157.3 (C_M**C**O), 156.7 (N=**C**C_A or N=**C**C_C), 156.5 (N=**C**C_T), 137.4 (C_B), 136.8 (C_S), 136.0 (C_N**C**C_O), 132.0 (C_D**C**-py), 129.9 (C_N), 128.6 (C_D), 122.8 (C_R), 119.6 (C_A), 119.5 (C_T), 118.6 (C_C), 115.0 (C_E), 114.5 (C_M), 68.0 (C_F), 67.5 (C_L), 37.1 (C_Q), 34.3 (C_O), 31.2 (C_P), 28.1 (C_G or C_K), 27.5(C_G or C_K), 26.9 (C_H, C_I or C_K), 25.5 (C_H, C_I or C_K), 25.4 (C_H, C_I or C_K); LRMS (ESI +ve) 479 $[M+H]^+$; HRMS (NSI +ve) 479.2684 $[M+H]^+$ (calc. for $C_{32}H_{34}N_2O_2$ 479.2693 $[M+H]^+$). Crystals suitable for x-ray crystallography were grown from 1:1 ^{t}BuOMe-CH_2Cl_2 *via* slow evaporation.

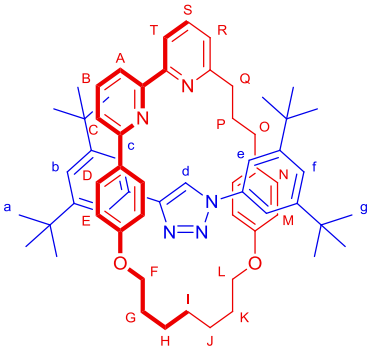

87

Rotaxane 87: A dry CEM microwave vial was charged with macrocycle **74** (11.9 mg, 0.025 mmol), azide **32** (5.78 mg, 0.025 mmol), alkyne **34**[2] (5.4 mg, 0.025 mmol), and $[Cu(MeCN_4)].PF_6$ (8.4 mg, 0.023 mmol). CH_2Cl_2 (2.5 mL) was added and the reaction mixture stirred at 80 °C for 72 h. After this time the reaction mixture was poured into EDTA-$NH_{3\ (aq)}$ (50 mL) and extracted with CH_2Cl_2 (3 × 50 mL). The combined organic extracts were washed with brine (50 mL), dried over $MgSO_4$, and reduced *in vacuo*. Chromatography (eluting in 1:1 petrol-CH_2Cl_2 up to 10% MeCN) gave **87** (9.23 mg, 40%) as a colourless solid; m.p. 157 – 159 °C (CH_2Cl_2); ^{1}H NMR (400 MHz, $CDCl_3$) δ 10.08 (s, 1H, H_d), 7.75 (t, *J* = 7.7, 1H, H_B), 7.68 – 7.63 (m, 2H, H_S and H_T), 7.57 – 7.53 (m, 3H, H_c and H_A), 7.51 (d, *J* = 1.6, 2H, H_e), 7.44 (t, *J* = 1.7, 1H, H_f), 7.36 (t, *J* = 1.7, 1H, H_b), 7.22 – 7.15 (m, 2H, H_C and H_R), 6.88 (d, *J* = 8.6, 2H, H_D), 6.33 (d, *J* = 8.5, 2H, H_M), 6.22 (d, *J* = 8.6, 2H, H_N), 6.17 (d, *J* = 8.5, 2H, H_E), 4.31 – 4.23 (m, 2H, H_O), 4.20 – 4.10 (m, 4H, H_Q and one each of H_F and H_L), 4.05 – 3.94 (m, 4H, H_P and one each of H_F and H_L), 2.69 – 2.50 (m, 2H, H_G), 2.37 – 2.30 (m, 2H, H_K), 2.19 – 2.15 (m, 2H, H_H), 1.93 – 1.89 (m, 2H, one of H_I and one of H_J), 1.84 – 1.71 (m, 2H, one of H_I and one of H_J), 1.16 (s, 18H, one of H_a or H_g), 1.14 (s, 18H, one of H_a or H_g). LRMS (ESI +ve) 925 $[M+H]^+$; HRMS (NSI +ve) 924.6147 $[M+H]^+$ (calc. for $C_{62}H_{77}N_5O_2$ 924.6150 $[M+H]^+$).

Diastereoisomeric rotaxanes (D,*R*$_{mp}$)-96 and (D,*S*$_{mp}$)-96: A dry CEM microwave vial was charged with macrocycle **74** (11.9 mg, 0.025 mmol), azide **90** (8.68 mg, 0.025 mmol), alkyne **34**[2] (5.4 mg, 0.025 mmol), and $[Cu(MeCN_4)].PF_6$ (8.4 mg, 0.023 mmol). CH_2Cl_2 (2.5 mL) was added and the reaction mixture stirred at 80 °C for 72 h. After this time the reaction mixture was poured into EDTA-$NH_{3\ (aq)}$ (50 mL) and extracted with CH_2Cl_2 (3 × 50 mL). The combined organic extracts were washed with brine (50 mL), dried over $MgSO_4$, and reduced *in vacuo*. Chromatography (eluting in 1:1 petrol-CH_2Cl_2 up to 10% MeCN) gave (D,*S*$_{mp}$)-**96** (9.84 mg, 38%) and (D,*R*$_{mp}$)-**96** (10.36 mg, 40%) as colourless solids.

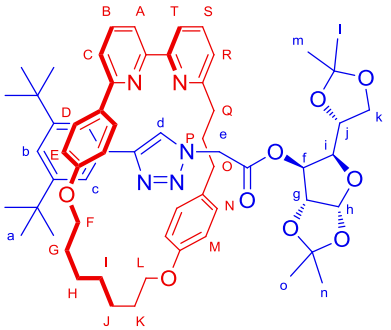

(D,R_{mp})-**96**

Rotaxane (D,R_{mp})-96: m.p. 168 – 170°C ; ^{1}H NMR (600 MHz, $CDCl_3$) δ 8.61 (s, 1H, H_d), 7.75 (t, *J* = 7.8, 1H, H_B), 7.74 (t, *J* = 7.7, 1H, H_S), 7.69 (d, *J* = 1.9, 1H, H_c), 7.54 (d, *J* = 7.9,1H, H_T), 7.52 (d, *J* = 7.2, 1H, H_A), 7.50 (d, *J* = 7.2, 1H, H_C), 7.43 (d, *J* = 8.7, 2H, H_D), 7.35 (t, *J* = 1.8, 1H, H_b), 7.26 (d, *J* = 7.0, 1H, H_R), 6.86 (d, *J* = 8.5, 2H, H_N), 6.55 (d, *J* = 8.5, 2H, H_M), 6.46 (d, *J* = 8.8, 2H, H_E), 5.86 (d, *J* = 18.2, 1H, H_e(*S*)), 5.18 (d, *J* = 3.6, 1H, H_h), 4.97 (d, *J* = 3.0, 1H, H_f), 4.17-4.12 (m, 1H, H_j), 4.09-3.90 (m, 7H, H_F and H_L, H_i, and H_k), 3.97 (d, *J* = 3.4, 1H, H_g), 3.63 (d, *J* = 18.2, 1H, H_e(*R*)), 2.88-2.73 (m, 2H, H_Q), 2.67-2.57 (m, 2H, H_O), 2.07-1.83 (m, 3H, H_P and one of H_G, or H_K,), 1.79-1.57 (m, 7H, H_H and H_J and three of H_G, and H_K), 1.45 (s, 3H, H_n or H_o), 1.40 (s, 3H, H_l or H_m), 1.43-1.37 (m, 2H, H_I), 1.34 (s, 18H, H_a), 1.31 (s, 3H, H_l or H_m), 1.22 (s, 3H, one of H_n or H_o). ^{13}C NMR (101 MHz, $CDCl_3$) δ 165.7 (C_e**C**O), 163.0 (C_Q**C**C_R), 158.7 (C_E**C**O and C_C**C**CC_D), 158.1 (C_A**C**CC_T), 157.6 (C_AC**C**C_T), 157.2 (C_M**C**O), 150.7 (**C**^{t}Bu), 147.3 (**C**C_d), 137.0 (C_B or C_S), 136.9 (C_B or C_S), 133.0 (C_N**C**C_O), 131.9 (C_D**C**CC_C), 130.8 (C_c**C**CC_d), 129.7 (C_N), 128.5 (C_D), 123.5 (C_d), 122.3 (C_R), 121.4 (C_b), 120.4 (C_A), 120.3 (C_c), 120.3 (C_T), 119.6 (C_C), 115.6 (C_E), 114.4 (C_M), 111.9 (C_n**C**C_o), 109.3 (C_l**C**C_m), 104.8 (C_h), 82.8 (C_g), 79.4 (C_i), 76.8 (C_f), 72.2 (C_j), 67.9 (C_F or C_L), 67.0 (C_F or C_L), 66.2 (C_k), 50.0 (C_e), 37.2 (C_Q), 35.1 (C_O), 34.9 (**C**Me_3), 33.0 (C_P), 31.5 (C_a), 29.2 (C_G or C_K), 28.3 (C_G or C_K), 28.1 (C_I), 27.0 (C_l or C_m), 26.8 (C_n or C_o), 26.4 (C_n or C_o), 25.9 (C_H or C_J), 25.7 (C_H or C_J), 25.4 (C_m or C_l); LR-MS (ESI +ve): m/z 1037 $[M+H]^+$. Crystals suitable for single crystal X-ray diffraction were grown from 1:1 cyclohexane-Et_2O *via* slow evaporation.

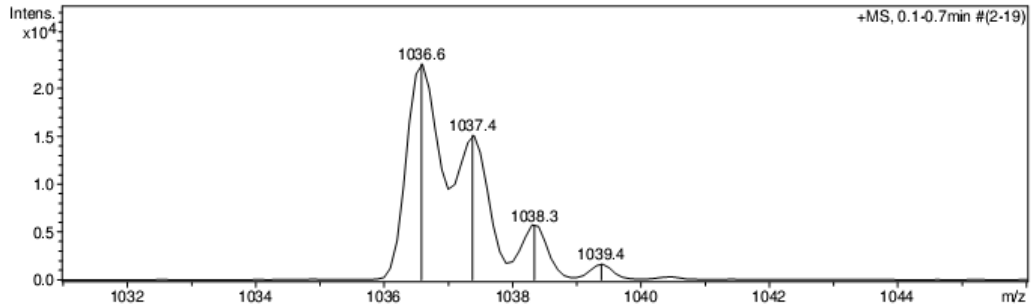
Intens.
x10^4
+MS, 0.1-0.7min #(2-19)
1036.6
1037.4
1038.3
1039.4
m/z

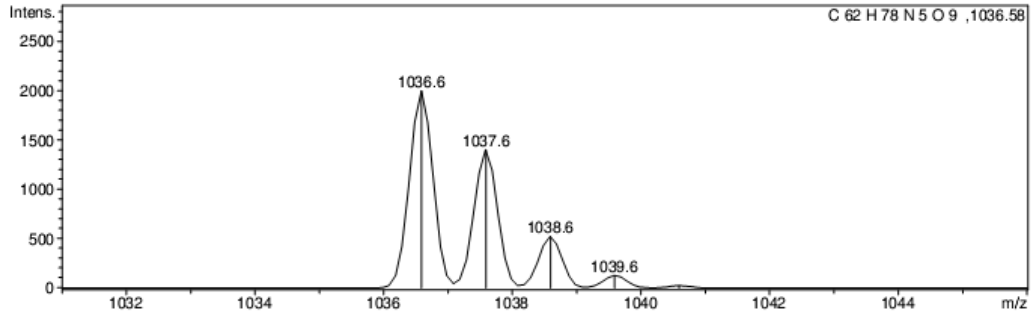
Intens.
C 62 H 78 N 5 O 9 ,1036.58
1036.6
1037.6
1038.6
1039.6
m/z

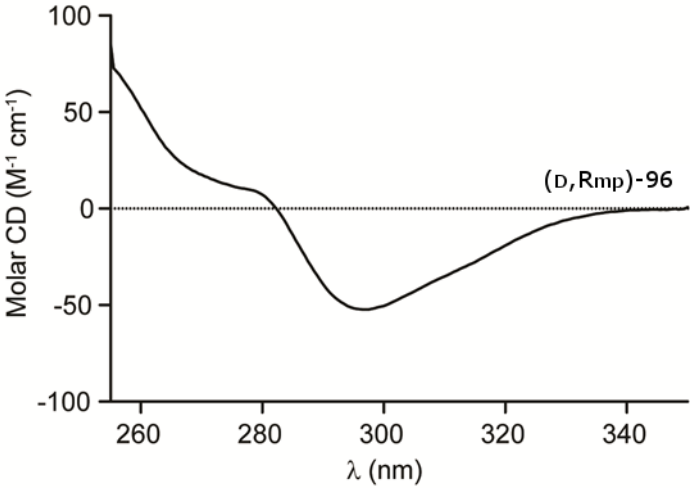
Molar CD (M-1 cm-1)
(D,Rmp)-96
λ (nm)

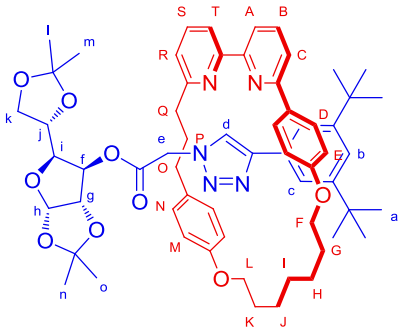

(D,S_{mp})-**96**

Rotaxane (D,S_{mp})-96: m.p. 209 – 211 °C; ^{1}H NMR (600 MHz, $CDCl_3$) δ 7.87 (d, *J* = 8.6, 2H, H_D), 7.78 (ap t, *J* = 7.8, 1H, H_B), 7.74 (ap t, *J* = 7.7, 1H, H_S), 7.57 (d, *J* = 7.8, H_A or H_C), 7.56 – 7.53 (m, 3H, H_c, H_A or H_C), 7.50 (d, *J* = 7.7, 1H, H_T), 7.39 (t, *J* = 1.6, 1H, H_b), 7.28 – 7.24 (m, 1H, H_R), 7.21 (d, *J* = 8.3, 2H, H_N), 6.90 (d, *J* = 8.7, 2H, H_E), 6.79 (d, *J* = 8.4, 2H, H_M), 6.51 (s, 1H, H_d), 6.31 (d, *J* = 18.9, 1H, H_e(*R*)), 5.59 (d, *J* = 3.4, 1H, H_h), 4.97 (d, *J* = 2.5, 1H, H_f), 4.88 (d, *J* = 18.9, 1H, H_e(*S*)), 4.25 – 4.18 (m, 1H, one of H_F), 4.21 – 4.18 (d, 1H, H_g), 4.12 – 4.06 (m, 1H, one of H_F), 3.97 (dd, *J* = 8.5, 2.6, 1H, H_i), 3.92 – 3.86 (m, 1H, one of H_L), 3.76 – 3.72 (m, 1H, one of H_L), 3.69 (dt, *J* = 8.4, 5.9, 1H, H_j), 3.64 (dd, *J* = 8.5, 5.2, 1H, one of H_k), 3.26 (dd, *J* = 8.4, 6.5, 1H, one of H_k), 2.92 – 2.85 (m, 1H, one of H_O), 2.78 (dt, 1H, *J* = 13.7, 4.6, 1H, one of H_Q), 2.71 – 2.61 (m, 2H, one of H_O and one of H_Q), 2.24 – 2.13 (m, 1H, one of H_P), 1.99 – 1.89 (m, 1H, one of H_P), 1.80 – 1.72 (m, 1H, one of H_K), 1.70 – 1.61 (m, 2H, H_G and one H_K), 1.56 – 1.51 (m, 2H, H_H or H_I or H_J) 1.51 (s, 3H, H_n or H_o), 1.42 (s, 3H, H_n or H_o), 1.41 (s, 18H, H_a), 1.40 – 1.34 (m, 2H, H_H or H_I or H_J), 1.23 – 1.19 (m, 2H, H_H or H_I or H_J), 1.17 (s, 3H, one of H_l or H_m), 0.57 (s, 3H, one of H_l or H_m); ^{13}C NMR (101 MHz, CDCl3) δ 167.0 (**C**=O), 163.5 (C_R**C**C_Q), 159.2 (C_E**C**O), 158.0 (C_A**C**CC_T or C_C**C**CC_D), 157.9 (C_A**C**CC_T or C_C**C**CC_D), 157.5 (C_AC**C**C_T), 157.5 (C_M**C**O), 151.0 (C_b**C**C_c), 147.8 (C_cC**C**C_d), 137.4 (C_B), 136.9 (C_S), 133.0 (C_N**C**C_O), 132.5 (C_CC**C**C_D), 130.5 (C_c**C**CC_d), 130.0 (C_N), 129.0 (C_D), 122.0 (C_R), 121.8 (C_b), 121.5 (C_d), 120.5 (C_c or C_C or C_A), 120.4 (C_c or C_C or C_A), 120.2 (C_T), 119.6 (C_C or C_A), 116.5 (C_E), 114.8 (C_M), 112.1 (C_n**C**C_o), 109.1 (C_l**C**C_m), 105.1 (C_h), 82.4 (C_g), 80.1 (C_k), 77.3 (C_f), 71.0 (C_j), 68.2 (C_F or C_L), 67.0 (C_F or C_L), 67.0 (C_k), 51.8 (C_e), 37.3 (C_Q), 35.1 (C_O), 35.0 (**C**Me_3), 31.7 (C_P), 31.6 (C_a), 28.5, 28.5, 28.4 (C_K, C_G + one of C_H, C_I or C_J), 26.8 (C_n or C_o), 26.6, 26.6 (C_n or C_o and C_l or C_m), 25.3 (one of C_H, C_I or C_J), 25.1 (one of C_H, C_I or C_J), 23.9 (C_l or C_m); LR-MS (ESI +ve): m/z 1037 $[M+H]^+$. Crystals suitable for single crystal X-ray diffraction were grown from 1:1 cyclohexane-Et_2O *via* slow evaporation.

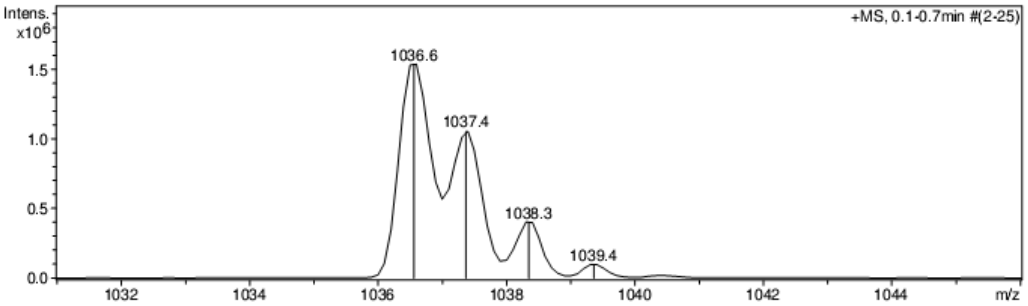
Intens.
x10^6
+MS, 0.1-0.7min #(2-25)
1036.6
1037.4
1038.3
1039.4
m/z

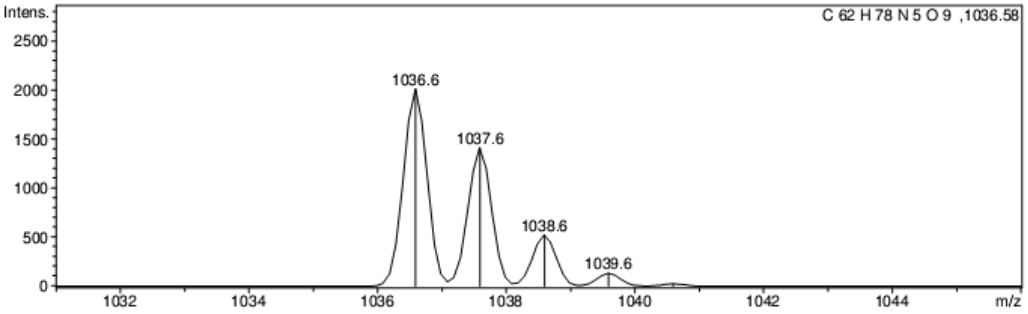
Intens.
C 62 H 78 N 5 O 9 ,1036.58
1036.6
1037.6
1038.6
1039.6
m/z

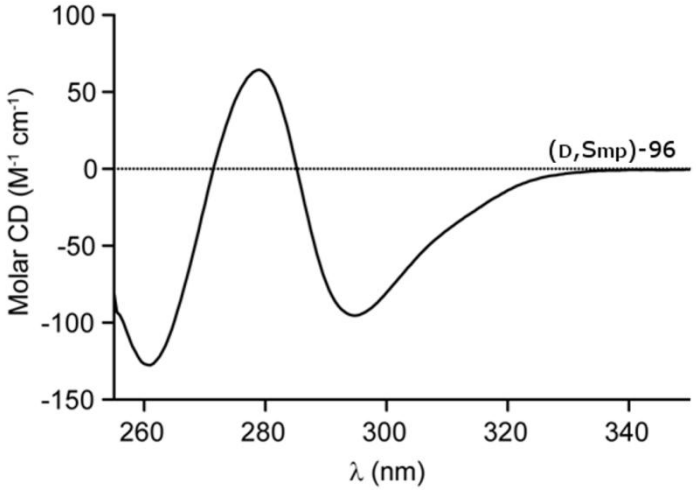
Molar CD (M-1 cm-1)
(D,Smp)-96
λ (nm)

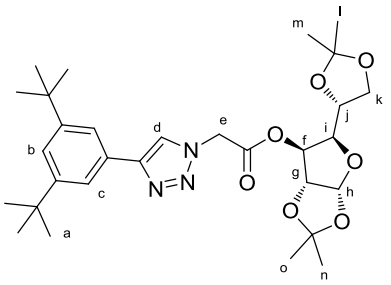

95

Thread 95: A dry CEM microwave vial was charged with azide **90** (8.7 mg, 0.025 mmol), alkyne **34**[2] (5.5 mg, 0.026 mmol) and [Cu(MeCN$_4$)].PF$_6$ (11.5 mg, 0.031mmol). CH_2Cl_2 (2 mL) was added *via* syringe and the reaction mixture stirred at 80 °C for 16 h. The crude reaction mixture was diluted with CH_2Cl_2 (50 mL) and washed with EDTA-NH_3 solution (50 mL). The aqueous phase was extracted with CH_2Cl_2 (2 × 50 mL), and the combined organic phases dried over $MgSO_4$ and reduced *in vacuo*. Chromatography (eluting in 1:1 petrol-CH_2Cl_2 →10% MeCN) yielded thread **95** as a white foam (4.6 mg, 33%); m.p. 89 – 91 °C; ^{1}H NMR (400 MHz, $CDCl_3$) δ 7.92 (s, 1H, H_d), 7.67 (d, *J* = 1.8, 2H, H_c), 7.43 (t, *J* = 1.8, 1H, H_b), 5.88 (d, *J* = 3.7, 1H, H_h), 5.37 (d, *J* = 3.0, 1H, H_f), 5.30 (d, *J* = 17.6, 1H, one of H_e), 5.25 (d, *J* = 17.6, 1H, one of H_e), 4.56 (d, *J* = 3.7, 1H, H_g), 4.18 (m, 1H, H_i), 4.11 – 3.97 (m, 3H, H_j and H_k), 1.52 (s, 3H, one of H_n or H_o), 1.40 (s, 3H, one of H_n or H_o), 1.37 (s, 18H, H_a), 1.31 (s, 3H, one of H_l or H_m), 1.30 (s, 3H, one of H_l or H_m); ^{13}C NMR (101 MHz, $CDCl_3$) δ 165.3, 151.4, 149.4, 129.4, 122.7, 120.8, 120.3, 112.6, 109.7, 105.1, 83.1, 79.8, 78.0, 72.3, 67.5, 50.8, 35.0, 31.5, 27.0, 26.7, 26.2, 25.2; LRMS (ESI +ve) 558 $[M+H]^+$; HRMS (NSI +ve) 558.3163 $[M+H]^+$ (calc. for $C_{30}H_{43}N_3O_7$ 558.3174 $[M+H]^+$).

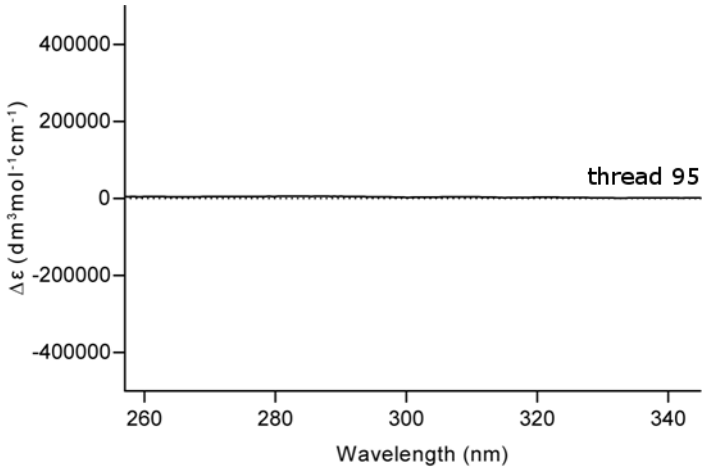

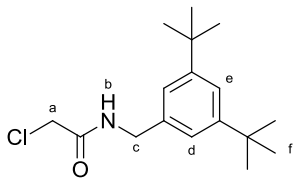

110

2-Chloro-N-(3,5-di-tert-butylbenzyl)acetamide (110): To a solution of 2-chloroacetyl chloride (59 μL, 1.0 mmol) in THF (0.5 mL) at 0 °C was added a solution of 3,5-di-*tert*-butylbenzylamine[3] (150 mg, 0.684 mmol), DMAP (41.8 mg, 0.342 mmol), Et_3N (0.20 mL, 1.43 mmol) in THF (0.65 mL). After 1 h the reaction mixture was diluted with H_2O (10 mL) and extracted with $CHCl_3$ (10 mL). The organic phase was washed with sat. $NaHCO_{3(aq.)}$ (10 mL), dried over $MgSO_4$ and reduced *in vacuo*. Chromatography (eluting in petrol → 50% Et_2O) gave α-chloroacetamide **110** as a pale yellow crystalline solid (176 mg, 87%); m.p. 127 – 129 °C (CH_2Cl_2); ^{1}H NMR (400 MHz, $CDCl_3$) δ 7.39 (t, *J* = 1.8, 1H, H_e), 7.14 (d, *J* = 1.8, 2H, H_d), 6.80 (br s, 1H, H_b), 4.49 (d, *J* = 5.6, 2H, H_c), 4.11 (s, 2H, H_a), 1.33 (s, 18H, H_f); ^{13}C NMR (101 MHz, $CDCl_3$) δ 165.7, 151.5, 136.3, 122.2, 122.0, 44.5, 42.7, 34.9, 31.5; LRMS (EI +ve) 295 $[M]^+$; HRMS (EI +ve) 295.1693 $[M]^+$ (calc. for $C_{17}H_{26}{}^{35}ClNO$ 295.1697 $[M]^+$).

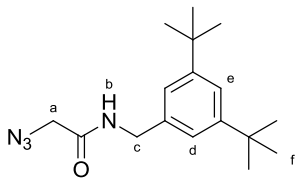

111

2-Azido-N-(3,5-di-tert-butylbenzyl)acetamide (111): A CEM vial was charged with α-chloroacetamide **110** (77 mg, 0.26 mmol), NaN_3 (180 mg, 2.76 mmol) and DMF (2.5 mL) and the reaction mixture heated at 60 °C for 16 h. The reaction was diluted with H_2O (25 mL) and extracted with Et_2O (2 × 25 mL). The organic extracts were washed with brine (25 mL), dried over $MgSO_4$ and reduced *in vacuo*. Chromatography (eluting in petrol → 50% Et_2O) gave 2-azidoacetamide **111** as a white crystalline solid (63 mg, 80%); m.p. 91 – 93 °C (CH_2Cl_2); ^{1}H NMR (400 MHz, $CDCl_3$) δ 7.39 (t, *J* = 1.7, 1H, H_e), 7.13 (d, *J* = 1.7, 2H, H_d), 6.58 (br s, 1H, H_b), 4.46 (d, *J* = 5.6, 2H, H_c), 4.02 (s, 2H, H_a), 1.33 (s, 18H, H_f); ^{13}C NMR (101 MHz, $CDCl_3$) δ 166.4, 151.6, 136.6, 122.4, 122.1, 52.9, 44.3, 35.0, 31.6; HRMS (NSI +ve) 303.2184 $[M+H]^+$ (calc. for $C_{17}H_{26}N_4O$ 303.2179 $[M+H]^+$).

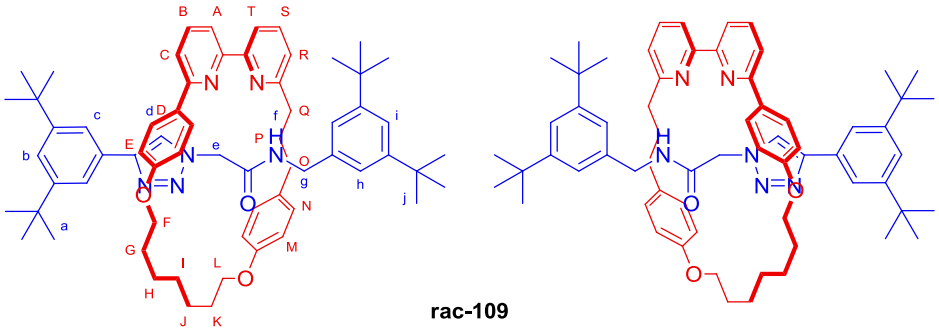

rac-109

Rotaxane rac-109: A dry CEM microwave vial was charged with macrocycle **74** (11.9 mg, 0.025 mmol), half-thread **111** (7.56 mg, 0.025 mmol), alkyne **34** (5.4 mg, 0.025 mmol), and $[Cu(MeCN_4)].PF_6$ (8.4 mg, 0.023 mmol). CH_2Cl_2 (2.5 mL) was added and the reaction stirred at 80 °C for 72 h. After this time the reaction mixture was poured into EDTA-NH_3 solution (50 mL) and extracted with CH_2Cl_2 (3 × 50 mL). The combined organic extracts were washed with brine (50 mL), dried over $MgSO_4$, and concentrated *in vacuo*. Chromatography (eluting in 1:1 petrol-CH_2Cl_2 →10% MeCN) isolated **rac-109** as a white solid (22.1 mg, 89%); m.p. 165 – 167 °C; ^{1}H NMR (400 MHz, $CDCl_3$) δ 9.04 (t, *J* = 5.3, 1H, H_f), 7.78 (t, *J* = 7.8, 1H, H_B or H_S), 7.77 (t, *J* = 7.8, 2H, H_B or H_S), 7.70 (s, 1H, H_d), 7.69 (d, 2H, H_c), 7.67 (d, *J* = 7.3, 1H, H_A), 7.60 (d, *J* = 7.3, 1H, H_T), 7.57 – 7.54 (m, 3H, H_D and H_R), 7.41 (t, *J* = 1.8, 1H, H_b), 7.28 (d, *J* = 7.9, 1H, H_C), 7.17 (t, *J* = 1.7, 1H, H_i), 6.87 (d, *J* = 1.7, 2H, H_h), 6.76 (d, *J* = 8.5, 2H, H_N), 6.65 (d, *J* = 8.6, 2H, H_M), 6.57 (d, *J* = 8.7, 2H, H_E), 4.77 (d, *J* = 15.9, 1H, one of H_e), 4.11 (m, 1H, one of H_F or H_L), 3.99 – 3.85 (m, 3H, three of H_F and H_L), 3.78 (d, *J* = 15.9, 1H, one of H_e), 3.63 (dd, *J* = 14.6, 6.0, 1H, one of H_g), 3.40 (dd, *J* = 14.6, 4.7, 1H, one of H_g), 2.62 (m, 4H, H_O and H_Q), 1.85 (m, 4H, H_P and one of H_F or H_L), 1.53 (m, 2H, H_G or H_K), 1.40 (s, 18H, H_a), 1.11 (s, 18H, H_j); ^{13}C NMR (101 MHz, $CDCl_3$) δ 163.4 (N-**C**(O)-C_e), 163.2 (C_R**C**C_Q), 159.1 (N=**C**-C_A or N=**C**-C_C or N=**C**-C_R or N=**C**-C_T), 159.0 (C_E**C**O), 157.5 (C_M**C**C_O), 156.8, 156.8 (two of N=**C**-C_A, N=**C**-C_C, N=**C**-C_R or N=**C**-C_T), 151.1 (C_b**C**C_c), 150.3 (C_h**C**C_i), 148.0 (C_eC**C**C_d), 137.5 (C_B or C_S), 137.4 (C_B or C_S), 136.9 (C_g**C**C_h), 132.2 (C_N-**C**-C_O), 131.6, 130.5, 129.5, 128.8, 122.7 (C_h), 122.6 (one of C_A, C_C, C_R or C_T), 122.5 (C_d), 121.8 (C_b), 121.1 (C_i), 120.4 (C_c), 120.3, 120.2, 120.2 (three of of C_A, C_C, C_R or C_T), 115.7 (C_D or C_E), 114.6 (C_N), 68.0, 66.6, 51.7 (C_e), 43.8 (C_g), 36.7 (C_Q), 35.0 (**C**-^{t}Bu$_a$), 34.9 (C_O), 34.6 (**C**-^{t}Bu$_j$), 32.2 (C_P), 31.6 (C_a), 31.3 (C_j), 31.0, 29.0, 28.1, 27.8, 25.6, 24.9; LR-MS (ESI +ve): m/z 995.5 $[M+H]^+$.

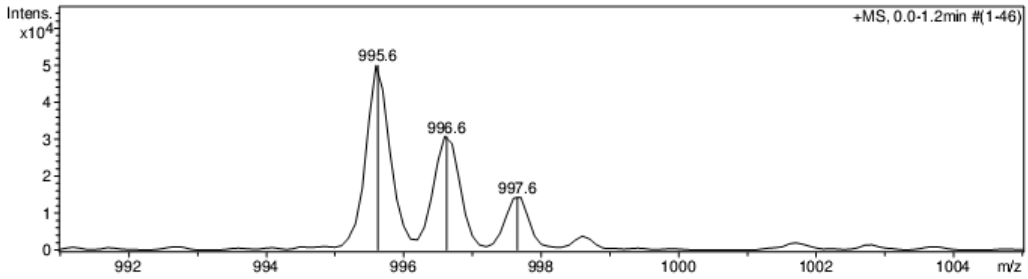
Intens.
x10^4
+MS, 0.0-1.2min #(1-46)
995.6
996.6
997.6
992
994
996
998
1000
1002
1004
m/z

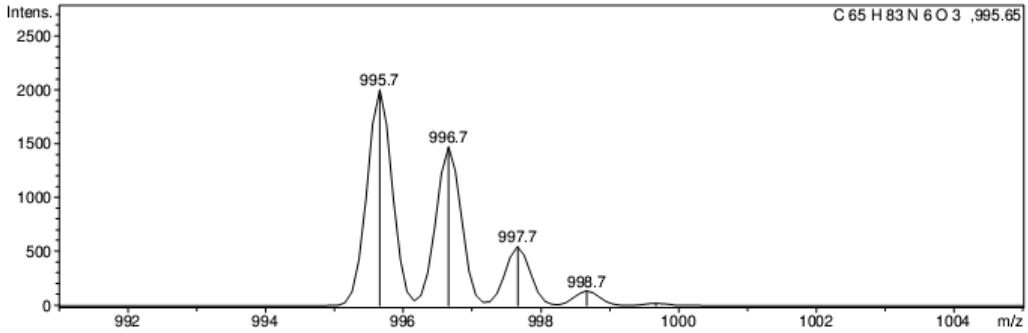
Intens.
C 65 H 83 N 6 O 3 ,995.65
995.7
996.7
997.7
998.7
992
994
996
998
1000
1002
1004
m/z

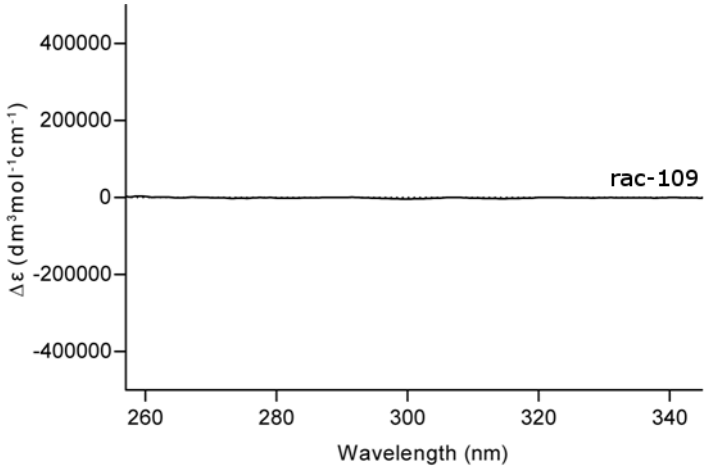
rac-109
Δε (dm³mol⁻¹cm⁻¹)
Wavelength (nm)

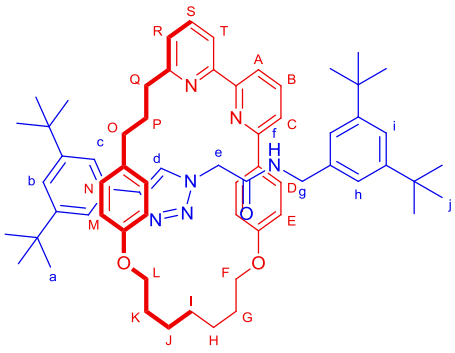

(R_{mp})-109

Rotaxane (R_{mp})-109: A CEM vial was charged with 3,5-di-*tert*-butylbenzylamine (11.4 mg, 0.052 mmol) and PhMe (125 µL) and the mixture stirred at 0 °C. $AlMe_3$ (33 µL, 2 M in toluene, 0.052 mmol) was added and the reaction mixture stirred at rt for 15 min to produce a solution of the corresponding aluminium amide. A CEM vial was charged with rotaxane (D,S_{mp})-**100** (12.8 mg, 0.013 mmol), aluminium amide solution was added (158 µL, 0.052 mmol) and the reaction mixture heated at 80 °C for 16 h. The reaction was diluted with CH_2Cl_2 (50 mL) and washed with a 10% solution of potassium sodium tartrate. After standing for 20 min the organic phase was separated and the aqueous phase extracted with CH_2Cl_2 (2 × 50 mL), the combined organic extracts were washed with brine (50 mL), dried over $MgSO_4$ and reduced *in vacuo*. Chromatography (1:1 petrol-CH_2Cl_2, 0→10% MeCN) afforded the enantiomerically pure (R_{mp})-**113** as a white solid (6.1 mg, 50 %); m.p. 173 – 175 °C.

Spectroscopic data were identical to that reported for racemic rotaxane **109** with the exception of the circular dichroism spectra.

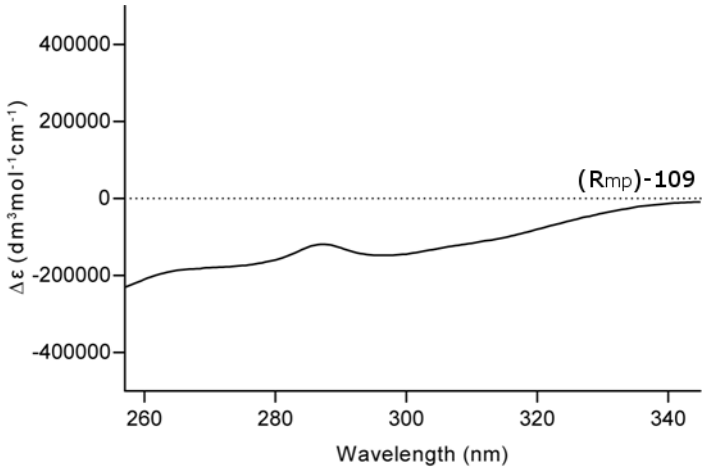

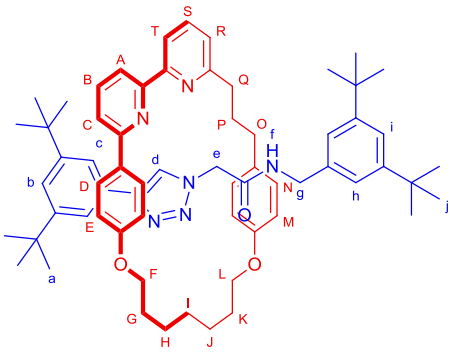

(*S*$_{mp}$)-109

Rotaxane (*S*$_{mp}$)-109: An identical procedure to that for (*R*$_{mp}$)-**109** but employing rotaxane (D,*R*$_{mp}$)-**96** afforded (*S*$_{mp}$)-**109** as a white solid (5.9 mg, 48 %); m.p. 171 – 173 °C.

Spectroscopic data were identical to that reported for racemic rotaxane **109** with the exception of the circular dichroism spectra.

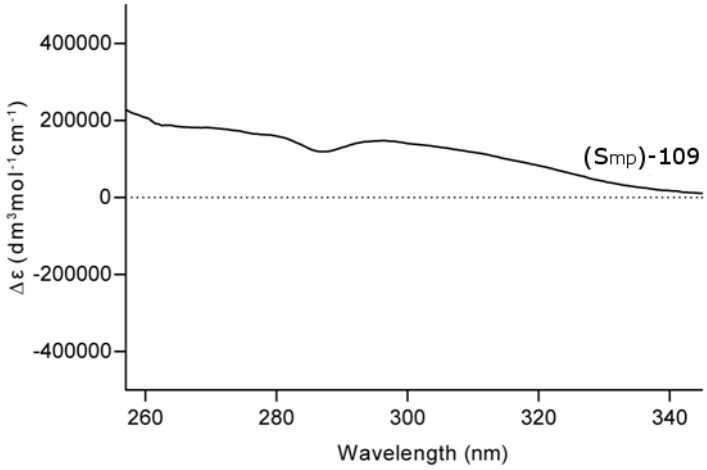

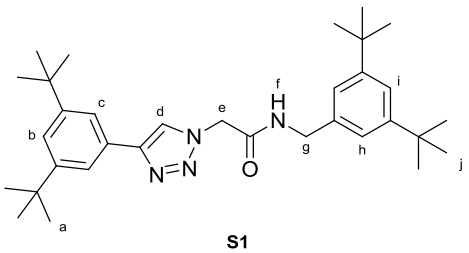

S1

Thread S1: A dry CEM vial was charged with azide **111** (7.56 mg, 0.025 mmol), ethynyl-3,5-di-tert-butylbenzene (**34**) (5.36 mg, 0.025 mmol), $[Cu(MeCN_4)].PF_6$ (0.9 mg, 0.003 mmol), CH_2Cl_2 (2.5 mL) and the reaction was heated at 80 °C for 16 h. The reaction mixture was poured into EDTA-NH_3 solution (50 mL) and extracted with CH_2Cl_2 (3 × 50 mL), the organic extracts dried ($MgSO_4$) and the solvent removed *in vacuo*. Chromatography (eluting in 1:1 petrol-CH_2Cl_2 → 10% MeCN) gave thread **S1** as a white crystalline solid (12.0 mg, 93%); m.p. 83 – 85°C (CH_2Cl_2); ^{1}H NMR (400 MHz, $CDCl_3$) δ 7.99 (s, 1H, H_d), 7.67 (d, *J* = 1.8, 2H, H_c), 7.44 (t, *J* = 1.8, 1H, H_b), 7.33 (t, *J* = 1.7, 1H, H_i), 7.03 (d, *J* = 1.7, 2H, H_h), 6.51 (t, *J* = 5.2, 1H, H_f), 5.13 (s, 2H, H_e), 4.44 (d, *J* = 5.6, 2H, H_g), 1.37 (s, 18H, H_a), 1.27 (s, 18H, H_j); ^{13}C NMR (101 MHz, $CDCl_3$) δ 165.1 (**C**=O), 151.5 (C_b=**C**-C^{t}Bu), 151.4 (C_h=**C**-C^{t}Bu), 149.5 (C-**C**=C_d), 136.1 (C_h=**C**-C_g), 129.2 (C_c-**C**-triazole), 122.8 (C_b), 122.0 (C_i), 121.9 (C_h), 121.0 (C_d), 120.3 (C_c), 53.3 (C_e), 44.4 (C_g), 35.0 (C-**C**-$(CH_a)_3$), 34.8 (C-**C**-$(CH_j)_3$), 31.5 (C_a), 31.4 (C_j); HRMS (NSI +ve) 517.3894 $[M+H]^+$ (calc. for $C_{33}H_{48}N_4O$ 517.3901 $[M+H]^+$).

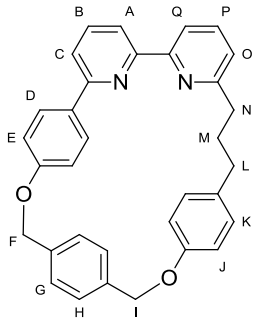

119

Macrocycle 119: A dry 2 L round bottomed flask was charged with bis-phenol **75** (2.01 g, 5.23 mmol), K_2CO_3 (7.23 g, 52.3 mmol), DMF (1.9 L) and 1,4-bis(bromomethyl)benzene (1.38 g, 5.23 mmol). The reaction mixture was stirred at 80 °C for 72 h after which time the solvent was removed *in vacuo*. The residue was extracted with refluxing Et_2O (3 × 200 mL), the extracts combined and reduced *in vacuo*. The residue was purified by flash chromatography (1:1 petrol-CH_2Cl_2 0→10% MeCN) and the fractions containing macrocycle **119** were subsequently purified by GPC (eluting in CH_2Cl_2) to yield macrocycle **119** (152 mg, 0.313 mmol, 6%); m.p. 188 – 190 °C; ^{1}H NMR (600 MHz, $CDCl_3$) δ 7.87 (d, *J* = 8.9, 2H, H_E), 7.78 (ap. t, *J* = 7.8, 1H, H_B), 7.67 (ap. t, *J* = 7.6, 1H, H_P), 7.65 (dd, *J* = 7.8, 0.7, 1H, H_C), 7.58 (dd, *J* = 7.7, 0.6, 1H, H_A), 7.53 (d, *J* = 7.6, 1H, H_Q), 7.34 (d, *J* = 8.1, 2H, H_H), 7.27 (d, *J* = 8.2, 2H, H_G), 7.18 (d, *J* = 7.5, 1H, H_O), 7.04 (d, *J* = 8.6, 2H, H_K), 6.74 (m, 2H, H_D), 6.67 (m, 2H, H_J), 5.24 (s, 2H, H_F), 5.18 (s, 2H, H_I), 2.92 (ap. t, 2H, H_N), 2.62 (ap. t, 2H, H_L), 2.18 – 2.11 (m, 2H, H_M); ^{13}C NMR (151 MHz, $CDCl_3$) δ 162.7 (N=**C**-C_N), 159.1 (C_E=**C**-O), 157.81 (N=**C**-C_C), 157.0 (N=**C**-C_A or N=**C**-C_Q), 156.9 (N=**C**-C_A or N=**C**-C_Q), 155.7 (C_J=**C**-O), 137.4 (C_B), 137.2 (C_F-**C**=C_G and C_H=**C**-C_I), 136.8 (C_P), 135.0 (C_K=**C**-C_L), 132.8 (C_D=**C**-py), 129.5 (C_K), 128.6 (C_E), 127.6 (C_H), 126.7 (C_G), 122.5 (C_O), 119.9 (C_A or C_Q), 119.8 (C_A or C_Q), 119.1 (C_C), 116.7 (C_D), 116.0 (C_J), 70.9 (C_F), 69.8 (C_I), 38.2 (C_N), 35.0 (C_L), 32.1 (C_M); HRMS (NSI +ve) 485.2227 $[M+H]^+$ (calc. for $C_{33}H_{29}N_2O_2$ 485.2224 $[M+H]^+$).

Diastereoisomeric rotaxanes (D,R_{mp})-120 and (D,S_{mp})-120: A dry CEM microwave vial was charged with macrocycle **119** (12.1 mg, 0.025 mmol), azide **90** (26.04 mg, 0.075 mmol), alkyne **34** (16.2 mg, 0.075 mmol), and [Cu(MeCN$_4$)].PF$_6$ (8.9 mg, 0.024 mmol). CH_2Cl_2 (2.5 mL) was added and the reaction mixture stirred. *N*,*N*-Diisopropylethylamine (0.22 mL, 1.25 mmol) was added and the reaction heated at 30 °C for 16 h. After this time the reaction mixture was poured into EDTA-$NH_{3\ (aq)}$ (50 mL) and extracted with CH_2Cl_2 (3 × 50 mL). The combined organic extracts were washed with brine (50 mL), dried over Na_2SO_4, and reduced *in vacuo*. Chromatography (eluting in $CHCl_3$ with 0.8% EtOH up to 100% Et_2O) gave (D,S_{mp})-**120** (17.5 mg, 75%) and (D,R_{mp})-**120 (**4.3 mg, 17%) as colourless films.

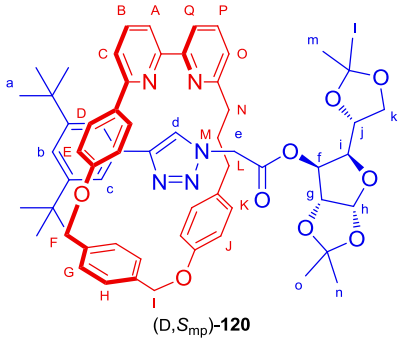

(D,S_{mp})-**120**

Rotaxane (D,S_{mp})-120: m.p. 134 - 146 °C; ^{1}H NMR (600 MHz, $CDCl_3$) δ 7.71 (ap. t, *J* = 7.8, 1H, H_B), 7.68 (ap. t, *J* = 7.9, 1H, H_P), 7.66 (br. d, 2H, H_c), 7.56 (d, *J* = 7.7, 1H, H_A), 7.53 (d, *J* = 7.7, 1H, H_O), 7.45 – 7.42 (m, 6H, H_D, H_G and H_H), 7.40 (d, *J* = 7.7, 1H, H_C), 7.37 (s, 1H, H_b), 7.22 (d, *J* = 7.8, 1H, H_Q), 6.99 – 6.95 (m, 4H, H_E and H_K), 6.53 (br. s, 2H, H_J), 5.43 (d, *J* = 14.2, 1H, one of H_F), 5.31 (d, *J* = 14.2, 1H, one of H_F), 5.29 (d, *J* = 3.5, 1H, H_h), 5.14 (d, *J* = 14.3, 1H, one of H_I), 4.95 (d, *J* = 14.3, 1H, one of H_I), 4.74 (d, *J* = 18.1, 1H, one of H_e), 4.38 (d, *J* = 2.4, 1H, H_f), 3.96 (m, 1H, H_j), 3.88 (dd, *J* = 9.0, 2.5, 1H, H_i), 3.81 – 3.78 (m, 2H, one of H_e and one of H_k), 3.72 (d, *J* = 3.4, 1H, H_g), 3.58 (dd, *J* = 8.3, 6.5, 1H, one of H_k), 2.91 (td, *J* = 13.3, 4.8, 1H, one of H_N), 2.76 (td, *J* = 13.3, 3.9, 1H, one of H_N), 2.73 – 2.68 (m, 1H, one of H_L), 2.53 (ddd, *J* = 13.7, 10.7, 2.9, 1H, one of H_L), 2.20 – 2.12 (m, 1H, one of H_M), 1.93 – 1.84 (m, 1H, one of H_M), 1.46 (s, 3H, H_n or H_o), 1.35 (s, 18H, H_a), 1.30 (s, 3H, H_l or H_m), 1.15 (s, 3H, H_n or H_o), 0.85 (s, 3H, H_l or H_m); ^{13}C NMR (151 MHz, $CDCl_3$) δ 164.2 (C_e**C**O or C_N**C**C_O), 164.1 (C_e**C**O or C_N**C**C_O), 159.3 (C_C**C**CC_D), 158.2 (C_E**C**O), 157.6 (C_A**C**N), 156.7 (C_Q**C**N), 156.3 (C_J**C**O), 151.2 (C_b**C**C_c), 147.2 (C_cC**C**C_d), 138.9 (C_H**C**C_I), 137.4 (C_B), 137.2 (C_F**C**C_G), 136.8 (C_P), 134.3 (C_D**C**-py), 134.1 (C_K**C**C_L), 130.9 (C_c**C**CC_d), 130.2 (C_K), 129.5 (C_D), 128.6 (C_G), 128.1 (C_H), 123.0 (C_Q and C_d), 121.7 (C_b), 120.9 (C_C), 120.7 (C_A), 120.1 (C_c), 119.9 (C_O), 116.8 (C_E), 114.2 (br, C_J), 111.7 (C_n**C**C_o), 109.4 (C_l**C**C_m), 104.8 (C_h), 82.3 (C_g), 79.9 (C_i), 77.4 (C_f), 71.4 (C_j), 69.6 (C_F), 68.5 (C_I), 67.5 (C_k), 50.6 (C_e), 37.2 (C_N), 35.1 (**C**Me_3), 35.1 (C_L), 31.8

(C_M), 31.7 (C(**C**H_3)$_3$), 27.0 and 26.9 (one of C_l and C_m, and one of C_n and C_o), 26.7 (one of C_n and C_o), 24.7 (one of C_l and C_m); LR-MS (ESI +ve): m/z 1043 $[M+H]^+$

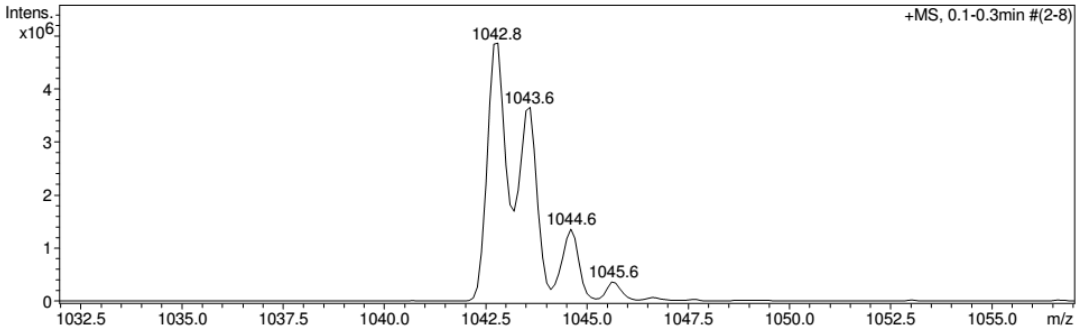

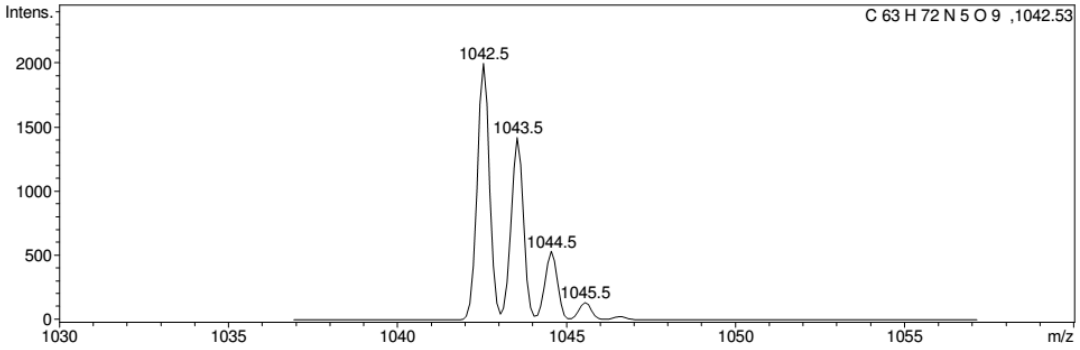

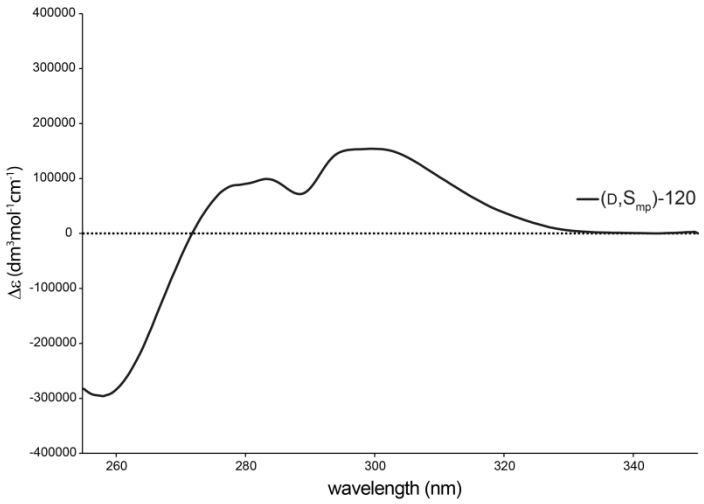

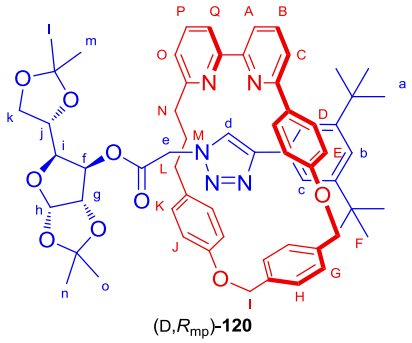

(D,R_{mp})-**120**

Rotaxane (D,R_{mp})-120: m.p. 75 - 83 °C; ^{1}H NMR (600 MHz, $CDCl_3$) δ 9.51 (s, 1H, H_d), 7.67 (ap. t, 1H, H_P), 7.65 (m, 1H, H_B), 7.64 (d, *J* = 1.8, 2H, H_c), 7.59 (d, *J* = 7.8, 2H, H_H), 7.50 (d, *J* = 7.4, 1H, H_A or H_Q), 7.49 (d, *J* = 7.4, 1H, H_A or H_Q), 7.47 (d, *J* = 8.0, 2H, H_G), 7.27 (t, *J* = 1.8, 1H, H_b), 7.26 (d, *J* = 7.7, 1H, H_C), 7.17 (d, *J* = 7.7, 1H, H_O), 7.07 (d, *J* = 8.0, 2H, H_E), 6.82 (d, *J* = 8.5, 2H, H_D), 6.72 (d, *J* = 8.7, 2H, H_J), 6.51 (br. s, 2H, H_K), 5.63 (d, *J* = 3.5, 1H, H_h), 5.32 (d, *J* = 14.1, 1H, one of H_F), 5.28 (d, *J* = 14.4, 1H, one of H_F), 5.25 (d, *J* = 14.2, 1H, one of H_I), 5.10 (d, *J* = 14.2, 1H, one of H_I), 4.50 (d, *J* = 2.8, 1H, H_f), 4.12 – 4.06 (m, 2H, H_g and H_j), 4.01 – 3.97 (m, 2H, H_i and one of H_k), 3.95 (dd, *J* = 8.8, 4.3, 1H, one of H_k), 3.36 (br. d, *J* = 18.7, 1H, one of H_e), 2.95 – 2.84 (m, 2H, H_N), 2.50 – 2.43 (m, 1H, one of H_L), 2.40 – 2.34 (m, 1H, one of H_L), 2.20 (d, *J* = 18.8, 1H, one of H_e), 2.03 – 1.92 (m, 1H, one of H_M), 1.87 – 1.77 (m, 1H, one of H_M), 1.49 (s, 3H, H_n or H_o), 1.37 (s, 3H, H_n or H_o), 1.24 (s, 3H, H_l or H_m), 1.21 (s, 18H, H_a), 1.13 (s, 3H, H_l or H_m); ^{13}C NMR (151 MHz, $CDCl_3$) δ 163.5 (C_N**C**C_O), 162.7 (C_e**C**O), 160.0 (C_C**C**CC_D), 157.7 (C_Q**C**=N), 157.7 (C_E**C**O), 157.0 (C_A**C**=N), 156.1 (C_J**C**O), 150.8 (C_b**C**C_c), 146.9 (C_cC**C**C_d), 138.4 (C_H**C**C_I), 137.6 (C_F**C**C_G), 136.8 (C_B or C_P) 136.7 (C_B or C_P), 135.3 (C_D**C**-py), 135.1 (C_K**C**C_L), 131.3 (C_c**C**CC_d), 130.3 (C_K), 129.7 (C_E), 129.2 (C_H), 128.8 (C_G), 125.6 (C_d), 122.3 (C_O), 121.5 (C_C or C_b), 121.3 (C_C or C_b), 120.7 (C_Q), 120.3 (C_c), 119.7 (C_A), 116.6 (C_D), 114.4 (C_J), 111.9 (C_n**C**C_o), 109.3 (C_l**C**C_m), 105.0 (C_h), 82.8 (C_g), 79.8 (C_i), 76.3 (C_f), 72.4 (C_j), 69.6 (C_F), 68.9 (C_I), 67.1 (C_k), 48.0 (C_e), 36.6 (C_N), 35.0 (**C**Me_3), 34.8 (C_L), 31.5 (C(**C**H_3)$_3$), 31.2 (C_M), 27.0 and 26.9 (one of C_n or C_o, and one of C_n or C_o), 26.8 (one of C_n or C_o), 25.3 (one of C_l or C_m); LR-MS (ESI +ve): m/z 1043 $[M+H]^+$

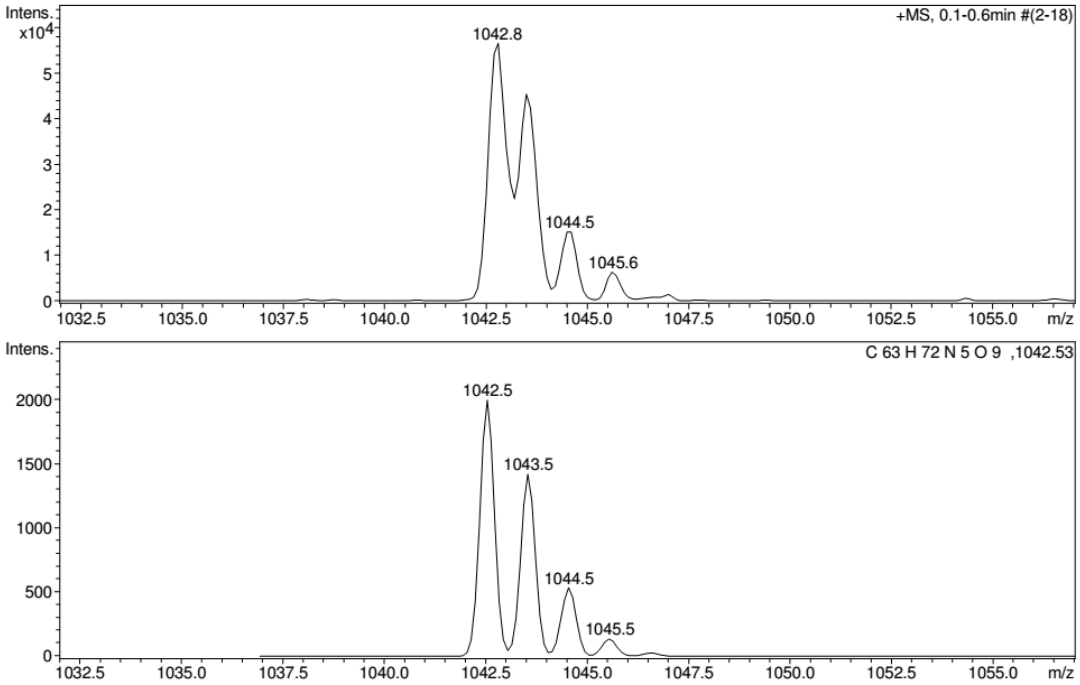
Intens.
x10^4
+MS, 0.1-0.6min #(2-18)
1042.8
1044.5
1045.6
m/z
Intens.
C 63 H 72 N 5 O 9 ,1042.53
1042.5
1043.5
1044.5
1045.5
m/z

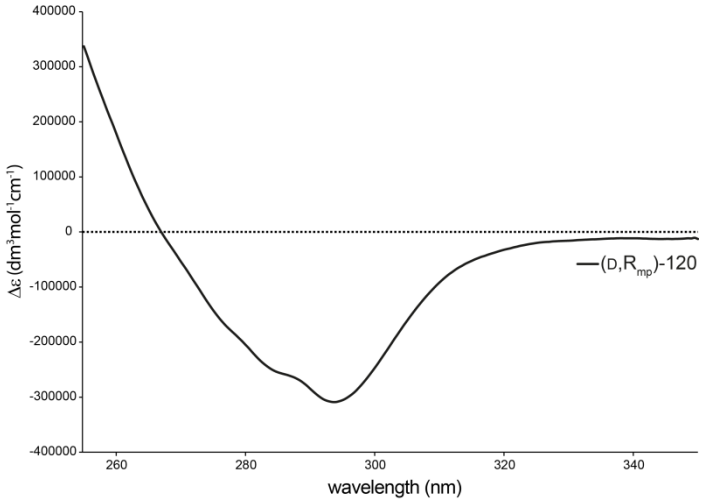
Δε (dm³mol⁻¹cm⁻¹)
wavelength (nm)
—(D,R_mp)-120

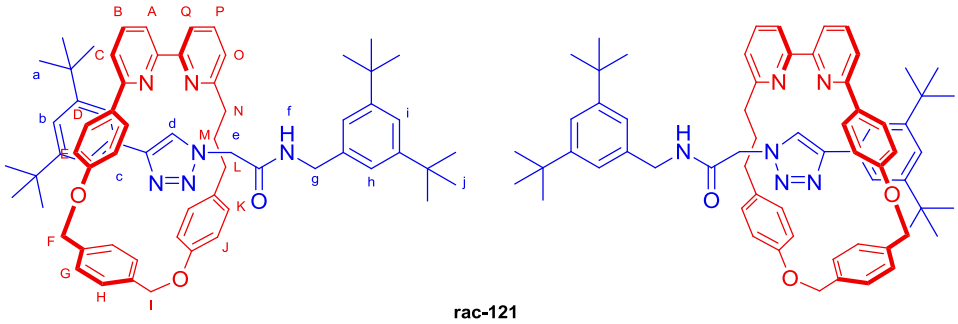

rac-121

Rotaxane rac-121: A dry CEM microwave vial was charged with macrocycle **119** (12.1 mg, 0.025 mmol), azide **90** (22.7 mg, 0.075 mmol), alkyne **34** (16.2 mg, 0.075 mmol), and $[Cu(MeCN_4)].PF_6$ (8.9 mg, 0.024 mmol). CH_2Cl_2 (2.5 mL) was added, followed by *N*,*N*-diisopropylethylamine (0.22 mL, 1.25 mmol) and the reaction stirred at 30 °C for 16 h. After this time the reaction mixture was poured into EDTA-NH_3 solution (50 mL) and extracted with CH_2Cl_2 (3 × 50 mL). The combined organic extracts were washed with brine (50 mL), dried over Na_2SO_4, and concentrated *in vacuo*. Chromatography (eluting in $CHCl_3$) isolated **rac-121** as a colourless solid (18.3 mg, 73%); ^{1}H NMR (600 MHz, $CDCl_3$) δ 9.61 (t, *J* = 3.6, 1H, H_f), 7.81 (ap. t, *J* = 7.8, 1H, H_B), 7.75 (ap. t, *J* = 7.8, 1H, H_P), 7.74 - 7.69 (m, 5H, H_A, H_Q, H_c, and H_d), 7.67 (d, *J* = 8.2, 2H, H_H), 7.44 (dd, *J* = 7.8, 0.7, 1H, H_C), 7.42 (t, *J* = 1.8, 1H, H_b), 7.38 (d, *J* = 8.1, 2H, H_G), 7.20 (dd, *J* = 7.1, 1.6, 1H, H_O), 7.17 (d, *J* = 8.8, 2H, H_E), 7.02 (br. t, *J* = 1.6, 1H, H_i), 6.82 (d, *J* = 8.6, 2H, H_J), 6.69 (br. d, *J* = 1.5, 2H, H_h), 6.65 (d, *J* = 8.5, 2H, H_D), 6.64 (d, *J* = 8.4, 2H, H_K), 5.34 (d, *J* = 14.7, 1H, one of H_F), 5.30 (d, *J* = 14.0, 1H, one of H_I), 5.24 (d, *J* = 14.0, 1H, one of H_I), 5.16 (d, *J* = 14.7, 1H, one of H_F), 4.48 (d, *J* = 15.2, 1H, one of H_e), 4.17 (d, *J* = 15.2, 1H, one of H_e), 2.66 - 2.60 (m, 1H, one of H_L), 2.54 – 2.47 (m, 2H, H_N), 2.39 – 2.32 (m, 2H, one of H_L and one of H_g), 2.06 – 1.99 (m, 1H, one of H_g), 1.96 – 1.86 (m, 1H, one of H_M), 1.78 – 1.70 (m, 1H, one of H_M), 1.41 (s, 18H, H_j), 1.04 (s, 18H, H_a); ^{13}C NMR (151 MHz, $CDCl_3$) δ 163.9 ($C_N\underline{C}C_O$), 162.9 ($C_e\underline{C}O$), 159.9 ($C_C\underline{C}CC_D$), 157.9 ($C_E\underline{C}O$), 156.4 ($C_A\underline{C}CC_Q$), 156.0 ($C_AC\underline{C}C_Q$), 155.9 ($C_J\underline{C}O$), 151.3 ($C_h\underline{C}C_i$), 149.7 ($C_a\underline{C}C_b$), 147.9 ($C_cC\underline{C}C_d$), 137.9 (C_B or C_P), 137.8 (C_B or C_P), 137.6 ($C_H\underline{C}C_I$), 136.8 ($C_F\underline{C}C_G$), 136.3 ($C_g\underline{C}C_h$), 133.7 ($C_K\underline{C}C_L$), 132.3 ($C_D\underline{C}$-py), 130.6 ($C_c\underline{C}CC_d$), 129.8 (C_K), 129.5 (C_E), 129.4 (C_H), 127.4 (C_G), 123.7 (C_O), 122.1 (C_b), 121.6 (C_h), 121.4 (C_C and C_d), 120.5 (C_A or C_Q), 120.3 (C_c), 120.0 (C_A or C_Q), 119.3 (C_i), 115.7 (C_J), 115.3 (C_D), 68.7 (C_F), 68.3 (C_I), 51.9 (C_e), 43.7 (C_g), 37.2 (C_N), 35.5 (C_L), 35.1 ($\underline{C}^tBu_a$), 34.8 ($\underline{C}^tBu_j$), 32.7 (C_M), 31.7 (C_j), 31.4 (C_a);

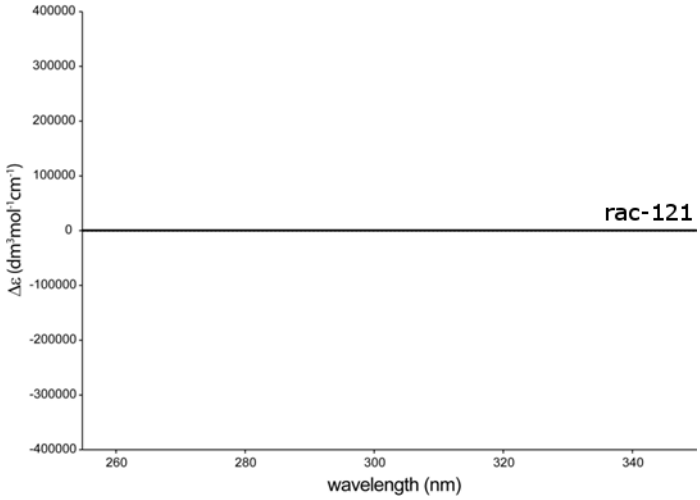
400000
300000
200000
100000
0
-100000
-200000
-300000
-400000
Δε (dm³mol⁻¹cm⁻¹)
rac-121
260
280
300
320
340
wavelength (nm)

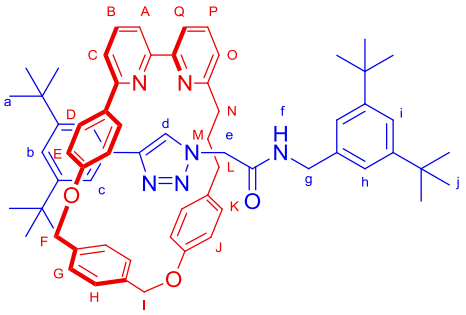

(R_{mp})-**121**

Rotaxane (R_{mp})-121: A CEM vial was charged with 3,5-di-*tert*-butylbenzylamine (72.5 mg, 0.331 mmol) and PhMe (0.80 mL) and the mixture stirred at rt. $AlMe_3$ (110 μL, 2 M in toluene, 0.220 mmol) was added and the reaction mixture stirred at rt for 15 min to produce a solution of the corresponding aluminium amide. A CEM vial was charged with rotaxane (D,S_{mp})-**120** (23.0 mg, 0.022 mmol), aluminium amide solution was added (0.91 mL, 0.052 mmol) and the reaction mixture heated at 100 °C for 16 h. The reaction was diluted with CH_2Cl_2 (50 mL) and washed with NH_3-EDTA $_{(aq.)}$ solution (50 mL). The organic phase was separated and the aqueous phase extracted with CH_2Cl_2 (2 × 50 mL), the combined organic extracts were washed with brine (50 mL), dried over Na_2SO_4 and reduced *in vacuo*. Chromatography (eluting in $CHCl_3$) afforded the enantiomerically pure (R_{mp})-**121** as a colourless film (14.5mg, 66 %); m.p. 74 - 84 °C; LR-MS (ESI +ve): m/z 1002 $[M+H]^+$.

Spectroscopic data were identical to that reported for rotaxane **rac-121** with the exception of the circular dichroism spectra.

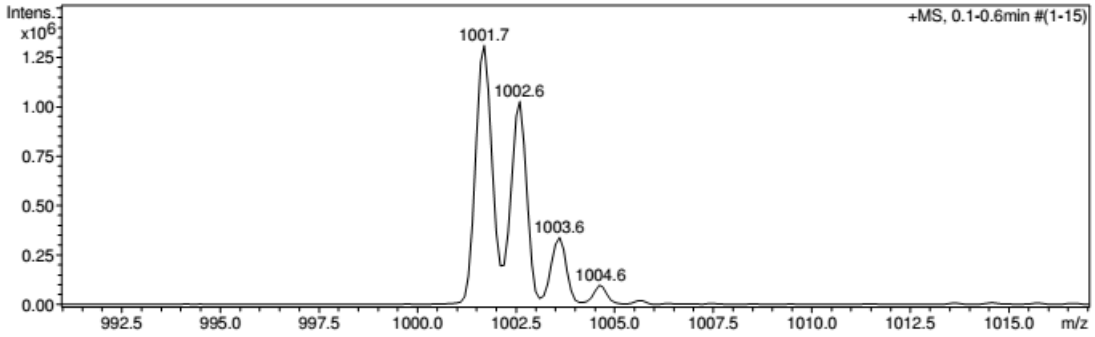
Intens.
x10^6
1.25
1.00
0.75
0.50
0.25
0.00
+MS, 0.1-0.6min #(1-15)
1001.7
1002.6
1003.6
1004.6
992.5
995.0
997.5
1000.0
1002.5
1005.0
1007.5
1010.0
1012.5
1015.0
m/z

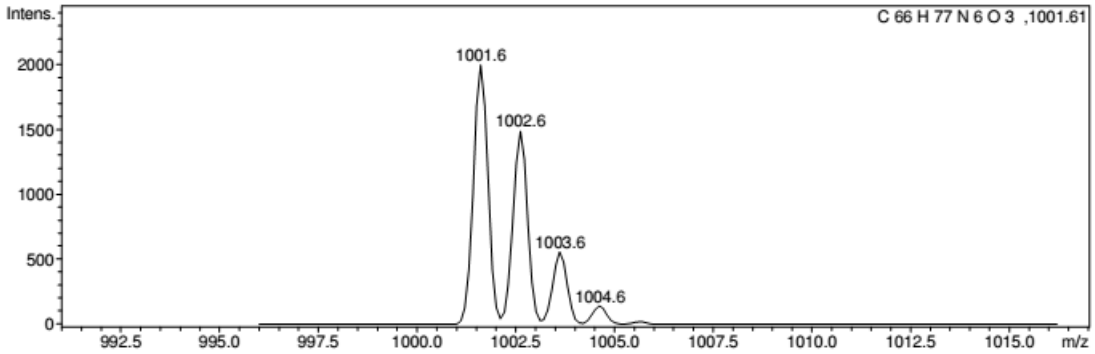
Intens.
2000
1500
1000
500
0
C 66 H 77 N 6 O 3 ,1001.61
1001.6
1002.6
1003.6
1004.6
992.5
995.0
997.5
1000.0
1002.5
1005.0
1007.5
1010.0
1012.5
1015.0
m/z

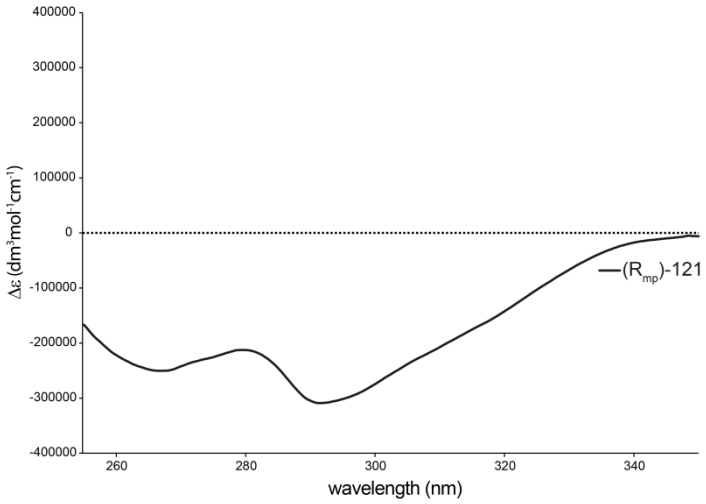
400000
300000
200000
100000
0
-100000
-200000
-300000
-400000
Δε (dm³mol⁻¹cm⁻¹)
—(R_mp)-121
260
280
300
320
340
wavelength (nm)

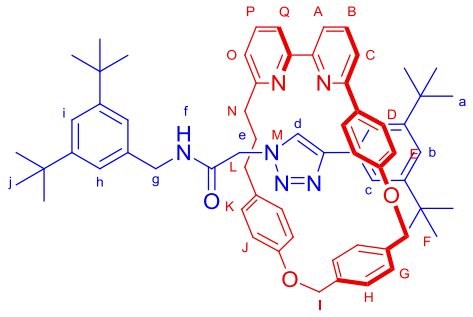

(S_{mp})-**125**

Rotaxane (S_{mp})-121: An identical procedure to that for (R_{mp})-**121** but employing rotaxane (D,R_{mp})-**120** afforded (S_{mp})-**121** as a colourless solid (10.1 mg, 46 %); m.p. 74 - 84 °C; LR-MS (ESI +ve): m/z 1002 $[M+H]^+$.

Spectroscopic data were identical to that reported for rotaxane **rac-121** with the exception of the circular dichroism spectra.

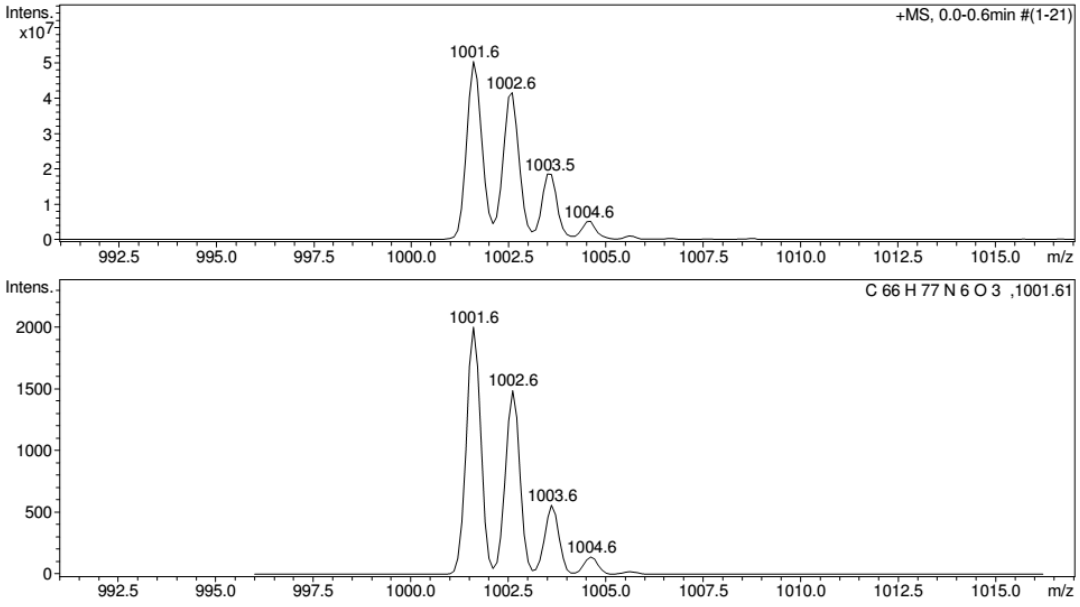

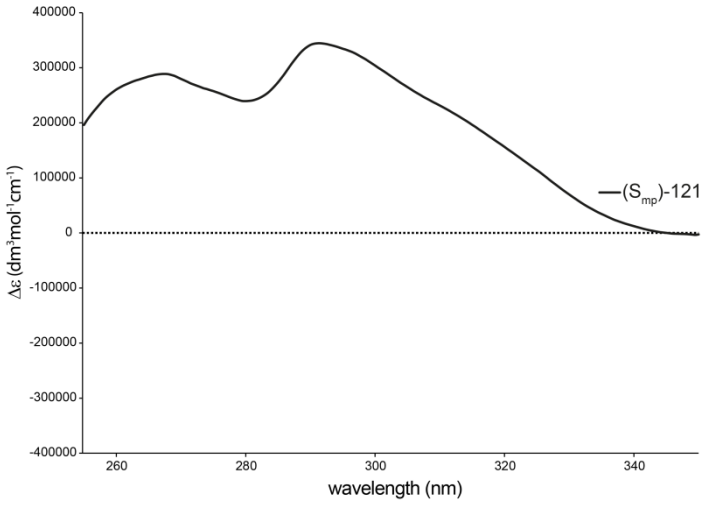

4.4 – Analytical Data

4.4.1 – HPLC chromatograms

Samples were run on a RegisPack column with at a concentration of ~1×10^{-4} M and injection volume = 10μL, in a solution of 1:9 hexane-IPA, with an isocratic gradient of 1:9 hexane-IPA at a flowrate of 1.5 mL/min.

4.4.1.1 – HPLC-MS Report for rotaxane rac-109

Compound Mass Spectrum List Report

Analysis Info

Analysis Name	D:\Data\Stephen Goldup\Rob\RB_6-racemate_1_01_465.d	Acquisition Date	19/10/2012 11:55:57
Method	chiral lcms_465.m	Operator	Ian Sanders
Sample Name	RB_racerot4	Instrument	esquire6000
Comment			

Acquisition Parameter

Ion Source Type	ESI	Ion Polarity	Positive	Alternating Ion Polarity	off
Mass Range Mode	Std/Normal	Scan Begin	50 m/z	Scan End	2800 m/z
Capillary Exit	166.0 Volt	Skimmer	40.0 Volt	Trap Drive	79.5
Accumulation Time	300000 µs	Averages	7 Spectra	Auto MS/MS	off

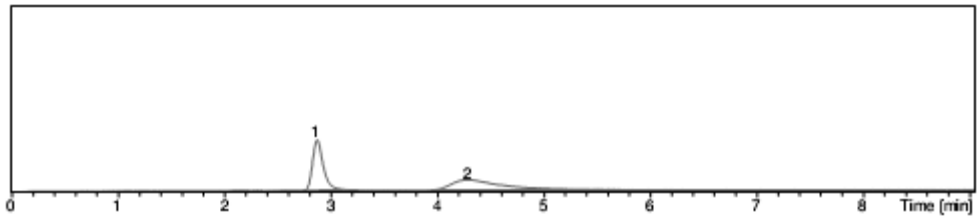

#	RT [min]	Area	Chromatogram	Intens.	Max. m/z	Area Frac. %
1	2.9	737.14	UV Chromatogram, 190-900 nm	109	995.4	50.2
2	4.3	730.09	UV Chromatogram, 190-900 nm	25	995.5	49.8

Cmpd 1, 2.9 min

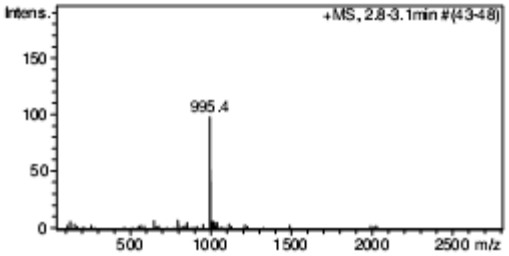

#	m/z	I	Res.	I %
1	995.4	98	2711	100.0
2	996.4	55	2436	56.2
3	997.5	52	3282	53.2
4	998.1	9	4504	9.2

Compound Mass Spectrum List Report

Cmpd 2, 4.3 min

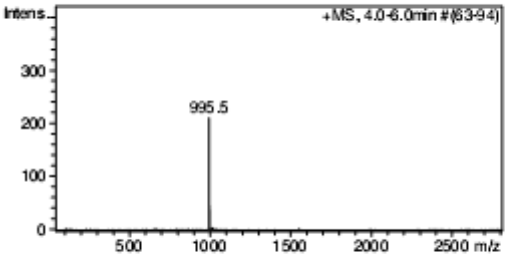

#	m/z	I	Res.	I %
1	995.5	210	2588	100.0
2	996.4	134	2622	63.8
3	997.5	47	2843	22.3
4	998.4	12	2801	5.5

4.4.1.2 – HPLC-MS Report for (R_{mp})-109

Compound Mass Spectrum List Report

Analysis Info

Analysis Name	D:\Data\Stephen Goldup\Rob\RB_(Rmp)6_2_01_468.d	Acquisition Date	19/10/2012 12:35:31
Method	chiral lcms_468.m	Operator	Ian Sanders
Sample Name	RB_E1_1	Instrument	esquire6000
Comment			

Acquisition Parameter

Ion Source Type	ESI	Ion Polarity	Positive	Alternating Ion Polarity	off
Mass Range Mode	Std/Normal	Scan Begin	50 m/z	Scan End	2800 m/z
Capillary Exit	166.0 Volt	Skimmer	40.0 Volt	Trap Drive	79.5
Accumulation Time	300000 µs	Averages	7 Spectra	Auto MS/MS	off

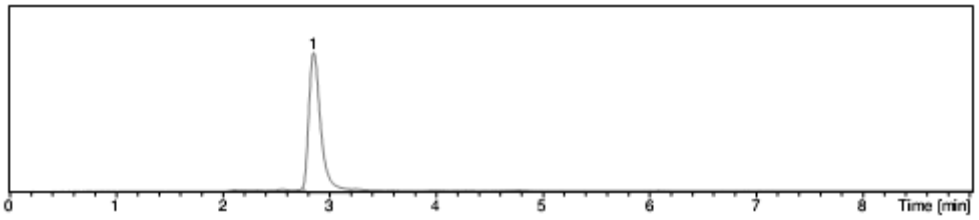

#	RT [min]	Area	Chromatogram	Intens.	Max. m/z	Area Frac. %
1	2.9	3630.0	UV Chromatogram, 190-900 nm	293	995.4	100.0

Cmpd 1, 2.9 min

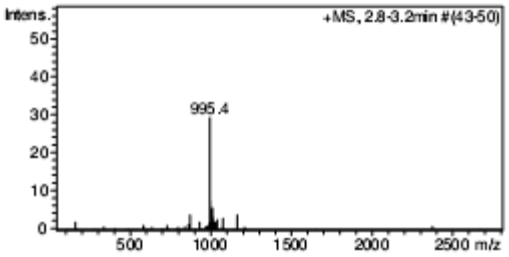

#	m/z	I	Res.	I %
1	995.4	29	3520	100.0
2	996.4	16	2877	55.8
3	997.4	10	2596	34.6
4	998.6	5	3630	17.2

4.4.1.3 – HPLC-MS Report for (S_{mp})-109

Compound Mass Spectrum List Report

Analysis Info

Analysis Name	D:\Data\Stephen Goldup\Rob\RB_(Smp)6_1_01_469.d	Acquisition Date	19/10/2012 12:45:32
Method	chiral lcms_469.m	Operator	Ian Sanders
Sample Name	RB_E2_F49	Instrument	esquire6000
Comment			

Acquisition Parameter

Ion Source Type	ESI	Ion Polarity	Positive	Alternating Ion Polarity	off
Mass Range Mode	Std/Normal	Scan Begin	50 m/z	Scan End	2800 m/z
Capillary Exit	166.0 Volt	Skimmer	40.0 Volt	Trap Drive	79.5
Accumulation Time	300000 µs	Averages	7 Spectra	Auto MS/MS	off

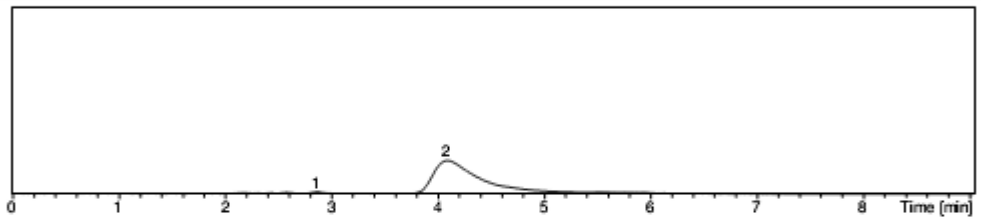

#	RT [min]	Area	Chromatogram	Intens.	Max. m/z	Area Frac. %
1	2.9	14.872	UV Chromatogram, 190-900 nm	3	995.6	0.7
2	4.1	2110.513	UV Chromatogram, 190-900 nm	69	995.5	99.3

Cmpd 1, 2.9 min

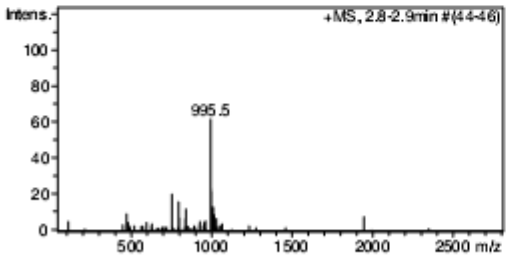

#	m/z	I	Res.	I %
1	995.5	62	2031	100.0
2	996.5	41	2728	66.0
3	997.5	23	2595	37.4

4.4.1.4 – HPLC-MS Report for rac-121

REGIS® TECHNOLOGIES, INC.
8210 Austin Avenue
Morton Grove, IL 60053

E-mail: teds@registech.com
Phone: (847) 583-7661
Toll Free: (800) 323-8144
Fax: (847) 967-1214
www.registech.com

LC Chiral Screening Data Report

C:\CHEM32\1\DATA\TJS2013\SIG2000596.D

Column Name	:	(R,R)-Whelk-O 1
Catalog #	:	780201
Column Size	:	250 mm x 4.6 mm
Particle Size	:	5 micron
Sample Name	:	Xyl-R
Mobile Phase	:	Hexane/Ethanol (90/10)
Flow Rate	:	2.0 mL/min
Injection Vol	:	10.0 uL
Pressure	:	78.1 bar

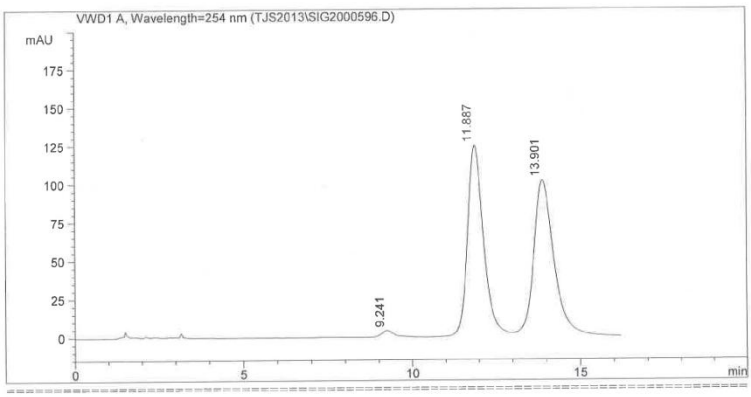

Peak #	RT [min]	Width [min]	Area	Area %
1	9.24	0.405	115.46	1.42
2	11.89	0.542	4000.45	49.27
3	13.90	0.669	4003.60	49.31

4.4.1.5 – HPLC-MS Report for (R_{mp})-121

REGIS® TECHNOLOGIES, INC.
8210 Austin Avenue
Morton Grove, IL 60053

E-mail: teds@registech.com
Phone: (847) 583-7661
Toll Free: (800) 323-8144
Fax: (847) 967-1214
www.registech.com

LC Chiral Screening Data Report

C:\CHEM32\1\DATA\TJS2013\SIG2000598.D

Column Name	:	(R,R)-Whelk-O 1
Catalog #	:	780201
Column Size	:	250 mm x 4.6 mm
Particle Size	:	5 micron
Sample Name	:	Xyl-E2
Mobile Phase	:	Hexane/Ethanol (90/10)
Flow Rate	:	2.0 mL/min
Injection Vol	:	10.0 uL
Pressure	:	78.4 bar

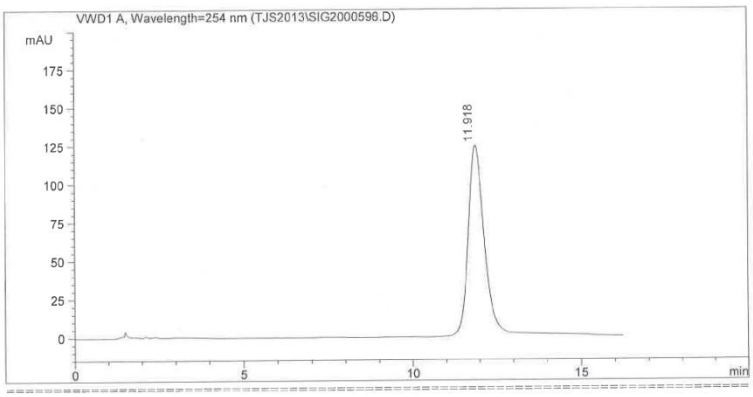

Peak #	RT [min]	Width [min]	Area	Area %
1	11.92	0.503	4130.11	100.00

4.4.1.6 – HPLC-MS Report for (S_{mp})-121

REGIS® TECHNOLOGIES, INC.
8210 Austin Avenue
Morton Grove, IL 60053

E-mail: teds@registech.com
Phone: (847) 583-7661
Toll Free: (800) 323-8144
Fax: (847) 967-1214
www.registech.com

LC Chiral Screening Data Report

C:\CHEM32\1\DATA\TJS2013\SIG2000597.D

Column Name	:	(R,R)-Whelk-O 1
Catalog #	:	780201
Column Size	:	250 mm x 4.6 mm
Particle Size	:	5 micron
Sample Name	:	Xyl-E1
Mobile Phase	:	Hexane/Ethanol (90/10)
Flow Rate	:	2.0 mL/min
Injection Vol	:	10.0 uL
Pressure	:	77.8 bar

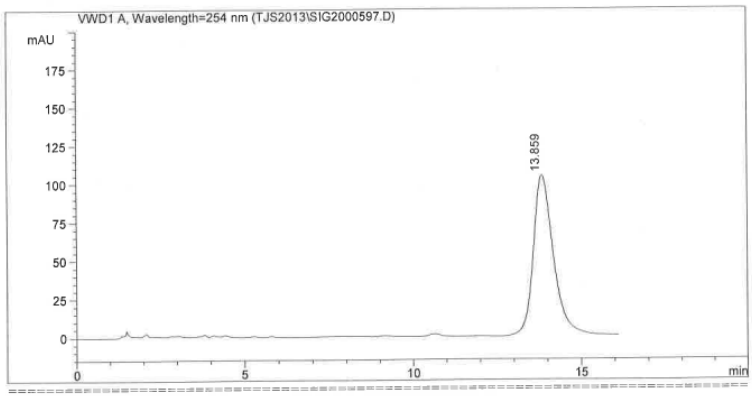

Peak #	RT [min]	Width [min]	Area	Area %
1	13.86	0.627	4355.43	100.00

4.4.2 – X-Ray Crystallographic Data

4.4.2.1 – Rotaxane (D,R_{mp})-96

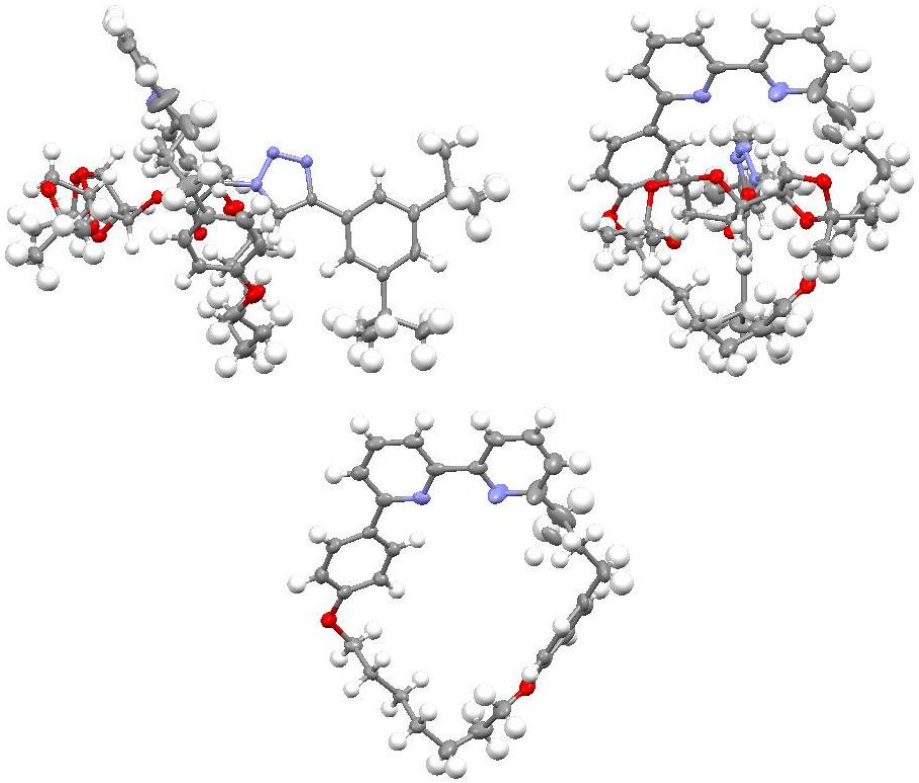

A specimen of $C_{62}H_{77}N_5O_9$, approximate dimensions 0.100 mm x 0.160 mm x 0.170 mm, was used for the X-ray crystallographic analysis. The X-ray intensity data were measured.

The integration of the data using an orthorhombic unit cell yielded a total of 47617 reflections to a maximum θ angle of 66.36° (0.84 Å resolution), of which 9593 were independent (average redundancy 4.964, completeness = 98.5%, R_{int} = 5.36%, R_{sig} = 4.86%) and 7857 (81.90%) were greater than $2\sigma(F^2)$. The final cell constants of a = 10.4088(7) Å, b = 16.2050(11) Å, c = 33.6784(19) Å, volume = 5680.7(6) $Å^3$, are based upon the refinement of the XYZ-centroids of reflections above 20 σ(I). The calculated minimum and maximum transmission coefficients (based on crystal size) are 0.8976 and 0.9379.

The structure was solved and refined using the Bruker SHELXTL Software Package, using the space group P 21 21 21, with Z = 4 for the formula unit, $C_{62}H_{77}N_5O_9$. The final anisotropic full-matrix least-squares refinement on F^2 with 705 variables converged at R1 = 5.55%, for the observed data and wR2 = 14.07% for all data. The goodness-of-fit was 0.977. The largest peak in the final difference electron density synthesis was 0.907 $e^-/Å^3$ and the largest hole was -0.459 $e^-/Å^3$ with an RMS deviation of 0.050 $e^-/Å^3$. On the basis of the final model, the calculated density was 1.212 g/cm^3 and F(000), 2224 e^-.

4.4.2.2 – Rotaxane (D,S_{mp})-96

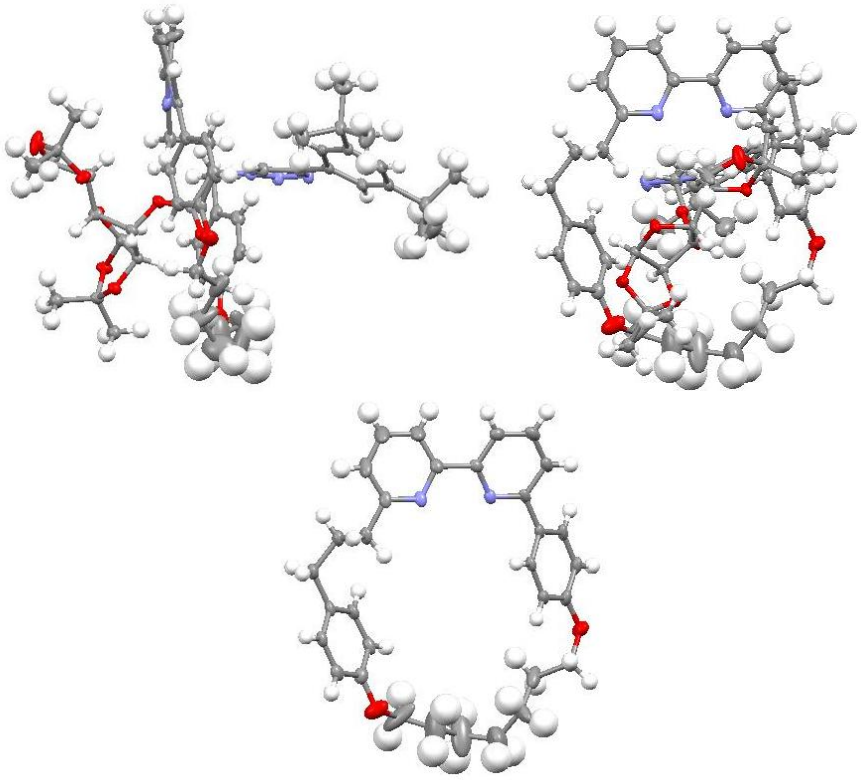

A specimen of $C_{62}H_{78}N_5O_{9.50}$, approximate dimensions 0.070 mm x 0.080 mm x 0.220 mm, was used for the X-ray crystallographic analysis. The X-ray intensity data were measured.

The total exposure time was 16.56 hours. The frames were integrated with the Bruker SAINT software package using a narrow-frame algorithm. The integration of the data using an orthorhombic unit cell yielded a total of 54954 reflections to a maximum θ angle of 60.24° (0.89 Å resolution), of which 7124 were independent (average redundancy 7.714, completeness = 96.4%, R_{int} = 3.14%, R_{sig} = 1.79%) and 6994 (98.18%) were greater than $2\sigma(F^2)$. The final cell constants of a = 13.6896(3) Å, b = 18.8091(4) Å, c = 21.8375(4) Å, volume = 5622.9(2) $Å^3$, are based upon the refinement of the XYZ-centroids of 9323 reflections above 20 σ(I) with 6.201° < 2θ < 116.3°. Data were corrected for absorption effects using the multi-scan method (SADABS). The ratio of minimum to maximum apparent transmission was 0.918. The calculated minimum and maximum transmission coefficients (based on crystal size) are 0.8671 and 0.9548. The structure was solved and refined using the Bruker SHELXTL Software Package, using the space group P 21 21 21, with Z = 4 for the formula unit, $C_{62}H_{78}N_5O_{9.50}$. The final anisotropic full-matrix least-squares refinement on F^2 with 696 variables converged at R1 = 4.85%, for the observed data and wR2 = 13.26% for all data. The goodness-of-fit was 1.047. The largest peak in the final difference electron density synthesis was 1.072 $e^-/Å^3$ and the largest hole was -0.377 $e^-/Å^3$ with an RMS deviation of 0.050 $e^-/Å^3$. On the basis of the final model, the calculated density was 1.235 g/cm^3 and F(000), 2244 e^-.

4.5 – References

[46] Lahlali, H.; Jobe, K.; Watkinson, M.; Goldup, S. M. *Angew. Chem. Int. Ed.*, **2011**, *50,* 4151.

[47] Saiah, M.; Bessodes, M.; Antonakis, K. *Tet. Lett.* **1992**, *33,* 4317.

[48] S. Grunder, D. Munoz Torres, C. Marquardt, A. Blaszczyk, R. Krupke, M. Mayor, *Eur. J. Org. Chem.* **2011**, *3*, 478.

[49] Bouillon, A.; Lancelot, J.-C.; Sopakova de Oliveira Santos, J; Collot, V; Bovy, P. R.; Rault, S. *Tetrahedron*, **2003**, 59, 10043.